

Master's thesis in Molecular Medicine

**Characterization of innate immune  
signaling components involved in regulation  
of TSLP expression in airway cells upon  
Human Metapneumovirus infection**

Ida Haugan Nervik

Trondheim, June 2016



Norwegian University of  
Science and Technology



Childhood Airway Infection Research Group (CAIR)

Department of Laboratory Medicine, Children's and Women's  
Health, Faculty of Medicine

Norwegian University of Science and Technology



## Acknowledgements

First and foremost I would like to express my deepest gratitude to my supervisor, Dr. Ingvild Bjellmo Johnsen for excellent guidance, follow up and inspiration.

Thank you to the rest of the Virus in immunity and disease research group for a valuable, exciting and challenging year. Especially thanks to Youxian Li and Kristin Rian for excellent help and for sharing knowledge in the lab.

Sincere thank you to Cecilie Lund for the great cooperation, help and support, and for sharing the ups and downs of this experience with me. It would not have been the same, or as fun, without you.

Thank you to my roomies in Neufeldtsgate and to my friends for making these past two years memorable. Especially thank you to Christine Rindal for technical support and for all the fun we have had this year. Thank you to Karine Flem Karlsen for proofreading and valuable advice.

Last but not least, thank you to my family: my parents and my brother Didrik, and of course Dima the Labrador, for all the love and support.

Ida Nervik

Trondheim, May 2016



## Abstract

Viral respiratory tract infections have been linked to development of asthma, which affects approximately 235 million people around the world. Human metapneumovirus (hMPV) is a recently discovered virus recognized as a clinically important respiratory pathogen. Thymic stromal lymphopoietin (TSLP) is an interleukin 7 (IL-7) like cytokine that is expressed mainly by epithelial cells at barrier surfaces and induce immune responses by targeting immune cells that produce T helper 2 (Th2) cytokines. hMPV infection is known to induce TSLP expression in airway epithelial cells and in fibroblasts. Elevated TSLP-directed inflammation in the airways may contribute to respiratory disease and create a Th2-permissive environment that attribute to the development of asthma.

How TSLP is regulated in response to hMPV infection in human airway cells is poorly described. Pattern recognition receptor (PRR) components regulating induction of TSLP in response to respiratory syncytial virus (RSV) infection, and IFN- $\beta$  induction in response to hMPV has previously been assessed, but such characterization of the regulation of TSLP induction in response to hMPV has not previously been done. This study focuses on the regulation of TSLP in response to hMPV subgroup A1 infection in human airway cells. PRR components involved in the regulation of TSLP expression upon hMPV A1 infection in human airway cells were characterized applying siRNA-mediated knockdown method.

The results indicate that TSLP is induced in response to hMPV A1 infection in both airway epithelial cells and lung fibroblast. The long form TSLP isoform is predominantly induced upon hMPV infection. The RIG-I-MAVS signaling pathway is suggested to be essential in the induction of TSLP upon hMPV infection. TBK1 seems to be a key component in the lftTSLP induction pathway. Lung fibroblasts seem to be particularly important as a source of TSLP production upon respiratory virus infection.



## Abbreviations

°C	Degrees Celsius
2'5'-OAS	2'5'-Oligoadenylate synthetase
-ssRNA	Single Stranded Negative Sense RNA
A1	hMPV lineage A sub-lineage A1
AECs	Airway Epithelial Cells
aMPV	Avian metapneumovirus
APC	Antigen Presenting Cell
ASC	Apoptosis-associated speck-like protein containing a caspase-recruitment domain
ATCC	American Type Culture Collection
ATF-2	Activating Transcription Factor 2
ATP	Adenosine triphosphate
β-ME	2-Mercaptoethanol
CARD	Caspase recruitment domain
CARDIF	CARD adapter inducing IFN-β
CCL5	Chemokine (C-C motif) ligand 5
CD4+/8+	Cluster of differentiation 4+/8+
cDNA	Copy DNA
cDVGs	Copy-back defective genomes
COPD	Chronic Obstructive Pulmonary Disease
CPE	Cytopathic effect
CRD	Chronic respiratory disease
Ct	Threshold cycle
CT	Cytoplasmic tail
CXL10	C-X-C motif chemokine 10
DCs	Dendritic cells
dH <sub>2</sub> O	Distilled water
DAMPs	Danger associated molecular patterns
dDVGs	Deletion defective viral genomes
DFA	Direct Fluorescent Antibody
DICER	Helicase with RNAase motif
DIs	Defective Interfering RNAs
DMEM	Dulbeccos Modified Eagles Medium
DMSO	Dimethyl sulfoxide
DNA	Deoxyribonucleic acid
DPBS	Dulbeccos Phosphate Buffered Saline
dsRNA	Double stranded RNA
DVGs	Defective Viral Genomes

EtOH	Ethanol
ER	Endoplasmic reticulum
F	Fusion protein
F0	F protein precursor
F1	F protein subunit 1
F2	F protein subunit 2
FBS	Fetal Bovine Serum
FFU	Focus Forming Units
FFU/mL	Focus Forming Units per milliliter
FITC	Fluorescein isothiocyanate
FP	Fusion peptide
G	Attachment protein
h	Hours
HEK	Human Embryonic Kidney cells
hMPV	Human metapneumovirus
HRA	Heptad repeat A
HRB	Heptad repeat B
HRSV	Human respiratory syncytical
IFNAR	Type I IFN receptor complex
IFNs	Type I interferons
IgE	Immunoglobulin E
IKK	I $\kappa$ B kinase complex
IL	Interleukin
IL-7R- $\alpha$	IL-7 receptor $\alpha$ chain $\alpha$
IP-10	Interferon gamma-induced protein 10
IPS1	IFN- $\beta$ promoter stimulator 1
IRF	IFN Regulatory Factors
ISG	IFN-stimulated genes
JNK	Jun N-terminal kinase
L	Large polymerase protein
LB	Lysis buffer
LGP2	Laboratory of genetics and physiology 2
LRR	Leucine rich repeats
LRTI	Low respiratory tract infection
lftSLP	Long form TSLP
M	Matrix protein
MAPKs	Mitogen activated protein kinases
MAVS	Mitochondrial antiviral signaling
MDA5	Melanoma Differentiation Associated protein 5
MHC	Major histocompatibility complex
mm	Millimeter
mRNA	Messenger RNA
MOI	Multiplicity Of Infection



Mx	Myxovirus resistance proteins
N	Nucleoprotein
NEMO	NF- $\kappa$ B essential modulator
NF- $\kappa$ B	Nuclear Factor-Kappa B
NLRP3	NLR Family, Pyrin domain containing 3
NLRs	NOD-Like Receptors
nm	Nanometer
NOD	Nucleotide-Binding and Oligomerization Domain
NS1/NS2	Nonstructural proteins 1 and 2
nt	Nucleotides
NT	No transfection
ON	Over Night
ORF	Open Reading Frame
OptiMem 2%	OptiMem supplemented with 2% FBS and gent/glut+
P	Phosphoprotein
PAMPs	Pathogen-associated molecular patterns
PBS	Phosphate buffered saline
PFA	Paraformaldehyde
PFU	Plaque forming unit
p.i.	Post infection
PKR	Protein kinase R
PRR	Pattern recognition receptor
qRT-PCR	Quantitative Real-Time PCR
RANTES	Regulated on activation, normal T cell expressed and secreted
RD	Regulatory Domain
RGD	Arginine-glycine-aspartate motif
RIG-I	Retinoic acid-inducible gene 1
RISC	RNA-inducing Silencing Complex
RLRs	RIG-like receptors
RM	Reaction Mix
RNA	Ribonucleic acid
RNAP	The Ribonucleoprotein complex
RPMI	Rosewell Park Memorial Institute Medium
RSV	Respiratory syncytial virus
RT	Room Temperature
RTr	Reverse Transcriptase
sDVGs	Snap-back defective viral genomes
SeV	Sendai Virus
SF2	Superfamily 2
sfTSLP	Short form TSLP
SH	Small Hydrophobic protein
siRNA	Short interfering RNA
ss	Single stranded
STAT	Signal Transducer and Activator of Transcription

TAK1	Transformin growth factor $\beta$ -activated kinase 1
TANK	TRAF family member-associated NF- $\kappa$ B activator
TBK1	TANK-binding kinase 1
TCGM	Trypsin Containing Growth Medium
TCID50/mL	Tissue Culture Infection Dose 50% per milliliter
TE	Trypsin EDTA
TF	Transcription factor
TGF- $\beta$	Transforming Growth Factor- $\beta$
Thr	Threonine
Th1 and 2	T helper cell 1 and 2
TIR	Toll/IL-1 homology domain
TLRs	Toll-like receptors
TM	Trans-membrane domain
TNF	Tumor Necrosis Factor
TNF-R	Tumor Necrosis Factor Receptor
TRADD	Tumor necrosis factor receptor type 1 associated DEATH domain
TRAF	TNF-receptor-associated factor
TSLP	Thymic stromal lymphopoietin
TSLPR	Thymic stromal lymphopoietin receptor
URTI	Upper respiratory tract infection
VISA	Virus-induced signaling adapter

# Table of Contents

<b>1 Introduction</b> .....	<b>1</b>
1.1 Respiratory disease .....	1
1.1.1 <i>Asthma</i> .....	1
1.2 Human metapneumovirus (hMPV) .....	4
1.2.1 <i>Epidemiology and clinical manifestations of hMPV</i> .....	4
1.2.2 <i>Taxonomy of hMPV</i> .....	5
1.2.3 <i>Biology and replication of hMPV</i> .....	6
1.3 Defective interfering RNA (DIs) .....	10
1.4 The airway epithelium .....	12
1.4.1 <i>The airway epithelium as an anatomical barrier</i> .....	13
1.4.2 <i>The airway epithelium as a defense against invasive pathogens</i> .....	14
1.5 The innate immune response .....	14
1.5.1 <i>Pattern recognition receptors (PRRs)</i> .....	15
1.6 Cellular signaling through TLRs, RLRs and NLRs .....	18
1.6.1 <i>Transcription factors</i> .....	21
1.6.2 <i>IFN-<math>\beta</math> and the antiviral state</i> .....	22
1.7 Thymic stromal lymphopoietin (TSLP) .....	24
1.7.1 <i>Biology of TSLP</i> .....	24
1.7.2 <i>TSLP and asthma</i> .....	24
<b>2 Aims of the Study</b> .....	<b>27</b>
<b>3 Methodology</b> .....	<b>29</b>
3.1 Reagents used .....	29
3.2 Cell cultivation .....	30
3.2.1 <i>Cell lines</i> .....	30

3.2.2 Subcultivation of cell lines.....	31
3.2.3 Thawing of cells.....	31
3.3 Virus propagation.....	32
3.4 Virus isolation .....	33
3.5 Titration assay .....	33
3.6 DI+/- determination assay .....	36
3.8 Replication curve.....	36
3.9 Infection.....	36
3.10 Lysis .....	37
3.11 Time course .....	37
3.12 siRNA Knockdown.....	38
3.13 Knockdown pathway using kinase inhibitors .....	40
3.14 RNA isolation .....	41
3.15 cDNA synthesis/reverse transcriptase.....	41
3.16 qRT-PCR.....	42
3.17 Western Blot .....	46
3.18 Statistical analysis .....	47
<b>4 Results and discussion .....</b>	<b>49</b>
4.1 Propagation of hMPV A1 in LLC-MK2 cell culture.....	49
4.2 Determination of IFN- $\beta$ induction in virus stocks, DI+ and DI- stocks.....	54
4.3 Characterization of IFN- $\beta$ response and activation of related transcription factors upon hMPV A1 infection in airway epithelial cells.....	57
4.3.1 Kinetics for hMPV A1-triggered IFN- $\beta$ induction in airway epithelial cells.....	57
4.3.2 Activation of transcription factors upon infection with hMPV A1 in airway epithelial cells.....	58
4.4 Characterization of PRR signaling components involved in hMPV A1- triggered TSLP induction in airway epithelial cells .....	62

4.4.1 Kinetics for hMPV-triggered TSLP induction in airway epithelial cells.....	62
4.4.2 Efficiency of siRNA-mediated knockdown of PRR signaling components.....	63
4.4.3 Characterization of PRR signaling components involved in hMPV A1-triggered lTSLP expression in airway epithelial cells.....	64
4.5 Characterization of IFN- $\beta$ response and activation of related transcription factors upon hMPV A1 infection in lung fibroblasts.....	68
4.5.1 Kinetics for hMPV-triggered IFN- $\beta$ induction in lung fibroblasts.....	68
4.5.2 Activation of transcription factors upon infection with hMPV A1 in lung fibroblasts .....	69
4.6 Characterization of PRR signaling components involved in hMPV A1- triggered TSLP induction in lung fibroblasts.....	71
4.6.1 Kinetics for hMPV-triggered TSLP induction in lung fibroblasts.....	71
4.6.2 Characterization of PRR signaling components involved in hMPV A1-triggered TSLP expression in lung fibroblasts.....	72
4.6.3 The NLRP3-inflammasome involvement in hMPV-triggered TSLP induction in lung fibroblasts.....	80
<b>5 Conclusions.....</b>	<b>83</b>
<b>6 Future Studies.....</b>	<b>85</b>
<b>References.....</b>	<b>87</b>
<b>Appendix A: Instruments and Computer Software.....</b>	<b>93</b>



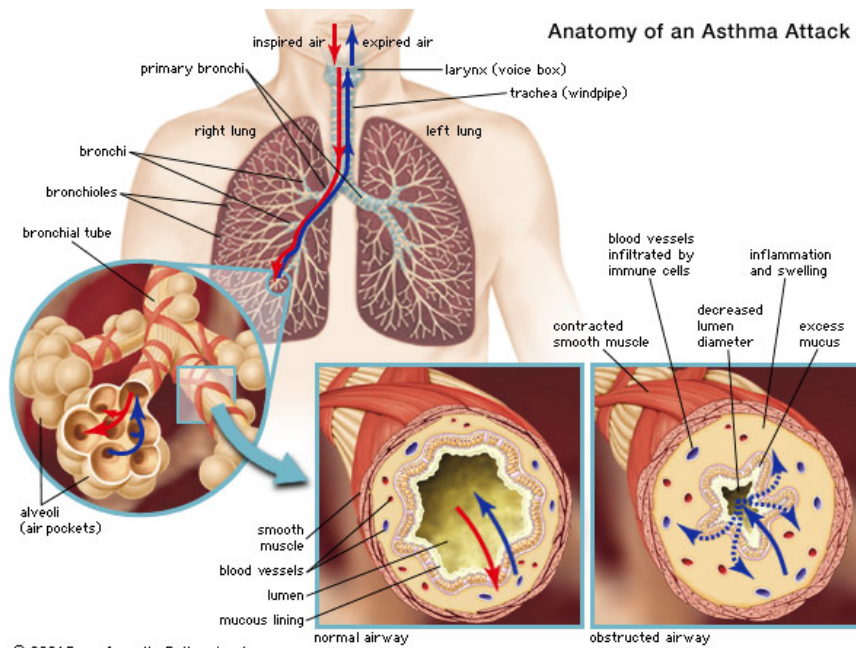
# 1 Introduction

## 1.1 Respiratory disease

Respiratory diseases are any disorders or diseases that affect the human respiration. The respiratory tract is exposed to the environment and may be affected by inhaled dust, gas and pathogens. Allergic or sensitivity reactions may affect the lung function. The respiratory tract has several mechanisms to defend itself against inhaled particles. The air is filtrated by cilia and mucus in trachea, and immune cells that travel in lymphatic vessels in the trachea walls destroy foreign particles that follow the inhaled air. In the bronchi, cilia is a key feature in removing substances from the airways. The particles are moved in a mucus layer by the “mucociliary escalator” up to the pharynx. Respiratory diseases can range from mild and self-limiting diseases such as the cold to serious conditions such as bacterial pneumonia, asthma, chronic obstructive pulmonary disorder (COPD), cystic fibrosis and lung cancer.

### 1.1.1 Asthma

Asthma is defined as a chronic inflammatory disorder of the airways. Because asthma has a low fatality rate, it receives less attention than other respiratory diseases, even though 235 million people around the world are affected (1). High prevalence of childhood asthma is observed and the prevalence is predicted to increase in the future. The inflammation cause wheezing, breathlessness, chest tightness and cough and is associated with increased bronchial hyper-responsiveness to a range of different stimuli. A number of different cell types are involved: mast cells, eosinophils, T lymphocytes, neutrophils and epithelial cells. The airway inflammation may be chronic or acute. The anatomy of an asthma attack is illustrated in Figure 1.1.



© 2001 Encyclopædia Britannica, Inc.

**Figure 1.1. The anatomy of an asthma attack.** The figure illustrates the anatomy of the lungs, with an enlarged illustration of the aveoli. The bottom figures illustrate the difference between a normal airway and an obstructed airway as in the case of an asthma attack. The asthma attack involves contraction of the smooth muscle of the alveoli, immune cells infiltrate the blood vessels, inflammation and swelling, the lumen area of the alveoli is decreased and mucus increases. The figure is borrowed from Encyclopædia Britannica (2).

The inflammation found in adults with asthma may begin during early childhood in high-risk individuals. Out of predisposing factors, atopy- the genetic predisposition for development of an antigen-specific IgE-mediated response to aeroallergens- is the strongest one for developing asthma. Respiratory tract infections as a result of viral infections have been linked to development of asthma. Asthma and viral infections have been linked in several ways. During infancy viruses are thought to be responsible for the asthmatic phenotype. Viruses such as respiratory syncytial virus (RSV) are known to be an inducer of this. However, there must be an additional genetic, environmental or developmental factor to contribute to the development of the asthmatic phenotype since close to all children have been infected by RSV by the age of two. Viral upper respiratory tract infections (URTI) have shown to play a role in patients with established asthma and may lead to acute worsening of airway obstructions and even hospitalization (3). Many children experience wheezing as a result of respiratory infections. For most of these children the wheezing will diminish with increased age, but for others, it will be the beginning of asthma (4).



Asthma pathogenesis can be classified into immune responses where CD4+ T-cell-dependent responses are T-helper type 1 (Th1) or 2 (Th2). The Th1 cells mediate delayed hypersensitivity reactions while Th2 promote B-cell-dependent humoral immunity. Interleukin (IL) -4, -5, -9 and -13 lead to Th2 differentiation and thus B-cell-dependent production of IgE, airway hyper-reactivity and tissue eosinophilia. Th1 cytokines like Type I Interferons (IFNs) and IL-12 lead to down-regulation of these Th2 responses, and they are inversely correlated with the general level of Th1 responses. Asthma pathogenesis is thus both based on the increase of Th2 responses but also the decrease in Th1 responses. The Th1 cells might be necessary for the development of Th2 responses, and might contribute to the allergic response but the overproduction of Th2 cytokines has nonetheless seemed to be the main cause of asthma pathogenesis. The Th2 hypothesis has been questioned to be the sole explanation for asthma after experiments of model systems and in humans. The resulting response of the allergic response include airway hyper-reactivity and mucus production, and these can develop without production of IgE or influx of eosinophils. Treatment that is specific for blocking the Th2 pathway has not yet showed efficient impact on asthma. Holtzman et al suggest that the primary response of airway epithelial cells and macrophages regulate Th2 behavior. Epithelial immune response genes are important in defense against viruses and may be involved in the asthma development. In this way, paramyxovirus infection and asthma may activate genes of the epithelial immune-response, a part of the innate immunity (5).

Allergic inflammation results from a complex immunological cascade that leads to a Th2-derived cytokine production, which triggers production of immunoglobulin IgE, eosinophilia and mucus. Dendritic cells (DCs) are professional antigen-presenting cells that are involved in the pathogenesis of allergic diseases. The initial signal that makes DCs induce production of pro-allergic Th2 cytokines is not known. Epithelial cells are located at the site where particles enter the body and are in close relation to DCs (6).

## 1.2 Human metapneumovirus (hMPV)

Human metapneumovirus (hMPV) was discovered by Bernadette van den Hoogen *et al* at the Department for Virology at Erasmus Medical Center in Rotterdam in 2001 (7).

### 1.2.1 Epidemiology and clinical manifestations of hMPV

hMPV is responsible for a large part of the URTI and lower respiratory tract infections (LRTI) in children. The most common diagnoses caused by hMPV infections are bronchiolitis, pneumonia and bronchitis. Children that have been diagnosed with LRTI caused by hMPV are most likely to be hospitalized, compared to infections by other viruses. This is due to the severe symptoms that have been observed in hMPV-associated LRTIs. It is believed that risk factors for hMPV are the same as for the closely related respiratory virus RSV. These risk factors are premature birth, comprised immune system, and underlying heart or lung disease. hMPV has been identified on every continent and infections seem to peak in the later winter and spring (8).

hMPV infection in experimental animals is associated with changes in the airway epithelial cells and increase of inflammatory cells in the lung interstitium. hMPV can, like RSV, be present in the lungs for several weeks. This proposes that the virus utilize specific strategies to overcome the host immune response. The airway epithelial cell infection leads to degeneration and/or necrosis, increase of neutrophils and prominent mucus. Later stages of hMPV infection include accumulation of intra-alveolar foamy macrophages. These features indicate that the airway inflammation is chronic and that the airway is obstructed and the mucociliary escalator is impaired. It correlates well with the bronchiolitis and wheezing that is observed in patients with hMPV infection (9). Increased levels of IL-8, together with asthma exacerbation in both adults and children is associated with hMPV infection (8). hMPV may, like RSV, induce alterations in the airway and be related to outbreak and exacerbation of childhood asthma. hMPV has been detected in respectively 8% and 4% of children hospitalized for acute expiratory wheezing. This suggests that hMPV might be a trigger for asthma (10, 11). Two chemokines that have been linked to RSV disease, IL-8 and regulated upon activation, normal T-cell expressed and secreted (RANTES), have been found in children positive for hMPV. IL-8 is a chemotactic factor mainly

for neutrophils while RANTES is a chemotactic factor for eosinophils. Children infected with hMPV had lower concentrations of RANTES and higher concentrations of IL-8 in their respiratory secretions compared to children infected with RSV (9, 11).

### 1.2.2 Taxonomy of hMPV

hMPV is a member of the Order *Mononegavirales*, the Family *Paramyxoviridae*, the Subfamily *Pneumovirinae* and the Genus *Metapneumovirus*, as illustrated in Figure 1.2. Below follows a brief description.

Human metapneumovirus was named so as it is the first member of the *Metapneumovirus* genus of the *Pneumovirinae* sub-family of the *Paramyxoviridae* family that was able to infect humans. Morphological, biochemical and genetic analysis revealed that hMPV was closely related to the, at that time, sole member of the *Metapneumovirus* genus, the avian pneumovirus C (aMPV). aMPV is an aetiological agent of upper respiratory tract disease in many birds. hMPV diverge from RSV and other pneumoviruses of the *Pneumovirinae* sub-family in that it has a different gene order and does not contain two non-structural proteins (9). Based on genotyping, hMPV strains have been classified into two main lineages, A and B, and four sub-lineages, A1, A2, B1 and B2 (12).

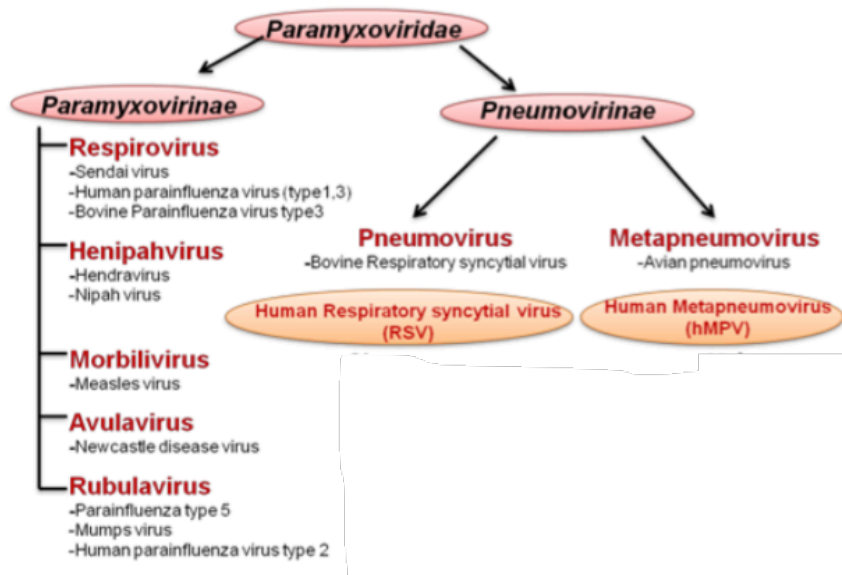


**Figure 1.2. Taxonomy of human metapneumovirus.** Human metapneumovirus is a member of the Order *Mononegavirales* (not illustrated), the Family *Paramyxoviridae*, the Subfamily *Pneumovirinae* and the Genus *Metapneumovirus*. The figure is modified from Kolli *et al* (13).

The Order *Mononegavirales* consist of enveloped viruses that contain a single stranded (ss) negative sense RNA molecule. The nucleocapsids of these viruses are helical and the infectious unit is the ribonucleoprotein that is found inside. On the surface they have spike-like structures. The Family *Paramyxoviridae* contains mainly spherical virions that are around 150-200nm in diameter. The genomes of these viruses are between 13,000 and 18,000 nucleotides in length. The RNA genomes do not have 5' cap structure or a 3' polyadenylate tail. The replication occurs in the cytoplasm, and virions bud from the plasma membrane. Most of the *Paramyxoviridae* members are respiratory viruses, and all infect vertebrates (14).

### 1.2.3 Biology and replication of hMPV

hMPV infection is initiated when the viral surface glycoproteins attach to receptors on the cell membrane. This initiates virus entry by fusion with the cellular membrane. The assumed life cycle of hMPV is shown in Figure 1.3. Most paramyxoviruses are dependent on two viral glycoproteins to enter the cell, one attachment protein and one fusion protein (F). For *Paramyxovirinae* it is proposed that the virus enters the cell by; 1) attachment protein binds to cellular receptors; 2) the bound attachment protein transmits a signal by direct interaction, to the F protein; 3) the F protein undergoes structural changes upon activation; 4) The F protein changes conformation from a pre-fusion to a post-fusion structure and this results in that the viral membrane merges with the plasma membrane; and 5) a fusion pore is created at the surface of the cell and the genome is delivered into the cytoplasm.

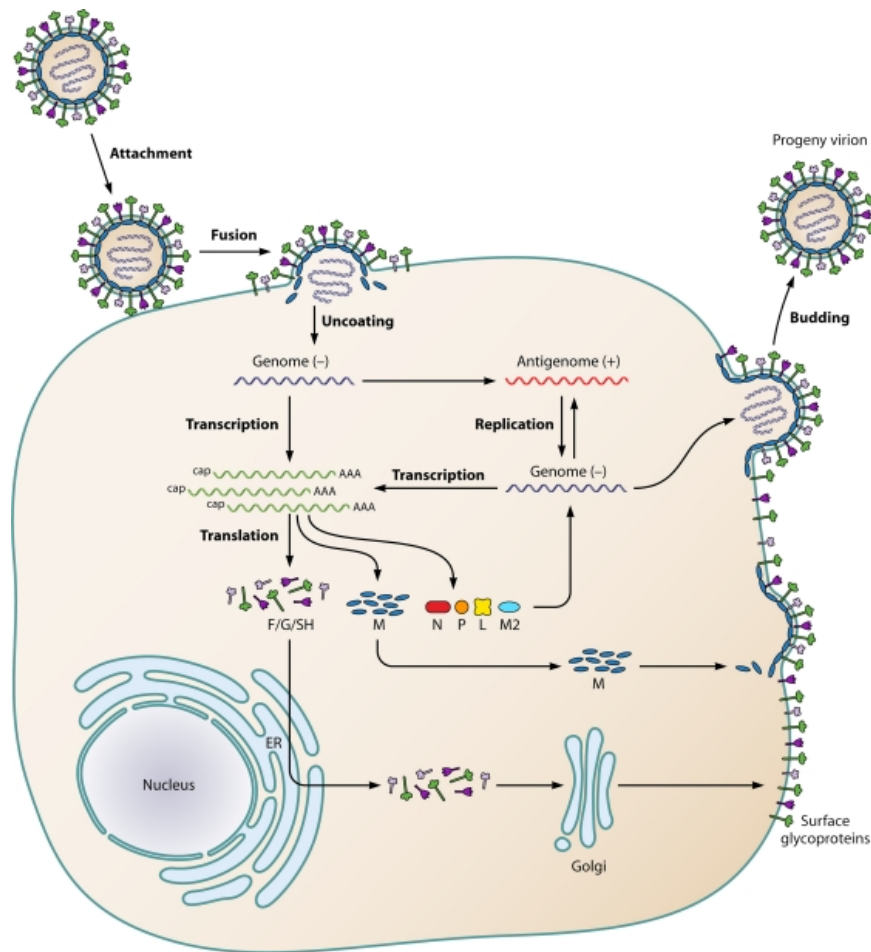


**Figure 1.3. The assumed hMPV life cycle.** The hMPV virion attaches to the plasma membrane of the host cell, and the two membranes fuse. The virion is uncoated and the RNAP complex, which contains the negative sense viral RNA, is released into the cytoplasm. The genome goes through primary transcription, and is then replicated to produce the antigenome (positive sense). The antigenome is further replicated to synthesize genomic RNA (negative sense) to produce additional antigenomes that are used as a template for secondary transcription. The M proteins and the RNPs are then transported by intracellular transport, to the plasma membrane. The viral glycoproteins F, G and SH are transported from the endoplasmic reticulum (ER) to the Golgi apparatus before they reach the plasma membrane. New virions are assembled and are released from the cell by budding. The figure is borrowed from Schildgen *et al* (15).

Unlike for other paramyxoviruses, only one glycoprotein is involved in the facilitation of virus entry for Pneumoviruses. Pneumoviruses have three glycoproteins on the surface of the virion; F, small hydrophobic (SH) and attachment (G). hMPV lacking G and SH are still infectious, and the F protein is able to perform the membrane fusion without a viral attachment protein and capable of completing the entry process. By attaching to the cellular receptors, F proteins activate the F-mediated membrane fusion (16).

The hMPV virions contain a lipid envelope that has three trans-membrane surface glycoproteins and surrounds the matrix (M) protein and the ribonucleoprotein (RNAP) complex. The RNAP complex consist of nucleoprotein (N), phosphor-protein (P), large polymerase protein (L), and the non-segmented single stranded negative sense RNA (–ssRNA) genome (15). An illustration of the hMPV virion is found in Figure 1.4.

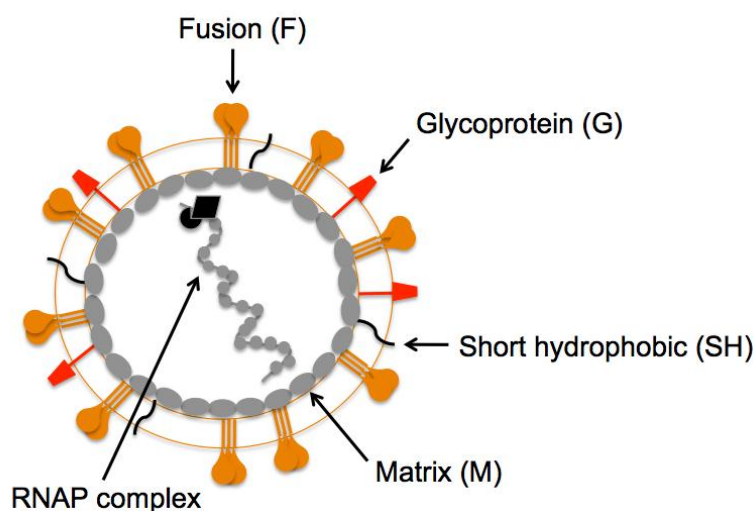


**Figure 1.4. Schematic representation of a human metapneumovirus (hMPV) virion.** The fusion (F, orange), attachment (G, red) and short hydrophobic (SH, black) proteins are glycoproteins on the surface of the virion. The inside lining of the membrane is coated by matrix proteins (M, gray ovals). The ribonucleoprotein (RNAP) complex (gray and black) is found within the viral envelope. The RNAP complex consist of the helical, genomic RNA that is wrapped by the nucleoprotein (N), the viral RNA-dependent, RNA polymerase (L), phosphoprotein (P), and matrix 2 protein (M2). The figure is borrowed from Cox *et al* (16).

The genomes of hMPV are around 13,000 nucleotides in size and contain 8 genes and 9 open reading frames (ORF). As seen in Figure 1.2, another close related virus is Sendai virus (SeV). A genomic map showing hMPV and compared to SeV and RSV is seen in Figure 1.5. The genomes of hMPV and RSV differ in several ways. RSV contains two genes that are not found in the hMPV genome, the nonstructural proteins NS1 and NS2. The position of SH and G genes differ between the two genomes. For RSV, the M2 and L ORF overlap. The position of SH and G genes differ between the two genomes. Sendai virus (SeV) lacks the M2, SH and G genes in hMPV and include a HN gene not found in hMPV. In addition the hMPV genome contains the M2 gene (15). The RSV genes NS1 and NS2 are involved in inhibition of IFN- $\beta$  signaling (5).

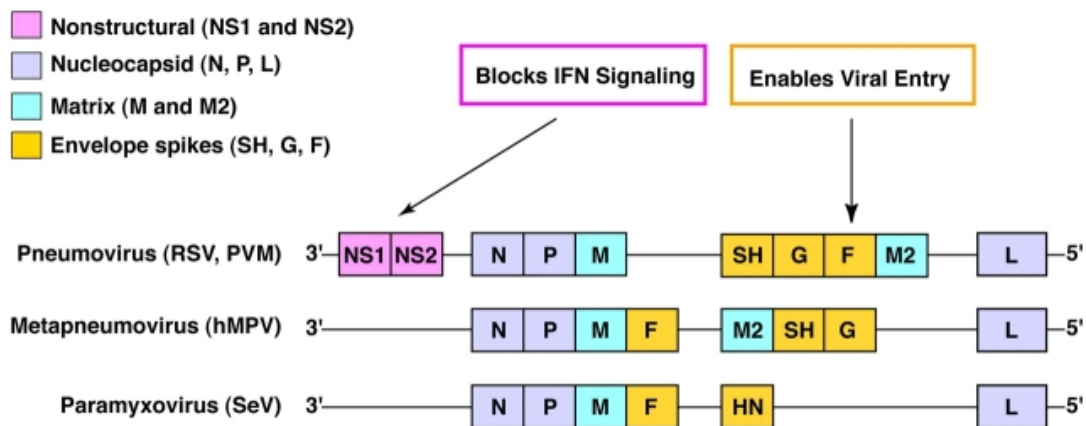


**Figure 1.5. Genomic map of hMPV, RSV, PVM and SeV.** The genomes of hMPV and RSV share many similarities but differ in several ways. RSV contains two genes that are not found in the hMPV genomes, the nonstructural proteins NS1 and NS2. For RSV, the M2 and L ORFs overlap (not illustrated). The position of SH and G genes differ between the two genomes. Sendai virus (SeV) lacks the M2, SH and G genes in hMPV and include a HN gene not found in hMPV. Pneumovirus of mice (PVM), Nucleoprotein (N), phosphoprotein (P), matrix protein (M), small hydrophobic protein (SH), fusion protein (F), attachment protein (G), and large polymerase protein (L). The figure is borrowed from Holtzman *et al* (5).

The F protein is synthesized as a precursor protein named F0. To become the activated protein with disulfide-linked F1 and F2 subunits, it requires cleavage by proteases. An illustration of the structural organization of the F gene is seen in Figure 4. The protein is not cleaved intracellularly and is depending on exogenous protease activation (15). Exogenous trypsin is required for propagation of hMPV in cell culture. Trypsin cleaves the F protein into the active variant that contains the F1 and F2 bound together through disulfide-bridges. Cleavage of the F protein happens at neutral pH at the plasma membrane of the cell (17). An illustration of the organization of the F protein is seen in Figure 1.6.

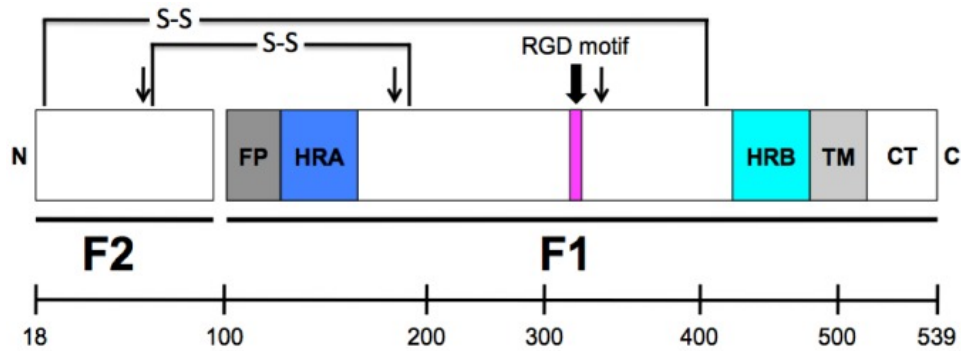


**Figure 1.6. Organization of the hMPV fusion (F) protein.** The F0 precursor protein is activated by cleavage into the F1 and the F2 subunits. They are bound together through disulfide bridges (S-S). The cleavage process is carried out by proteases. *In vitro* the cleavage is dependent on exogenous trypsin to be carried out. The F protein contains 522 amino acids plus signal sequence. The F1 subunit consists of 440 residues and the F2 subunit of 82 residues. The F1 subunit includes an extracellular domain, a trans-membrane domain and a cytoplasmic tail. Fusion peptide (FP), Heptad repeat A (HRA), Heptad repeat B (HRB), Trans-membrane domain (TM), Cytoplasmic tail (CT), Arginine-glycine-aspartate (RGD) motif. The C and N is here used to illustrate the C and the N terminus of the peptide. The figure is borrowed from Cox *et al* (16).

### 1.3 Defective interfering RNA (DIs)

Viruses have evolved mechanisms to counteract antiviral host responses. By doing so, the viruses can replicate and spread before being eliminated. Seasonal viruses are especially effective in counteracting host defenses. For example, Influenza virus and RSV encode proteins that antagonize the host response. Many of the antagonists target the RIG-like-receptor (RLR) pathway. The parainfluenza virus V protein blocks MDA5 signaling, while the C protein blocks IFN signaling and amplification of the RLR response. RSV proteins NS1 and NS2 interfere with IFN expression and signaling. These mechanisms allow the viruses to replicate, package and release from host cells without any antiviral host response for 1.5 to 3 days, called the “incubation period”. The incubation period is characterized by rapid virus growth and the patient does not experience symptoms. The antiviral response that follows will control the infection and clear the virus (18). The RSV antagonists NS1 and NS2 are not present in the hMPV genome. Therefore hMPV is believed to have a different strategy to evade the immune system and avoid the anti viral responses. It is thought that hMPV is a strong inducer of RIG-I and MAVS and thus IFN production. Viral defective interfering (DI) particles are shown to induce IFN expression during infection of cells *in vitro* (18). In addition to promote IFN expression, DI particles stimulate rapid and



strong expression of pro-inflammatory cytokines, chemokines, antiviral genes upon infection with the *Paramyxovirus* SeV. Stocks of SeV that do not carry DI particles are shown to not induce a potent response in the host even when at high Multiplicity of Infection (MOI). DI particles are in this way involved in promoting the transition from the innate to the adaptive immune response. It is believed that DIs become numbered during viral replication, and that these DIs are recognized by the cell as danger signals and thus stimulate the antiviral response of the host (18). This is illustrated in Figure 1.7.

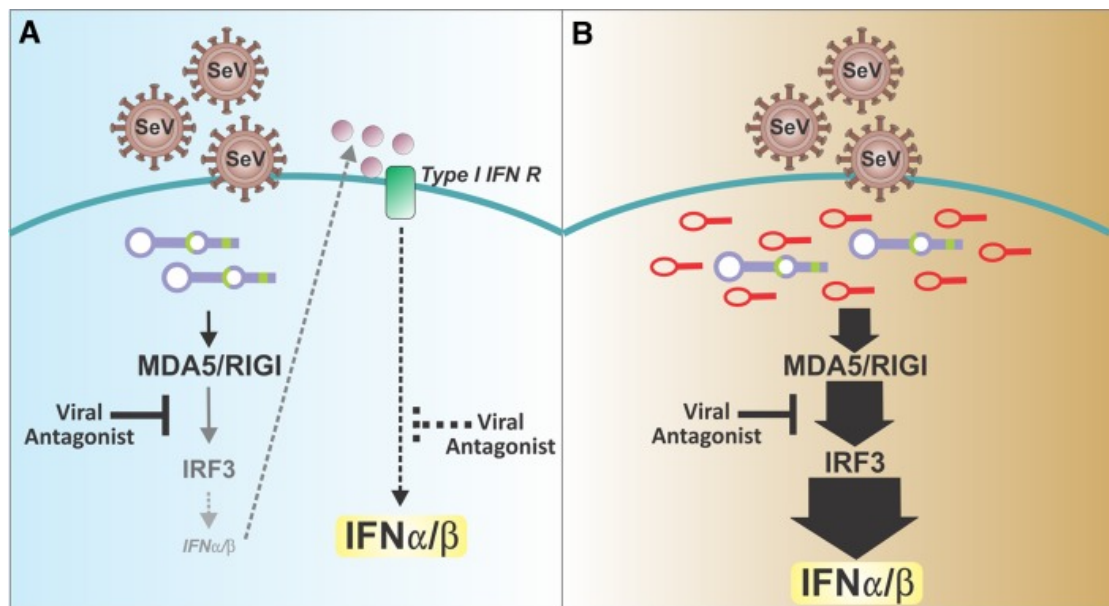


**Figure 1.7. An overview of the current and proposed models for the sequence of events of antiviral responses to infections with paramyxoviruses. A)** The current model: Recognition of virus is magnified by IFN signaling that promotes expression of viral receptors and signaling molecules. In this model it is assumed that there are expressed low levels of IFN. This will mean in the case of SeV infection, that the virus encoded antagonist proteins are only active to a certain degree. **B)** The proposed model: In the proposed model by the López laboratory it is assumed that defective viral genomes that become numbered during virus replication, are danger signals that stimulate the host to respond to overcome the viral antagonism. They assume that this response is independent of type I IFN feedback. The figure is borrowed from López (18).

Negative sense RNA viruses seem to produce defective viral genomes (DVGs) as spontaneous by-products of replication when the virus reaches high titers. DVGs are effectively recognized by the host and induce a potent antiviral response. DVGs are truncated versions of the viral genome that lack essential genes and thus the DVGs are unable to propagate without helper virus. There are two types of DVGs: Deletion DVGs (dDVGs) and Copy-back DVGs (cDVGs). The dDVGs are generated when the viral polymerase falls off the original template and reattaches further downstream. They share the 3' and 5' ends with their parental virus but are incomplete. The cDVGs,

and closely related Snap-back DVGs (sDVGs), consist of a segment of the genome that is flanked by the reverse complementary version of its 5' end. These are generated when the viral polymerase detaches from the template and reattaches to the newly synthesizing strand, which then copies back the 5' end of the genome (18).

Van den Hoogen *et al* suggested a hypothesis that DIs that are present in virus stocks could be responsible for the activation of the IFN pathway. Their results showed that sDVGs accumulate in hMPV stocks, and that these activate the IFN pathway upon infection. DIs does most likely play a significant role in hMPV pathogenesis as they easily accumulate (19).

#### **1.4 The airway epithelium**

Airway epithelial cells (AECs) line the airways and serve a number of functions, including first line of defense and amplification of cytokine response. The AECs are able to modulate a wide range of inflammatory responses through recruitment and activation of inflammatory cells. AECs are also able to release mediators that serve to recruit other epithelial cells and fibroblasts. AECs are in this way important in repair responses, and when these responses are unbalanced it could lead to airway dysfunction (20). In the alveolar part of the lung the most abundant cells are interstitial fibroblasts. They are found in the interstitial space and they are responsible for secretion of the extracellular matrix that supports the alveolar units. Fibroblasts that are stimulated by TGF- $\beta$  can transform into epithelial cells (21). The alveolus is illustrated in Figure 1.8 showing the different cell types involved.

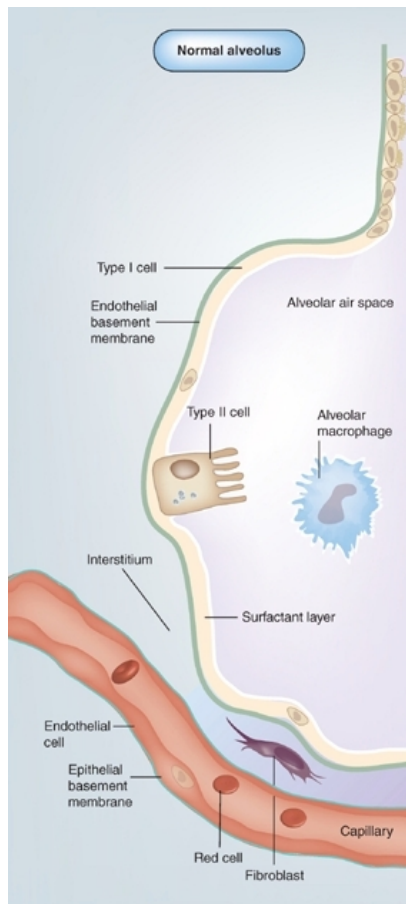


**Figure 1.8. The normal alveolus.**

The surface is made up of the squamous type I epithelial cells which forms the air-blood barrier, and the cuboidal type II, which are secretory cells. Type I cells are more susceptible to injury and cell death. Type II cells are able to proliferate and differentiate into Type I, and this is a key feature in re-epithelialization of the epithelial barrier. Fibroblasts are found in the interstitial space. The figure is modified from Manicone (22).

#### 1.4.1 The airway epithelium as an anatomical barrier

The first line of defense, the anatomical barriers of the airway epithelium, consists of physical and chemical barriers. These are important in defense against pathogens by making sure that they are unable to enter the body. Chemical barriers at these surfaces have antimicrobial activity and acid pH. If pathogens are able to breach the physical and chemical barriers they can survive in the extracellular spaces or infect cells.

When a foreign infectious agent invades the body, the cellular innate immune response begins right away. Surface or cytosolic receptors recognize the pathogens and the white blood cells macrophages and neutrophils are activated. These cells engulf and destroy extracellular pathogens by phagocytosis. Some receptors lead to activation of proteins that have beneficial effects like antimicrobial activity or they recruit fluid cells and molecules to the site of infection, leading to inflammation.

Local innate inflammation is beneficial in the process of eliminating pathogens or damaged cells. During inflammation a range of different processes take place: antimicrobial substances are increased, phagocytic cells eliminate pathogens,

dendritic cells take up and present pathogens to lymphocytes and in this way activates the adaptive immune response. Natural killer cells are able to recognize and kill virus-infected, altered or stressed cells. These inflammatory responses are absolutely necessary in fighting pathogens and damaged host cells but can also be harmful by leading to systemic consequences that cause damage of the tissues and worst case cause death. Regulatory mechanisms have evolved to prevent or limit these harmful responses (23).

#### **1.4.2 The airway epithelium as a defense against invasive pathogens**

The airway epithelium is an important player in the fight against respiratory pathogens. The lungs are protected against respiratory viruses by ciliated epithelial cells. Mucus that covers the apical site of the epithelium creates a semipermeable barrier where nutrients, water and gasses are exchanged while being impermeable for most pathogens. Most inhaled particles are cleared by mucus and cilia in this way on the epithelial surface. Both the innate and the adaptive immune system are regulated by the airway epithelial cells. The epithelial cells produce antiviral molecules such as pro-inflammatory cytokines that in turn recruit and activate other innate immune cells and initiate mechanisms of the acquired immune response. Once a virus has entered an airway epithelial cell, they are rapidly recognized by Pattern Recognition Receptors (PPRs) (24).

### **1.5 The innate immune response**

Innate immunity is part of the immune system in vertebrates evolved to eliminate invasive pathogens in the body. The innate immune system is highly conserved and works as the first line of defense independent of immunological memory. The innate immune response is able to discriminate between self and invasive pathogens, and recognize microbes through PRRs that are constitutively expressed. In comparison, acquired immunity is developed by clonal selection, involved in the late phase of infection and responsible for generating immunological memory. The acquired immune system involves a range of rearranged, specific receptors (25). Acquired immunity is dependent on activation from the innate immune system.

### 1.5.1 Pattern recognition receptors (PRRs)

PRRs are germline-encoded receptors independent of immunological memory, and expressed on all cells. Even though they are not as specific as receptors of the acquired immune system, they are able to discriminate between self and invasive pathogens. They recognize distinct pathogen-associated molecular patterns (PAMPs) on foreign microbes and danger-associated molecular patterns (DAMPs) on host derived molecules, and are able to initiate anti-pathogen and pro-inflammatory responses. The PAMPs can be the microbe itself or segments on the pathogen that are essential to pathogen survival and therefore are conserved (25). When a virus enters the host, the PAMPs on the pathogen are recognized by PRRs on the host cells. PRRs are divided into three categories, including toll-like receptors (TLRs), RLRs and nucleotide-binding oligomerization domain (NOD)-like receptors (NLRs). TLRs are membrane bound, found on the plasma membrane and on endosomal membranes, while NLRs and RLRs are found in the cytosol. When PAMPs are recognized by these PRRs, transcription factors and signaling pathways are activated leading to expression of antiviral, immune and inflammatory genes, resulting in inflammation and host immune responses (13).

#### *Toll-like receptors (TLRs)*

TLRs are type 1 integral membrane glycoproteins that contain leucine-rich-repeat (LRR) motifs on their extracellular domain and a cytoplasmic signaling domain homologous to that of the IL-1. This domain is therefore named the Toll/IL-1 homology (TIR) domain. A number of different immune cells express TLRs; antigen-presenting cells (APCs) including macrophages and DCs as well as B cells, specific types of T cells, and even non-immune cells such as fibroblasts and epithelial cells. Expression of TLRs is regulated in response to pathogens, cytokines and stress. Certain TLRs are expressed on the cell surface while others are found on endosomes. TLRs are stimulated by their ligand, and this recruits adaptor molecules containing a TIR domain to the cytoplasmic tail of the TLRs. This triggers a downstream signaling cascade that results in production of cytokines and chemokines with pro-inflammatory features (25).

### ***RIG-like receptors (RLRs)***

RLRs are intracellular PRRs that belong to the superfamily 2 (SF2)

helicases/ATPases. RLRs distinguish between self and non-self RNA and trigger signaling cascades to initiate host defense responses against viruses. They recognize pathogenic-derived RNA in the cytosol of most cells. There are three members of the RLR family; retinoic acid-inducible gene I (RIG-I) also known as DDX58; melanoma differentiation-associated gene 5 (MDA-5) also known as IFIH1 or helicard; and laboratory of genetics and physiology 2 (LGP2) (13).

RIG-I, MDA5 and LGP2 share conserved structural and functional domains. They inhabit a DExD/H-box capable of ATP hydrolysis activity *in vitro* that is involved in dsRNA interactions. The DExD/H-box is homologous to RNA helicase domains. The DExD/H-box have diverse functions including translocation along ss and ds nucleic acids, unwinding of db nucleic acids, annealing of complementary strands and displacement of proteins from ribonucleoprotein complexes. RLRs contain a regulatory domain (RD) located the C-terminus. The RD is involved in recognition of RNA, and is involved in regulation of RIG-I signaling activity. The RD works as an auto-inhibitory domain for RIG-I. The RD has also been termed the repressor domain, and expression of the RD of RIG-I or LGP2 can inhibit RIG-I-mediated signaling and deletion of the RIG-I RD region increases basal signaling activity (26).

RIG-I and MDA5 also share two N-terminal caspase activation and recruitment domain (CARD) regions, but these are not present in LGP2. These protein interaction CARDS are necessary for antiviral signal transduction downstream of RNA recognition. The CARDS are the primary effector domains that transduce an RNA detection signal downstream. Expression of the RIG-I or MDA5 CARDS alone is sufficient to induce unregulated signal transduction (26). An illustration of the composition of the three RLRs RIG-I, MDA5 and LGP2 is found in Figure 1.9.

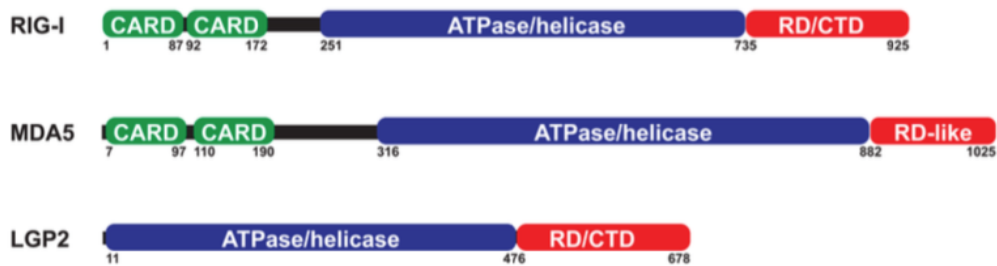


**Figure 1.9. RLR family members RIG-I, MDA5 and LGP2.** The three receptors have a central ATPase containing a DEXD/H box helicase domain. RIG-I and MDA5 contain N-terminal CARD domains that mediate downstream signaling. LGP2 lacks CARD. RIG-I and LGP2 contain a repressor domain (RD) in the C-terminal regulatory domain (CTD). Because MDA5 does not contain a RD, overexpression is sufficient to activate pathway signaling, while overexpression of RIG-I in the absence of an activating ligand does not result in activating signaling pathways. LGP2, lacking the CARD, has a dominant-negative phenotype. The RLRs are present in low levels in un-stimulated cells. The figure is modified from Dixit (27).

#### Retinoic acid-inducible gene I (RIG-I)

RIG-I senses the 5' triphosphate of viral genomes or viral derived transcripts of negative sense ssRNA viruses. RIG-I is known to recognize several RNA virus, including SeV and RSV (28).

#### Melanoma differentiation-associated gene 5 (MDA5)

MDA-5 senses long dsRNA, typically intermediate of the replication of positive sense ssRNA viruses. MDA-5 is essential in detecting picornaviruses and is a target of IFN inhibitory activity of paramyxovirus V protein (28).

#### Laboratory of genetics and physiology 2 (LGP2)

LGP2 is unable to sense RNA directly due to the lack of CARD. It is thus not capable of propagating an antiviral signal like RIG-I or MDA5, and LGP2 is therefore thought to have a distinct role in signaling (26). The role of LGP2 is not completely understood. However, it is shown that overexpression of LGP2 inhibit IFN induction in response to SeV, and LGP2 is believed to be an inhibitor of RIG-I while an activator of MDA5 in IFN induction (29).

#### *NOD-like receptors (NLRs)*

NLRs play major roles in the innate immune and inflammatory responses, and they have show to be involved in initiating responses against respiratory viruses (24). Some NLR members, like the NOD1 and NOD2, activate transcription of genes that encode inflammatory cytokines, while others, like NLRP3, is able to form multi-protein complexes called inflammasomes (23, 30).

NLR family, Pyrin Domain Containing 3 (NLRP3)

NLRP3 assemble with other proteins into the inflammasome complex that activate proteases necessary for converting inactive cytokines into their active and secreted form (23). The inflammasome consist of the adaptor apoptotic speck-containing protein with a CARD (ASC) and pro-caspase-1, and is involved in cleavage and activation of the pro-inflammatory cytokines IL-1 $\beta$  and IL-18 into secreted forms (24).

### **1.6 Cellular signaling through TLRs, RLRs and NLRs**

After PRRs recognize virus associated molecules, antiviral responses are initiated. The antiviral response includes production of cytokines and chemokines and further activation of the adaptive immune response. One of the main cytokines involved in viral immune response is IFN- $\beta$ . IFNs initiate both antigen-specific CD8<sup>+</sup> T cell responses and chemokines that stimulate lymphocytes and monocytes and recruit them to the site of infection. IFNs also upregulate effector molecules that help establish the 'antiviral state'. Transcription of IFNs is regulated by activation of transcription factors NF- $\kappa$ B, ATF2, IRF3 and IRF7. Activation of NF- $\kappa$ B and ATF2-c-Jun result in regulation of expression of genes that are involved in inflammation, in addition to interaction with IRF3 and IRF7 to enhance type I interferon induction (31). The RIG-I/MDA5-dependent signaling pathway leading to expression of IFN- $\beta$  is illustrated in Figure 1.10.



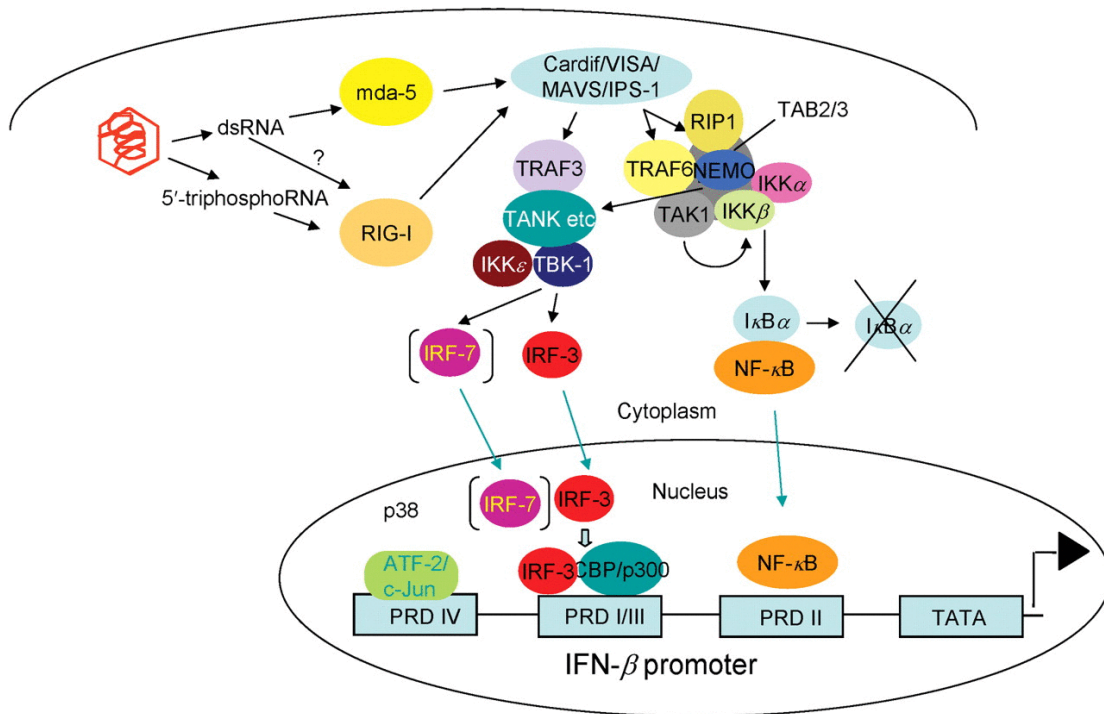


**Figure 1.10. MDA5- and RIG-I-dependent signaling.** The RNA helicases MDA5 and RIG-I are activated by viral RNA in the cytosol. RIG-I can be activated by both RNA molecules with 5' triphosphates and dsRNA, while MDA5 is only activated by the latter. The N-terminal CARD domains recruit the adaptor MAVS, which recruits signaling components that either signals further through the IRF-3 or the NF- $\kappa$ B pathways. It is believed that the downstream signaling that follows in these pathways are similar to the downstream signaling of TRIF in TLR3-dependent signaling. Activation of NF- $\kappa$ B requires TRAF6 and RIP1 recruitment and further the recruitment of the IKK complex and TAK1. TAK1 phosphorylates and thus activates the IKK $\beta$  subunit of the IKK complex which in turn phosphorylates I $\kappa$ B. This leads to ubiquitination of I $\kappa$ B, before it is degraded by the proteasome. When I $\kappa$ B is degraded, NF- $\kappa$ B is released and moves into the nucleus where it binds to the IFN- $\beta$  promoter. Activation of IRF-3 requires the recruitment of TRAF3. TRAF3 binds to TANK, TBK1 and IKK $\epsilon$  which then are activated and able to phosphorylate IRF-3 directly. The mechanism for how this happens is not yet fully understood. When IRF-3 is activated it can translocate into the nucleus and bind to the IFN- $\beta$  promoter. Co-factors such as CBP/p300 and RNA polymerase II assemble and stimulate transcription. The IFN- $\beta$  promoter has three known binding sites: for ATF-2/c-Jun (PRD IV), IRF-3 (PRD I/III) and NF- $\kappa$ B (PRD II). The figure is borrowed from Randall et al (32).

Below follows a closer look at signaling components that lead to activation of transcription factors in RIG-I- and MDA5-dependent signaling.

### **Mitochondrial antiviral signaling (MAVS)**

The adaptor protein mitochondrial antiviral signaling (MAVS) is also known as IPS1, VISA and CARDIF. MAVS contain CARD and associate with RIG-I or MDA-5 upon their activation, leading to downstream signaling kinases that lead to activation of NF- $\kappa$ B and IRF that again leads to transcription of genes involved in antiviral and pro-inflammatory responses (28), see Figure 1.10. The virus initiated innate immune response also relies on the RIG-I and MDA5-dependent pathway in fibroblasts and

other cell types. MAVS triggers NF- $\kappa$ B activation through TRAF6 and the IKK- $\alpha$ - $\beta$  complex or IRF3 activation through TRAF3 and the TBK1 and IKKe-kinase complexes in response to viral infection (33).

#### ***TNFR-associated factor 6 (TRAF6)***

The tumor necrosis factor receptor (TNF-R) associated factor (TRAF) family consist of intracellular proteins that bind to the cytoplasmic regions of receptors. In addition to the adaptor function, most TRAF function as E3 ubiquitin ligases involved to activate downstream proteins in signaling pathways. Signaling pathways that are TRAF-dependent usually lead to activation of NF- $\kappa$ B, mitogen-activated protein kinases (MAPKs) or IRFs (34). In RLR-signaling, dimerization of MAVS leads to recruitment of TRAFs, including TRAF6. These assemble at the mitochondrial outer membrane, a site for signaling complexes to assemble (34).

TRAF6 ubiquitinates NEMO and proteins that activates TAK1 and further leads to phosphorylation of the I $\kappa$ B kinase (IKK) complex. When IKK is activated, it phosphorylates the inhibitory I $\kappa$ B subunit of the NF- $\kappa$ B. NF- $\kappa$ B is in this way released and enter the nucleus where it activates gene expression (23).

#### ***TANK-binding kinase 1 (TBK1)***

TANK-binding kinase 1 (TBK1) and IRF3 are crucial in the IFN- $\alpha$ - $\beta$  induction, and therefore the cell has evolved many mechanisms to control the activation of TBK1/IRF3. TBK1 can be phosphorylated at multiple sites. The phosphorylation at S172 seems to be necessary to activate TBK1. IRF3 is one of the major downstream substrates of TBK1 in inducing IFN expression. TBK1 mediates phosphorylation of IRF3, and in this way promotes dimerization, nuclear translocation and involvement in transcription. Regulation of TBK1/IRF3 phosphorylation by kinases and phosphatases may determine the IFN induction, both in magnitude and duration, upon viral infection (35).

### 1.6.1 Transcription factors

The IFN- $\beta$  promoter has, as shown in Figure 7, binding sites for the transcription factors NF- $\kappa$ B, IRF3 and ATF2. The NF- $\kappa$ B and IRF transcription factor families are simultaneously activated in response to viral infection.

#### ***Nuclear factor kappa-light-chain-enhancer of activated B cells (NF- $\kappa$ B)***

NF- $\kappa$ B activation following viral infections involves phosphorylation and subsequent polyubiquitylation of I $\kappa$ B $\alpha$  through the IKK-dependent pathway. A number of inflammatory and immunoregulatory genes that are induced by paramyxovirus require NF- $\kappa$ B to be transcribed (36, 37). Optimal NF- $\kappa$ B activity also requires phosphorylation of the NF- $\kappa$ B protein p65 (33). RIG-I and MDA5 dependent activation of NF- $\kappa$ B in response to viral infection is illustrated in Figure 1.10.

#### ***Interferon Regulatory Factor 3 (IRF3)***

In contrast to NF- $\kappa$ B activation, IRF3 activation in the cytoplasm occurs directly through their C terminal phosphorylation by two kinases, TRAF family member-associated NF- $\kappa$ B activator (TANK)-binding kinase 1 (TBK1), and IKK-e (33). Transcription factors of the IRF family are essential players in virus-triggered type I IFN-gene expression (38). IRF3 is known to induce transcription of antiviral genes, and in the absence of IRF3 the cells will become persistently infected and keep producing new infectious virions. IRF3 is expressed in all cell types, however at different levels. TBK1/IKKe are protein kinases that are responsible for mediating IRF3-phosphorylation. When IRF3 is activated by RIG-I signaling it becomes polyubiquitinated and degraded by the proteasome. The TLR pathway and the SeV-activated RIG-I pathway are partially overlapping (39, 40). An illustration of the RIG-I-dependent activation of IRF3 is found in Figure 1.11.

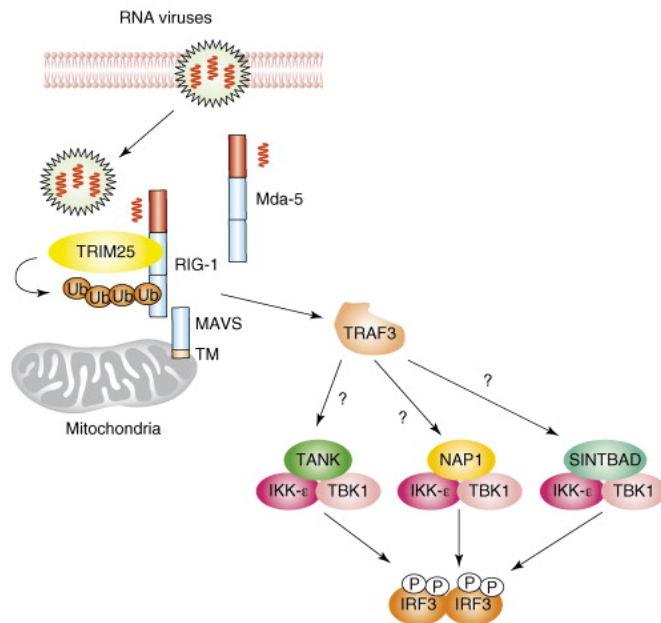


**Figure 1.11. RIG-I-dependent IRF3 activation.** RNA from viruses activate RIG-I through binding to their DExD/H box RNA helicases (the red boxes). The CARD domains on these receptors (the light blue boxes) are polyubiquitylated by the E3 ubiquitin ligase TRIM25 which is believed to lead to recruitment of the mitochondrial adaptor MAVS. MAVS signals to TRAF3 which activates IRF3 through TBK1 and IKK $\epsilon$  signaling and phosphorylation. TANK is necessary for TBK1 and IKK $\epsilon$  assembly. The figure is modified from Chau *et al* (33).

### Activating transcription factor 2 (ATF2)

ATF2 is a member of the leucine zipper family of DNA binding proteins and is found in the lung among other tissues. Upon antigen stimulation ATF2 can be activated through phosphorylation at amino acids Thr69 and Thr71 by upstream signaling factors p38 and JNK. ATF2 dimerizes with the transcription factor c-jun, which localizes the complex in the nucleus and makes where it works as a transcription activator of cytokines, pro-inflammatory genes and genes involved in apoptosis (41, 42).

### 1.6.2 IFN- $\beta$ and the antiviral state

IFNs are secreted cytokines that have antiviral features. They can be divided into type I, II and III, based on the amino acid sequence. IFN- $\alpha$  and - $\beta$  are produced in response to viral infections (32). Instead of referring to type I IFN, IFN- $\beta$  will be used as IFN- $\beta$  has been used in the experiments of this thesis. The virus-infected cell will secrete IFN- $\beta$  and the IFN- $\beta$  will bind to the IFN- $\alpha$ - $\beta$  receptor (IFNAR) on neighboring cells, and itself. By binding to the receptor it will activate the intracellular signaling

pathway that will lead to up-regulation of IFN- $\beta$ -responsive genes, which have direct or indirect antiviral effect. Viruses will not be able to replicate in an efficient manner in cells that are in the antiviral state (32).

Many different types of epithelial cells express IFNs. Transcription factors NF- $\kappa$ B, ATF2 and IRFs are involved in the regulation of IFN synthesis, as illustrated in Figure 1.10. When IFN- $\beta$  binds to its receptor, signaling to the nucleus goes through the Jak-STAT pathway, as illustrated in Figure 1.12. When STAT1/2 is activated it forms a complex with IRF-9 that trans-locates to the nucleus where it induces IFN-stimulated genes (ISGs) to produce antiviral proteins. The antiviral proteins include protein kinase R (PKR), 2'5'-oligoadenylate synthetase (2'5'-OAS), myxovirus resistance protein (Mx proteins) and these inhibit viral replication (24).

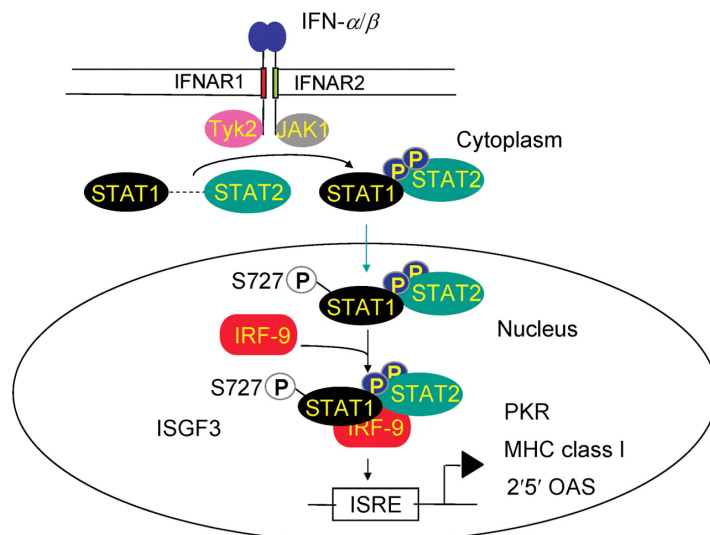


**Figure 1.12. Signalling pathway activated by IFN- $\alpha/\beta$ .** When IFN- $\alpha/\beta$  bind to the type I IFN receptor (IFNAR), the receptor-associated tyrosine kinases JAK1 and Tyk2 are activated and phosphorylate STAT1 on tyrosine 701 (Y701) and STAT2 on tyrosine 690 (Y690). When STAT1 and STAT2 are phosphorylated they interact with each other and the STAT1-STAT2 heterodimer translocates into the nucleus where it interacts with IRF-9, a DNA-binding protein. The IRF-9-STAT1-STAT2-heterotrimer, or the ISGF3 complex, binds to a sequence motif called the IFN-stimulated response element (ISRE), which leads to transcriptional activity. To be activated properly, STAT1 also requires phosphorylation of serine 727 (S727). The figure is borrowed from Randall *et al* (32).

Activation of PKR leads to apoptosis. 2'5'-OAS is involved in degradation of viral through cleavage of ssRNA. The Mx proteins reduce virus replication by impairing intracellular transport of viral proteins (24).

## 1.7 Thymic stromal lymphopoietin (TSLP)

Thymic stromal lymphopoietin (TSLP) was first identified in supernatants isolated from the mouse thymic stromal cell line Z210R.1 (43). Through characterization and cloning, it was identified as a short-chain four helix-bundle type I cytokine (44). A human homologue TSLP was identified through database search methods (45, 46).

### 1.7.1 Biology of TSLP

TSLP is an epithelial cell-derived IL-7-like cytokine. Induced by pathogens, it contributes to mucosal immunity and promotes inflammatory responses by Th1 as well as Th2 (47). TSLP is an important factor in the pathogenesis of asthma. Higher concentrations of TSLP is found in the lungs of asthmatics and this correlate with the increased Th2 responses and the severity of the disease (48).






There are two isoforms of the human TSLP. The translational products of the two isoforms are functionally different (49). Short form TSLP (sfTSLP) is constitutively expressed both at mRNA and protein level in cells of the oral mucosa and skin, the salivary glands and is released in the saliva. The sfTSLP have antimicrobial features and is not regulated in the same way as the long form TSLP (lfTSLP). The TSLP isoforms show opposite immune functions. sfTSLP is anti-inflammatory and expressed during steady-state conditions, while the lfTSLP is pro-inflammatory and solely expressed during inflammation (50). The TSLP receptor complex is a heterodimer consisting of the IL-7-receptor  $\alpha$  chain (IL-7R $\alpha$ ) and a TSLP binding chain called the TSLP receptor (TSLPR) (51).

### 1.7.2 TSLP and asthma

Under normal physiological circumstances, TSLP seems to be involved in CD4<sup>+</sup> T cell homeostasis in the peripheral mucosa associated lymphoid tissues. It is not fully understood which signals that control the steady-state TSLP production. In inflammatory settings, such as during viral infection, TSLP expression in epithelial cells is increased in response to inflammation. The local increase of TSLP affect and enhance the DC maturation and activation and stimulates resident macrophages. TSLP-activated DCs migrate to the lymph nodes and induce the CD4<sup>+</sup> T cells to produce Th2 inflammatory cytokines (52).

Immune cells, including eosinophils, fibroblasts neutrophils and mast cells, is attracted to the site of inflammation as a result of the chemokine production and is contributing to the following exacerbated pathology (51). An overview of the sources and direct and indirect targets of TSLP in asthma is found in Figure 1.13. TSLP has been linked to the initiation of allergic airway inflammation. TSLP alone is not sufficient in causing full airway inflammatory disease, however it induces innate responses that include mucus overproduction in the lung. To develop full airway inflammation foreign antigens as well as CD4+T cells are required. TSLP is a factor in the lung that generate Th2 allergic responses to the foreign antigen (52).

TSLP is showed to activate DCs that subsequently lead to a Th2-driven T cell response. TSLP is therefore an important epithelial cytokine that trigger DC-mediated allergic inflammation (6).

Cellular sources of TSLP	Cellular targets of TSLP	Actions
Epithelial Cells 	Dendritic Cells	↑ Co-stimulatory molecules, Th2 priming
Fibroblasts 	CD4+ T Cells	↑ Proliferation, Th2 differentiation
Dendritic Cells 	Mast Cells	↑ Cytokine production
	Eosinophils	↑ Extracellular trap formation, cytokine production
Basophils 	Basophils	↑ Expansion, cytokine production
	Treg Cells	↓ Suppressive activity
Mast Cells 	Lung natural helper innate type 2 cells	↑ Th2 cytokine production (with IL-33)

**Figure 1.13. Sources and targets of TSLP during asthma.** The overview show the TSLP cellular sources and targets of TSLP in asthma/lung inflammation, and the actions of TSLP on these targets. The figure is borrowed from West *et al* (48).

TSLP released by primary epithelial cells in response to relevant stimuli, activate cells of the innate immune system and induce them to producing high levels of Th2 pro-inflammatory cytokines (53). It is indicated that TSLP induction is occurring early during the viral infection cycle, as molecules sensing viral replication in the cytosol of AECs are activated (47). It has recently been shown that TSLP is expressed in response to RSV in airway epithelial cells and that the regulation is dependent on

RIG-I (54). However, a lot is still unknown regarding the TSLP induction pathway in response to hMPV and other respiratory viruses.



## 2 Aims of the Study

High prevalence of childhood asthma is observed and the prevalence is predicted to increase in the future. Viral respiratory tract infections have been linked to asthma. hMPV is a recently discovered virus recognized as a clinically important respiratory pathogen. TSLP is an IL-7-like cytokine that is expressed mainly by epithelial cells at barrier surfaces and induce immune responses by targeting immune cells that produce Th2 cytokines. How production of TSLP is regulated in airway epithelial cells during respiratory virus infection is poorly described. The hypothesis is that hMPV infection triggers TSLP expression in airway cells. Elevated TSLP-directed inflammation in the airways may contribute to respiratory disease and create a Th2-permissive environment that attribute to the development of asthma.

The objectives of the study were as follows:

1. Cultivate hMPV subgroup A1 and produce stocks for use in cell culture experiments
2. Characterize the IFN- $\beta$  response and activation of related transcription factors upon hMPV A1 infection in airway epithelial cell line A549 and lung fibroblast cell line WI-38
3. Assess the kinetics of TSLP mRNA induction in airway epithelial cell line A549 and lung fibroblast cell line WI-38 upon hMPV A1 infection
4. Study PRR signaling components involved in TSLP mRNA induction in airway epithelial cell line A549 and fibroblast cell line WI-38 upon hMPV A1 infection



### 3 Methodology

Below follows a description of the methods that were used for this thesis. A complete list of instruments and software used is found in Appendix A.

#### 3.1 Reagents used

Below, in Table 3.1, is a list of reagents used in the experiments conducted in this master thesis. The reagents are arranged according to experiment.

**Table 3.1. Reagents used.** Reagents used, manufacturer and catalog number, arranged according to experiment.

Product	Manufacturer
<b>Cell culture</b>	
DMEM	Bio Whittaker <sup>®</sup> , Lonza
DPBS	Sigma <sup>®</sup> life sciences, Sigma Aldrich
FBS, Lot. nr: 41F3715K	Gibco <sup>®</sup>
Gentamycin	Gibco <sup>®</sup>
Glutamine (L-glut)	Sigma Aldrich
OptiMem	Gibco <sup>®</sup> , life technologies
Pencillin-Streptomycin Solution	ATCC <sup>®</sup>
PBS	Bio Whittaker <sup>®</sup> , Lonza
RPMI	Gibco <sup>®</sup> , life technologies
Trypsin EDTA	Lonza
<b>siRNA transfection</b>	
Lipofectamine <sup>®</sup> RNAiMAX	Thermo Fisher Scientific
<b>RNA isolation and cDNA synthesis</b>	
β-ME (2-mercaptoethanol)	Sigma Aldrich
Ethanol (96%)	VWR
RNeasy kit	Quiagen
qScript <sup>™</sup> cDNA synthesis kit	Quanta Biosciences
<b>PCR</b>	
Perfecta SYBR Green FastMix, ROX <sup>™</sup>	Quanta Biosciences
RNase free water	VWR
<b>Virus isolation and titration assay</b>	
Human metapneumovirus direct immunofluorescence Assay (DFA)	Light diagnostics <sup>™</sup> EMD Millipore Corporation
Sendai Virus (SeV)	Cantell strain, Charles River Laboratories, Wilmington, MA
Sucrose	Sigma Aldrich

Syringe-driven Filter Unit, 0.8mm	Millex
Trypsin	Difco
Tween20/Sodium Azide	Light diagnostics EMD, Milipore Corporation

#### Western Blot

iBlot <sup>®</sup> Gel Transfer stacks Nitrocellulose, Mini	NOVEX by life technologies
TBS	
TBST	In-house
	In-house

## 3.2 Cell cultivation

### 3.2.1 Cell lines

#### *LLC-MK<sub>2</sub>*

The LLC-MK<sub>2</sub> cell line is a monkey kidney epithelial cell line known to be susceptible for and support growth of several different viruses (55). LLC-MK<sub>2</sub> has been reported to be the most successful cell line for hMPV cultivation (56). LLC-MK<sub>2</sub> cell line was obtained from American Type Culture Collection (ATCC®) number CCL-7<sup>TM</sup>. LLC-MK<sub>2</sub> cells were cultured in Opti-MEM with 5% fetal bovine serum (FBS), 20ug/mL gentamycin and 200mM glutamine. LLC-MK<sub>2</sub> was incubated in 5% CO<sub>2</sub> at 37°C. These cells were maintained and sub-cultivated by the research group engineer. These cells were used for the growth curve experiment as well as hMPV propagation and titration assay.

#### *A549*

A549 is a lung carcinoma epithelial cell line. The cells were maintained in RPMI 10% supplemented with 10% FBS, 20ug/mL gentamycin and 200mM glutamine. The cells were incubated in 5% CO<sub>2</sub> at 37°C. The cells were seeded in T75 flasks and split when they reached 75-80% confluency. These cells were used to study hMPV-mediated responses in airway epithelia, including kinetic studies, siRNA-mediated knockdown of signaling components and phosphorylation status of transcription factors.

#### *WI-38*

The WI-38 cells are lung fibroblasts. The cells were maintained in DMEM supplemented with 10% FBS, 100u/mL penicillin and 100ug/mL streptomycin. The cells were incubated in 5% CO<sub>2</sub> at 37°C. The cells were seeded in T75 flasks and split

when they reached 75-80% confluency. These cells were used to study hMPV-mediated responses in airway epithelia, including kinetic studies, siRNA-mediated knockdown of signaling components, phosphorylation status of transcription factors and confocal study.

### **HEK-293**

HEK-293 is an embryonic kidney cell line. The cells were maintained in DMEM supplemented with 10% FBS, 200mM glutamine and 20ug/mL gentamicin. The cells were incubated at 8% CO<sub>2</sub> at 37°C. These cells were maintained and sub-cultivated by the research group engineer. The cells were used to test induction of IFN-β and for controls used for Western blot.

### **3.2.2 Subcultivation of cell lines**

The cells were split when they reached 75-80% confluence. Medium was removed and cells were washed in 8mL PBS 37°C to remove dead cells. The cells were then trypsinated with 1mL TE at 37°C for 5 minutes. The trypsination step is to detach the cells from the flask surface. 5mL medium was then added to inhibit the trypsin, and the total 6mL cell supernatant/medium was transferred to a 15mL tube and centrifuged (5810R, Eppendorf) for 5 minutes, 1500rpm at 20°C. The supernatant was removed and the cell pellet was re-suspended in 2mL medium. To count cells, the Z2 Coulter<sup>®</sup> Particle Count and Size Analyzer (Bekcman Coulter) was used. 20μL of suspended cells were mixed in isoton. The function of the isoton is to dilute the cells in a neutral liquid that keeps the cells intact and don't cause lysis. Programme C (T<sub>1</sub>=10uM, T<sub>u</sub>=19uM) was used to count all cell lines.

### **3.2.3 Thawing of cells**

All cell stocks were kept in liquid nitrogen tanks and were thawed in water (37°C) and seeded in T75 flasks. The cells were kept in medium containing the cryoprotective agent dimethylsulfoxide (DMSO) when they were frozen, this to reduce the freezing point of the medium as well as to slow the cooling rate and thus reduce the risk of ice crystal formation which can cause damage to the cells (57). The medium was changed the next day of the thawing, as the DMSO is toxic for the cells in above 4°C (58).

### **3.3 Virus propagation**

The hMPV virus strain hMPV/NL/1/00 was received from Bernadette van den Hoogen at the Department of Virology, Erasmus MC, Rotterdam. This strain represents the hMPV subgroup A1.

hMPV was propagated in serial propagation using LLC-MK<sub>2</sub> cells. LLC-MK<sub>2</sub> cells are known to be the most successful cell line for hMPV cultivation (56). On day one 2M LLC-MK<sub>2</sub> cells were seeded in a T175 flask with 30mL medium. When the cells reached full confluence, at around day four, trypsin containing growth medium (TCGM) was added and the cells were infected with hMPV at MOI 0.01. The hMPV fusion protein requires cleavage of proteases to be activated and trypsin is therefore added to medium, to enhance the viral replication process. Four days after infection, a 5mL sample of the supernatant was collected. The rest of the medium was removed and replaced with fresh TCGM. The collected supernatant was used to infect a new flask with fully confluent LLC-MK<sub>2</sub> cells, generation two. The flask was incubated for 1 hour before the virus sample was removed and replaced with 30mL fresh TCGM. The serial propagation was continued for two more generations as illustrated in Figure 3.1. When the cytopathic effect (CPE) was considered substantial: CPE of 75-90%, the flasks were freezed and stored at -80°C until isolation. This was around day 8 or 9. It is important that the CPE doesn't exceed 90% because live cells are necessary for the virus to be able to replicate further.

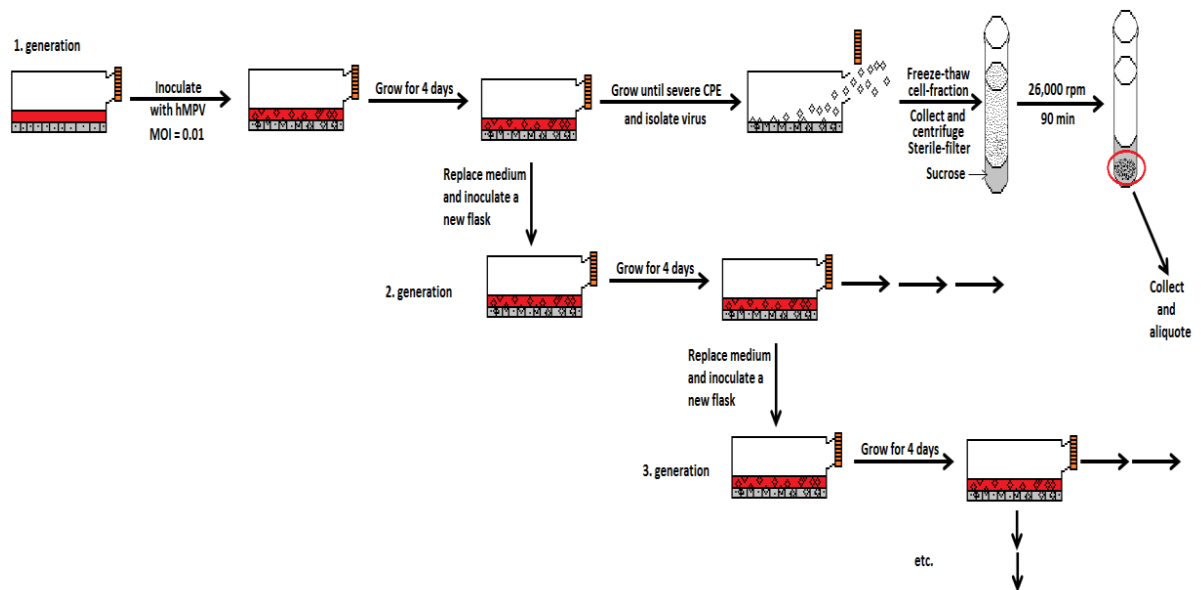


**Figure 3.1. Serial propagation.** HMPV was propagated using serial propagation. A flask with confluent LLC-MK2 cells were infected with hMPV at MOI 0,01 and incubated for four days. Supernatant from the infected flask was then transferred to a new flask, and this was continued for in total four generations. At day 8 or 9 the CPE were considered to be 75-90% and the flasks were frozen and the virus was isolated. The isolation steps are explained in section 3.4. The figure is allowed used by the author Jostein Malmo (unpublished).

### 3.4 Virus isolation

At the day of isolation, the virus flasks were thawed, the cells scraped and supernatant collected in tubes. The tubes were centrifuged at 1500rpm for 5 minutes at 4°C. To remove any cell residues the supernatant was sterile filtered using 0.8mm syringe-driven filter units (Millex). Six polymer tubes were sterilized in 70% ethanol before adding 2mL 20% sucrose. The filtered virus supernatant was carefully added on top of the sucrose, creating two layers. The tubes were then centrifuged in an ultracentrifuge (Sorvall Discovery 100SE, Hitachi) at 26 000rpm for two hours at 4°C. After centrifugation, the supernatant was removed and the pellet was re-suspended in 3mL of TCGM. The virus solution was aliquoted into tubes of 1mL and snap frozen in liquid nitrogen. The virus was stored at -80°C.

### 3.5 Titration assay

After isolation of virus, a titration assay was performed to find the titer for the specific stock that was isolated. The assay is based on plaque forming units (PFUs), which gives a number for how many live infectious particles present in the stock.

### Protocol

The titration assay was performed using LLC-MK<sub>2</sub> cells that were seeded in a 96 well plate with 5k cells/well. Four days after seeding the cells were infected with hMPV diluted in TCGM. A tenfold serial dilution as illustrated in Figure 3.2 was made. The dilution series included eight dilutions, and four parallels were infected for each dilution. Eight Eppendorf tubes were prepared, each with 900μL TCGM. 100μL of the virus stock was added to the first tube to obtain a 10<sup>-1</sup> dilution, and mixed. 100μL of the mixed 10<sup>-1</sup> solution was transferred to the next tube to obtain a 10<sup>-2</sup> dilution, and this was repeated till the last tube with a dilution of 10<sup>-8</sup>. The LLC-MK<sub>2</sub> cells were washed with PBS before 200μL of the appropriate virus dilution was added to their respective wells. The cells were incubated at 37°C with 5% CO<sub>2</sub> for four days. The cells were then washed with 200μL warm PBS and fixed with 80% Acetone for 10 minutes at -20°C. The acetone was replaced with 30μL direct fluorescent antibody (DFA), following incubation for 15 minutes at 37°C. The DFA monoclonal antibodies are labeled with fluorescein isothiocyanate (FITC), a green fluorescence that bind to cells infected with hMPV. Cells that were uninfected stained red due to the Evans blue. The DFA was then removed and the cells were washed with room-tempered PBS supplemented with Tween20. 100μL PBS was in the end added to the cells. A fluorescence microscope was used to determine infected wells, the 50% Tissue Culture Infective Dose per mL (TCID<sub>50</sub>/mL) and further the Focus Forming Unit per mL (FFU/mL) of the virus stock was calculated.

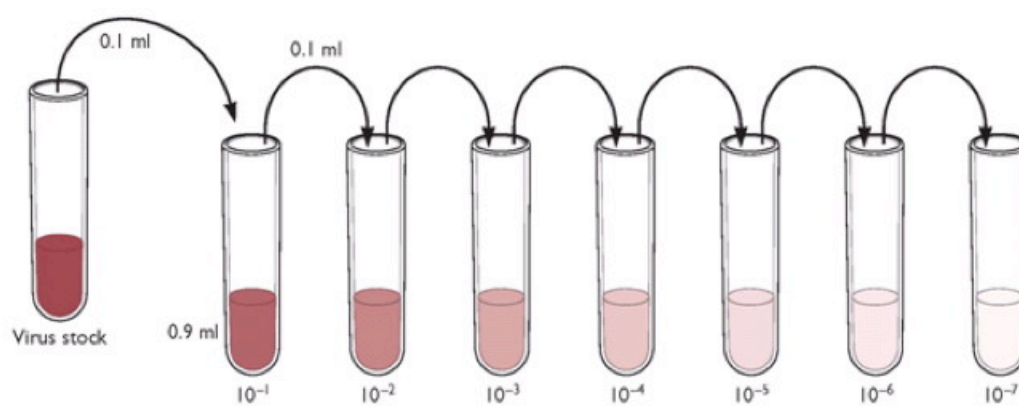


**Figure 3.2. 10-fold serial dilution.** A serial dilution of hMPV was made to infect the cells in the titration assay. 900μL TCGM was added to each tube. 100μL of the virus stock was added to the first tube, mixed, and 100μL was then transferred to the next tube to obtain a 10-fold serial dilution, with dilutions 10<sup>-1</sup> till 10<sup>-8</sup>. The figure is modified from Racaniello (59).



Focus forming assay is one method to measure the concentration of viruses in a sample. Confluent cells are infected with virus for a chosen time frame, before the cells are permeabilized and incubated with a fluorescent antibody against the virus. The cells are examined using a microscope. The TCID<sub>50</sub>-principle is based on the number of plaques that are infected at a specific dilution. At low dilutions, all wells will be infected while at high dilutions none of the wells will be infected. Wells with one fluorescent foci was considered positive. The dilution where 50% of the wells were considered positive was used, and the virus stock titer (expressed as FFU/mL) was calculated (59). To calculate the FFU/mL, Formula 3.1 was used. The mean of the plaques of the four parallels of the dilution was calculated (plaque mean).

$$\text{FFU/mL} = (\text{plaque mean} / \text{dilution factor}) / 0,2$$

**Formula 3.1. Calculation of FFU/mL.** This formula was used to calculate the FFU/mL of a virus stock from the titration assay. The plaque mean was calculated from the parallels of the dilution with at least two positive wells. The dilution factor is  $10^{-x}$ .

The FFU/mL was used to calculate the volume of virus that was needed to infect a particular number of cells at a particular MOI. The formula that was used to calculate this is shown in Formula 3.2.

$$\text{a) MOI} = ((\text{FFU})/\text{mL})/(\text{Number of cells}) \times V$$

$$\text{b) } V = (\text{MOI} \times \text{number of cells})/(\text{FFU}/\text{mL})$$

$$\text{c) } V = (\text{MOI } 1 \times 100\text{k cells})/(700\text{k FFU}/\text{mL}) = (100\text{k})/(700\text{k}) = 142,8\mu\text{L virus.}$$

**Formula 3.2. Calculating MOI.** **a)** The formula for calculating MOI. **b)** Algebraic alteration of the formula given in a) gives the formula for calculating the volume (V) of virus that is needed to infect a particular number of cells at a particular MOI. **c)** Example of using the formula to calculate the volume of virus when using a virus stock with FFU/mL = 700k in an experiment with 100k cells per well, and wishing to infect at MOI 1.

### **3.6 DI+/- determination assay**

To determine whether virus stocks were positive (+) or negative (-) of DI particles, a DI+/- estimation assay was performed. The assay was performed in HEK-293 cells. On day one, 30k cells were seeded in 48 well plates in DMEM. On day two, the medium was removed and OptiMem 2% was added. The cells were infected with hMPV at MOI 1. The medium was changed back to DMEM after two hours. The cells were lysed with 350 $\mu$ L 1% LB containing  $\beta$ -ME after 18 hours. RNA was isolated as explained in 3.14 and cDNA synthesized as explained in 3.16. qRT-PCR was then performed, using IFN- $\beta$  primers as listed in Table 3.2.

### **3.8 Replication curve**

To determine the peak time point of hMPV replication and thus the ultimate day for hMPV isolation, a replication curve experiment was performed.

Two flasks with 2M LLC-MK<sub>2</sub> cells were seeded. One was used as a “cell bank” to seed plates for the titration assay while the other was infected with hMPV. At confluence the virus flask was infected with hMPV at MOI 0.01. The cells were incubated at 5% CO<sub>2</sub> 37°C in 5mL TCGM for one hour. The TCGM was then replaced with 30mL fresh TCGM. The TCGM was replaced every fourth day. A titration assay was performed for days 0, 2, 4, 6, 7, 8, 9, 10, 12 and 14 to determine the titer peak time point, the highest FFU/mL. At those specific days 400 $\mu$ L of the supernatant was collected and centrifuged for 5 minute at 20°C, 1500rpm. 175 $\mu$ L of the supernatant was then lysed with 175 $\mu$ L RLT lysis buffer with 1:100  $\beta$ -ME and stored at -80°C. qRT-PCR was eventually performed on all samples using primers for the hMPV N-gene, found in Table 3.2. 100 $\mu$ L of the supernatant was used in titration assay as explained in section 3.5.

### **3.9 Infection**

Prior to infection, all cell lines except HEK-293 were washed with PBS. The appropriate volume Opti-MEM supplemented with 2% FBS and antibiotics was then added according to well plate. Which antibiotics used for the specific cell lines is found in section 3.2.1. In the case of HEK experiments, the medium was removed after two hours of infection as the HEK cells tolerate being maintained in the OptiMem medium poorly. The A549 and WI-38 cells were kept in the infection

medium till lysis to increase infection rate. MOI tests were performed by other members of the research group and MOI 1 was considered the most appropriate concentration.

### **3.10 Lysis**

Cells were lysed with lysis buffer (LB) according to which analysis methods that were further used. Cells used for qRT-PCR were lysed with RLT LB with 1:100  $\beta$ -ME (10 $\mu$ L/1mL RLT). 350 $\mu$ L lysis buffer was used for lysis per well. Cells used for Western blot were lysed in 150 $\mu$ L 1% LB containing phosphate inhibitors NaOvan (200mM),  $\beta$ -glycerolphosphate (2M), NaF (1M), PMSF (0,3M), Pepstatin (1mM), Leupeptin (5mg/mL). The 1% LB consist of Tris (50mM, pH 7.5), NaCl (150mM), Glycerol, Triton X-100 (1%), EDTA (2mM) and H<sub>2</sub>O.

### **3.11 Time course**

Time course experiments were conducted using both A549 and WI-38 cell lines. Both mRNA and protein levels were analyzed.

#### ***Protocol for qRT-PCR***

50k WI-38 cells were seeded in 24 well plates. The next day cells were washed with PBS and OptiMem 2% FBS was added. The cells were then infected with hMPV at MOI 1. The cells were lysed in 350 $\mu$ L LB supplemented with  $\beta$ -ME.

#### ***Protocol for SDS-PAGE and Western Blot***

200k WI-38 cells were seeded in 2mL medium in 6-well plates or 100k cells in 1mL medium in 12-well plates. The next day cells were washed with PBS and OptiMem 2% FBS was added. The cells were then infected with hMPV at either MOI 1 or MOI 0.5. MOI 0.5 was considered to be OK for potent stocks, or was used to spare virus. The cells were lysed in 150 $\mu$ L 1% LB supplemented with phosphatase and protease inhibitors, concentrations are found in section 3.10. Lysates were put on ice and stored at -20°C. The SDS PAGE and Western blot protocols were followed as explained in 3.18.

### 3.12 siRNA Knockdown

Knockdown experiments were performed to determine the role of signaling components involved in the regulation of hMPV-triggered TSLP induction. As control siAllstar and no siRNA medium and hMPV infected cells were used. Both A549 and WI-38 cell lines were used for these experiments.

To silence genes that are suspected to be involved in the regulation of TSLP upon hMPV infection, a RNA interference (RNAi) method was used. Knockdown using small interfering RNA (siRNA) was performed. siRNA molecules are double stranded RNA (dsRNA) molecules that are around 20-25 basepairs (bp) long with a 2 nucleotide 3' overhang. These overhangs are recognized by the enzymatic machinery of RNAi, and result in degradation of target messenger RNA (mRNA) (60). The siRNA binds to the protein complex Dicer in the cell, which cuts the siRNA into fragments. The antisense strand becomes connected to the RNA-induced Silencing Complex (RISC). The strand directs the RISC to the mRNA, which results in basepairing. The mRNA is further cleaved. An illustration of the principle is found in Figure 3.3.

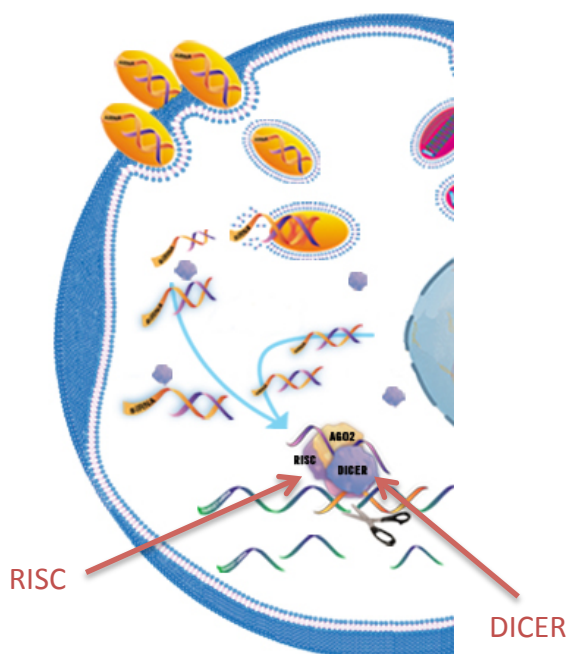


**Figure 3.3. The siRNA knockdown principle.** The siRNA molecules are delivered into the cell by the Lipofectamine RNAiMAX transfection reagent (yellow). The siRNA molecules are double stranded RNA with a two nucleotide 3' overhang that are recognized by the enzymatic machinery of RNAi and result in degradation of the target mRNA. The siRNA binds to the protein complex DICER which cuts the siRNA into fragments. The antisense strand becomes connected with the RNA-inducing Silencing Complex (RISC), and directs the RISC to the mRNA which results in basepairing. The mRNA is further cleaved, resulting in knockdown. The figure is modified from Mirus Bio (61).

#### ***Protocol for knockdown experiments, qRT-PCR***

SiRNA at a final concentration of 10nM was mixed with OptiMem without serum and antibiotics. The medium was prepared without antibiotics and serum as these components can interfere with the RNAiMAX complex and thus disrupt the transfection. RNAiMAX diluted 1:10 in OptiMem was added to the siRNA, and incubated at room temperature (RT) for 20 minutes. A complete list of the siRNA sequences that were used is found in Table 3.2. Cells were seeded in complete medium without antibiotics. The cells were incubated over night (ON) and the medium was replaced with fresh medium. The cells were incubated at 37°C for 24 hours. The cells were then infected at MOI 1. OptiMem supplemented with 2% FBS was used during the infection. 18 hours p.i., the cells were lysed in 350µL buffer RLT. RNA was isolated as explained in 3.14, cDNA synthesized as explained in 3.18, and qRT-PCR was performed as explained in 3.16. 18h infection was chosen, as this was the time point where we expected the highest induction of lftSLP, based on the time course experiments that were performed.

#### ***Protocol for test siRNA, Western Blot***

1µL siRNA at a final concentration of 10µM was mixed with 200µL OptiMem without serum or antibiotics, and 2µL RNAiMAX and added to a well of a 12-well plate. The mix was incubated at RT for 20 minutes. Cells were seeded in complete medium without antibiotics. The cells were incubated ON and the medium was replaced with fresh medium. The cells were then incubated at 37°C for 24 hours. The cells were lysed in 150µL 1% LB supplemented with phosphatase and protease inhibitors found in Section 3.10. Western Blot was performed as explained in 3.17.

**Table 3.2. siRNA sequences.** A complete list of siRNA sequences used for siRNA-mediated knockdown experiments. Concentrations of 10 $\mu$ M was used.

siRNA	ID#	Manufacturer
Allstar	1027280	Quiagen
RIG-I	sc-61480	Santa Cruz
MDA5	sc-61010	Santa Cruz
LGP2	sc-93967	Santa Cruz
MAVS	sc-75755	Santa Cruz
TRAF6	004712-00	Thermo Scientific
TBK1	S761	Ambion
NLRP3	S41554	Ambion
Caspase1	S2408	Ambion

### 3.13 Knockdown pathway using kinase inhibitors

These experiments were performed to observe the effect of hMPV-triggered TSLP induction by inhibiting TANK-binding kinase 1 (TBK1) kinases. Amlexanox is an inhibitor of TBK1 and IKK $\epsilon$  (62). BX795 inhibits the catalytic activity of TBK1/IKK $\epsilon$  by blocking their phosphorylation (63).

#### *Protocol*

On day one 30k cells were seeded in 250 $\mu$ L in 48-well plates. On day two, kinase inhibitors diluted in OptiMem 2% were added to the cells. Kinase inhibitors BX795 and Amlexanox were used. Concentrations 2 $\mu$ M and 4 $\mu$ M were used for both inhibitors. After 30 minutes incubation in RT, the cells were infected. On day three, the cells were lysed in 350 $\mu$ L LB RLT with  $\beta$ -ME. The lysates were stored at -80 $^{\circ}$ C. RNA was isolated and qRT-PCR was performed as explained in section 3.16.

### 3.14 RNA isolation

RNA isolation was performed following the Qiagen RNeasy kit instructions. 350µL 70% EtOH was added to the samples and transferred to spin columns before centrifuged for 15 seconds at 10,000rpm. Following wash with RW1 and buffer RPE buffers, RNA was collected in 30µL RNase-free water. NanoDrop was used to measure the RNA concentration and purity. For 260/280 a ratio around 2.0 is considered pure while significantly lower ratio may indicate the presence of protein or other contaminants that absorb strongly near 280nm. For 260/230 a ratio around 2.0-2.2 was considered pure (57). RNA was stored at -80°C. Following isolation the RNA was used to synthesize cDNA by using the reverse transcriptase method.

### 3.15 cDNA synthesis/reverse transcriptase

RNA was transcribed into cDNA using TC-512 (TECHNE) machine, program Nu Quanta. The qScript™ cDNA synthesis kit was used. 4µL Reaction Mix (RM) and 1µL Reverse Transcriptase (RTr) was used per well. For each well, 10µL sample, 5µL water, 4µL RM and 1µL RTr was used, making to total volume of each well 20µL. Two controls were used, -RNA and -RT. The -RNA control contained 4µL RM, 1µL RTr and 10µL water while the -RT control contained 4µL RM, 6µL water plus 5µL of the “Medium sample” RNA. The Nu Quanta program steps are found in Table 3.3. cDNA was stored at 4°C. The cDNA was further used for qRT-PCR.

**Table 3.3. cDNA synthesis cycles.** The thermal cycles of the cDNA synthesis using the Nu Quanta program of the TC-512 TECHNE machine.

Step	Temperature	Time (minutes)
1	22°C	5
2	42°C	30
3	85°C	5

### 3.16 qRT-PCR

qRT-PCR was used to determine the expression of specific genes upon hMPV A1 infection in cell lines HEK, A549 and WI-38.

#### *The polymerase chain reaction (PCR)*

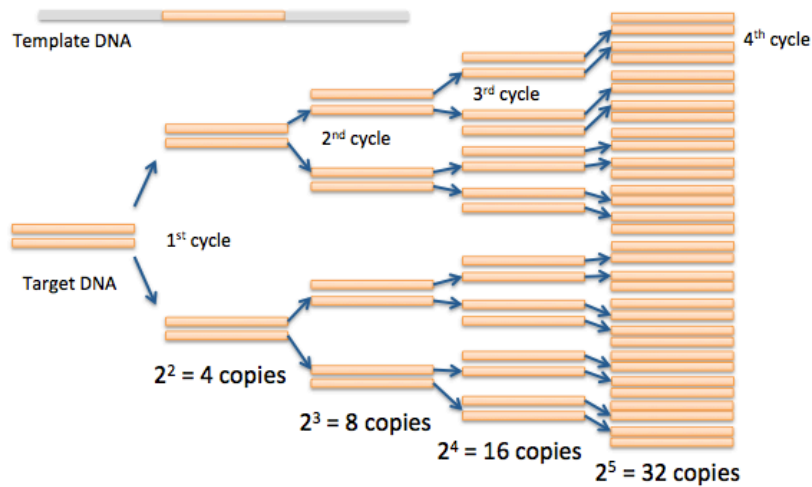
DNA is amplified by the polymerase chain reaction (PCR). The PCR amplification process consists of three stages. First is the denaturation step, where the double stranded DNA (dsDNA) is exposed to heat to divide the DNA into single stranded DNA (ssDNA). The second step is the annealing step. The temperature is lowered and specific primers attach to the ssDNA. The third and last step is elongation, where enzymes carry out extension of primers with nucleotides to copy the original DNA (64). The DNA amplification is illustrated in Figure 3.4a.

#### *SYBR Green*

PerfeCTa<sup>®</sup> SYBR Green FastMix (Quanta BioSciences) was used to measure the amount of PCR product. SYBR Green is a fluorescent dye that binds to the minor groove on dsDNA. The fluorescence is measured real-time during the PCR reaction. Amplification of the DNA is linked to cycles. When the fluorescence signal exceeds a chosen threshold, this cycle is called the threshold cycle (Ct) (65), as seen in Figure 3.4b.



a)



b)

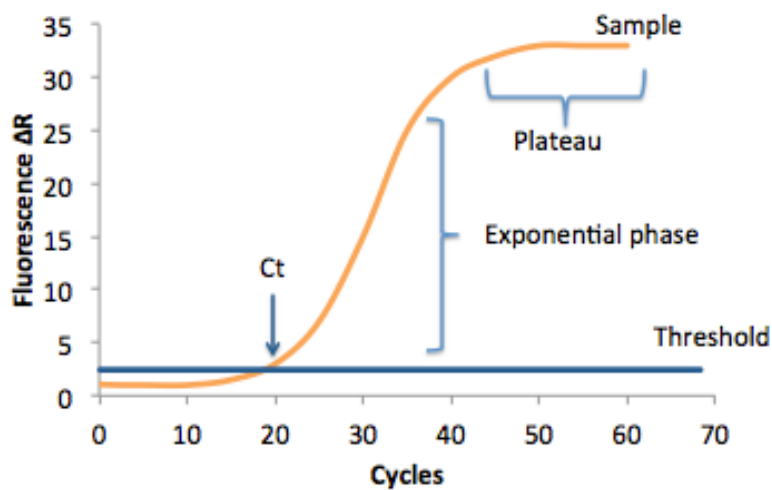


**Figure 3.4. The PCR principle.** a) This figure illustrates the principle of amplification of a target gene that is the basis of the PCR method. The template DNA is denatured and two new strands are synthesized. The step is repeated for several cycles. b) This figure illustrates the principle of qRT-PCR. When the amplification of a sample (orange) reaches a certain cycle that exceeds a chosen threshold (blue), a fluorescence signal is detected. This cycle is called the cycle threshold (Ct). The product amount is doubling for each cycle during the exponential phase. When the reaction components are being consumed, the reaction slows down, and in the plateau phase the reaction has stopped.

### The 2 $\Delta\Delta$ CT method

The relative quantification method is one way to analyze data from real-time quantitative PCR experiments. The other way is by absolute quantification which determines the input copy number of the target gene, this by relating the PCR signal to a standard curve. The relative quantification is based on the 2 $\Delta\Delta$ CT method, which measures the relative changes in gene expression for qRT-PCR experiments. Relative quantification is the change in expression of the target gene relative to a reference gene or reference sample such as an untreated control or a sample at time zero in a time-course study. When using the relative quantification method, certain equations and assumptions are required. The 2 $\Delta\Delta$ CT method is use for this. The amount of target equation is found in Formula 3.3. The use of this formula should give the mean fold change at time zero close to 1 because  $2^0=1$  (66).

$$\text{a) Amount of target} = 2^{-\Delta\Delta CT}$$

$$\text{b) } \Delta\Delta CT = ((C_{T,\text{target}} - C_{T,\text{Control}})_{\text{Time x}} - (C_{T,\text{Target}} - C_{T,\text{Control}})_{\text{Time 0}})$$

**Formula 3.3. The amount of target equation used in the 2 $\Delta\Delta$ CT method.** a) The amount of target is calculated by this formula where b) Time x is any given time point. Time 0 represents the 1x expression of the target gene normalized to the control. The mean  $C_T$  values for both the target and the control is determined at time 0. When using this formula, the value of the mean fold change at time 0 should be close to 1 because  $2^0=1$ . A full derivation for the formula is found in Livak *et al* (66).

### Protocol

A master mix containing 10 $\mu$ L SYBR Green, 1 $\mu$ L Forward primer, 1 $\mu$ L Reverse primer and 6.5 $\mu$ L dH<sub>2</sub>O for each well was prepared. 18.5 $\mu$ L of the master mix was added to each well of a 96 well-plate. The primers used are found in Table 3.6. 1.5 $\mu$ L cDNA, diluted 1:2 with dH<sub>2</sub>O, was then added. The plate was centrifuged Rotina 35 (Hettich Zentrifugen) for 15 seconds. The qRT-PCR is performed using the Step One Plus Real-Time PCR System machine (Applied Biosystems). Three parallels of each of the cDNA samples were used. For the negative RNA and negative RT controls, either 1 or 3 parallels were used. The steps of qRT-PCR are found in Table 3.4.

**Table 3.4. The thermal cycle steps of qRT-PCR.** The steps of qRT-PCR using the Step One Plus Real-Time PCR System machine from Applied Biosystems.

Step	Temperature	Time (seconds)
Denaturing	95°C	00:20
PCR cycling	95°C	00:03
Final elongation	60°C	00:30

To establish the kinetics for hMPV A1 infected A549 and WI-38 cells, primers for IFN- $\beta$  and the sTSLP and lTSLP genes were used for time course experiments. To establish the significance of different genes involvement in TSLP regulation upon hMPV A1 infection, knockdown experiments were carried out. The lTSLP primers were used to establish expression of lTSLP upon hMPV A1 infection in cells that were used for knockdown experiments. To determine infection rate, primers for the N-protein of hMPV were used. The primer efficiency has previously been tested by members of the research group.

**Table 3.6. Primers used for qRT-PCR.** An overview of the primers used in qRT-PCR.

Target	Manufacturer	Direction	Primer sequence
lTSLP	Sigma	Forward	5'-GGGCTGGTGTTAACTTACGACTTCA-3'
	Aldrich	Reverse	5'-ACTCGGTACTTTTGGTCCCCTCA-3'
sTSLP	Sigma	Forward	5'-CGTAAACTTTGCCGCCTATGA-3'
	Aldrich	Reverse	5'-TTCTTCATTGCCTGAGTAGCATTTAT-3'
IFN- $\beta$	Invitrogen	Forward	5'-GCCGCATTGACCATCTATGAGA-3'
		Reverse	5'-GAGATCTTCAGTTTCGGAGGTAAC-3'
hMPV N-gene	Sigma	Forward	5'-CATATAAGCATGCTATATTTAAAAGAGTCTC-3'
	Aldrich	Reverse	5'-CCTATTTCTGCAGCATATTTGTAATCAG-3'
GAPD	Sigma	Forward	5'-GAAGGTGAAGGTCGGAGTC-3'
H	Aldrich	Reverse	5'-GAAGATGGTGATGGGATTTC-3'

### **3.17 Western Blot**

The term Western Blot is here used as a collective term for several methods used to analyze expression of proteins. Western blotting was performed to determine whether specific transcription factors were activated in response to hMPV infection in human airway cells. Proteins are often activated by phosphorylation, and to measure activation of transcription factors, antibodies against phosphorylated transcription factors were used.

#### ***Protocol SDS PAGE***

NuPAGE® gels were used, usually 10% or 4-12% Bis-TrisGel. Type of gel used was chosen on basis of the size of the proteins to achieve high distribution of the proteins that were being observed. Running buffer was prepared by mixing 950mL dH<sub>2</sub>O with 50mL 20x NuPAGE MOPS running buffer. Protein lysates were thawed on ice and centrifuged (5000rpm, 4°C for 5 minutes). Sample buffer containing 950µL 4xLDS, which contains a dye making it possible to visualize the samples in the gel, and 50µL of the reducing agent DTT (1M) was prepared, and mixed with cell lysate sample in a 3:1 concentration. The proteins were further denatured by heat block at 70°C for 10 minutes. Samples were short spun and loaded onto the gel and running buffer poured into the chamber. 4µL of Kaleidoscope and Magic Mark standards were used to determine the size of the proteins by comparing the standards to their corresponding bands. Electrophoreses was run on 200V for circa one hour.

#### ***Protocol dry blot***

After protein separation by electrophoresis, the proteins were blotted onto the membrane for further detection. Dry blot was performed using iBlot® Gel Transfer stacks Nitrocellulose Mini kit and the iBlot™ machine (Invitrogen). The membrane was washed with 1xTBS before it was blocked with Odyssey block buffer (diluted 1:1 in TBS) for one hour. The membrane was further washed 3x with TBST and incubated with primary antibody shaking in a cold environment overnight (ON). The membrane was the next day washed 3x5minutes with TBST and further incubated at room temperature with secondary antibody for 1h. The membrane was then washed with 2xTBST and washed with TBS. When the membrane was dry, Odyssey (LI-COR Biosciences) was used to develop photo of the membrane. Image Studio Software (LI-COR Biosciences) was used to analyze the blots. The primary

antibodies were diluted in TBST. For a complete overview of antibodies and their corresponding dilution, see Table 3.7.

**Table 3.7. Antibodies.** Antibodies used and their corresponding dilution in TBST. P = Phosphorylated.

Antibody	Dilution in TBST	Host	Manufacturer	Catalog number	Size (kDa)	Phosphorylation site
<b>Primary antibodies</b>						
P-ATF2	1:1000	Rabbit	CST	#9221	70	Thr71
P- IRF3	1:1000	Rabbit	CST	#4961	45-55	S396
P-65	1:1000	Rabbit	CST	#3033	65	S536
P-STAT1	1:1000	Rabbit	CST	#9167	84,91	Tyr701
B-aktin	1:20,000	Mouse	Sigma Aldrich	A1978	42	
TRAF6	1:10,000	Rabbit	Abcam	Ab33915	58	
<b>Secondary antibodies</b>						
680 GAR	1:20,000	Rabbit	Li-cor			
680 GAM	1:20,000	Mouse	Li-cor			
800 GAR	1:5000	Rabbit	Li-cor			
800 GAM	1:5000	Mouse	Li-cor			

### 3.18 Statistical analysis

Data are representative for three independent experiments unless else is stated. Excel was used to do all the statistical analysis in this thesis. The standard deviation is represented by error bars. To calculate the significance between two samples, two-sample unpaired Student's t test was used. P value < 0.05 was considered significant and is represented with an asterisk (\*).



## 4 Results and discussion

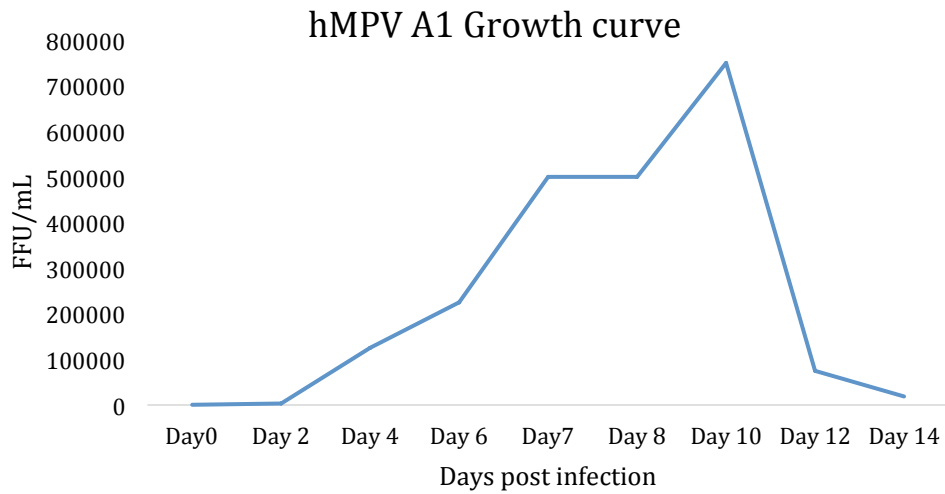
### 4.1 Propagation of hMPV A1 in LLC-MK2 cell culture

To find the optimal time point for hMPV replication a growth curve experiment was performed. It was used to establish an indication of when to isolate hMPV during propagation to yield the highest possible amount of virus. Based on the titration assay, the ideal time for harvesting virus would be on day 10 as seen in Figure 4.1a. High FFU/mL at day 10 may indicate that the replication is at its maximum on this day. Based on low Ct-value on day 8, as seen in Figure 4.1b, the replication maximum may be on this day. The low Ct-value stays fairly stable from day 8 and through day 14. The problem with using Ct-value as a basis for viral replication is that the Ct value is not able to register whether the mRNA is from live or dead virus. Because of this, consideration of the CPE effect was also taken into account when finding the optimal day for virus isolation. Figure 4.2 shows the cell morphology during a propagation of the hMPV A1 stock S26 in LLC-MK2 cells. The cells were considered to have CPE of 75-90% at day 8 or 9. As this day correlates closely to the replication max indicated by the FFU/mL and Ct-values, the virus flasks were frozen and virus isolated at day 8 or 9. The CPE value is important to ensure that there still are cells with normal morphology present that are adherent and available for virus replication. The growth curve experiment was conducted once.

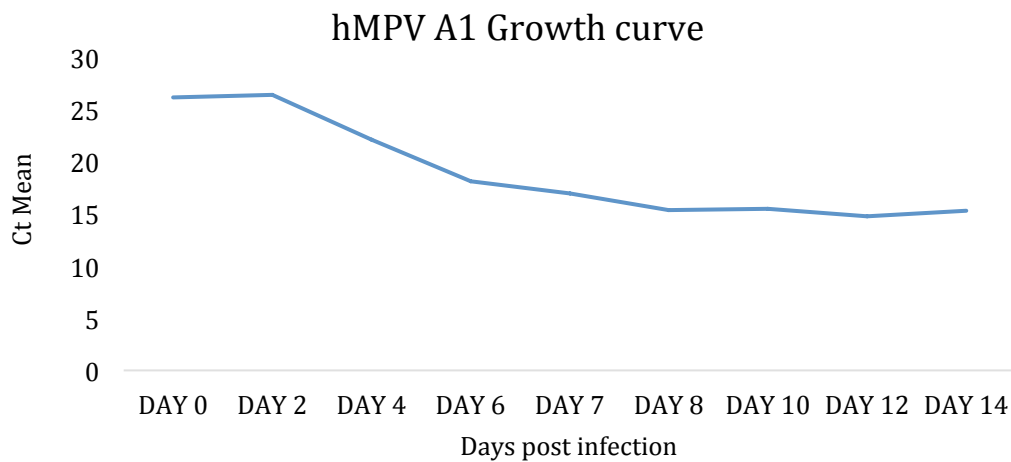




a)

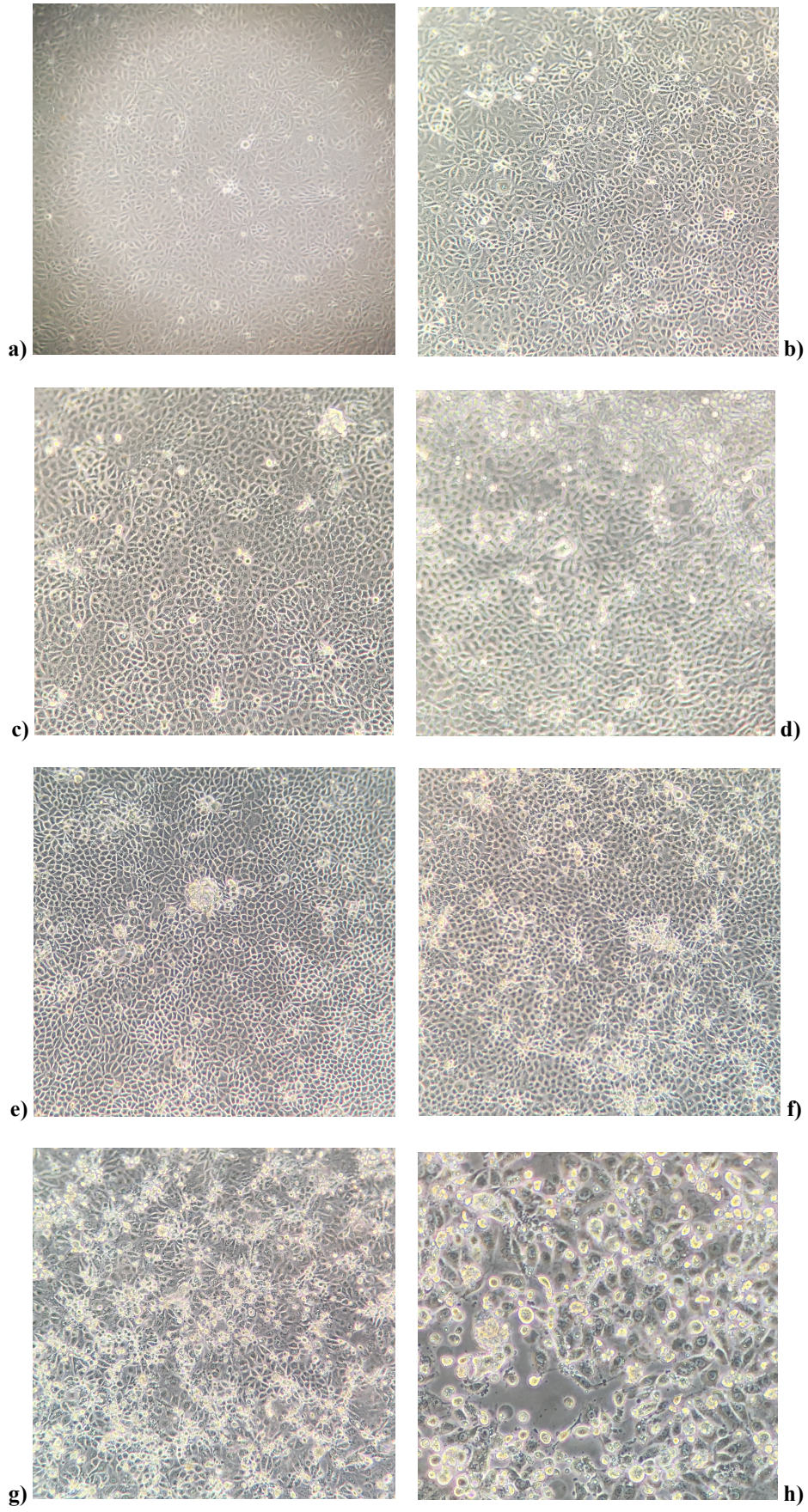


b)



**Figure 4.1. hMPV A1 growth curve.** The growth curve experiment was conducted to find the peak replication day for hMPV A1. LLC-MK2 cells were infected with hMPV A1S17 at confluency. Titration assays were performed to calculate the FFU/mL at days 2, 4, 6, 7, 8, 10, 12 and 14 p.i. qRT-PCR was applied to assess maximum virus using hMPV N-gene primers. The experiment was conducted once. **a)** FFU/mL **b)** Ct Mean value.

The cytopathic effect (CPE) was monitored during the growth curve experiment. When the CPE was considered to be at 75-90%, the flasks were frozen and the virus isolated. A picture of healthy cells, that show low or no CPE, is found in Figure 4.2a. Pictures of the day-to-day CPE development during hMPV propagation is presented in Figure 4.2b-m.



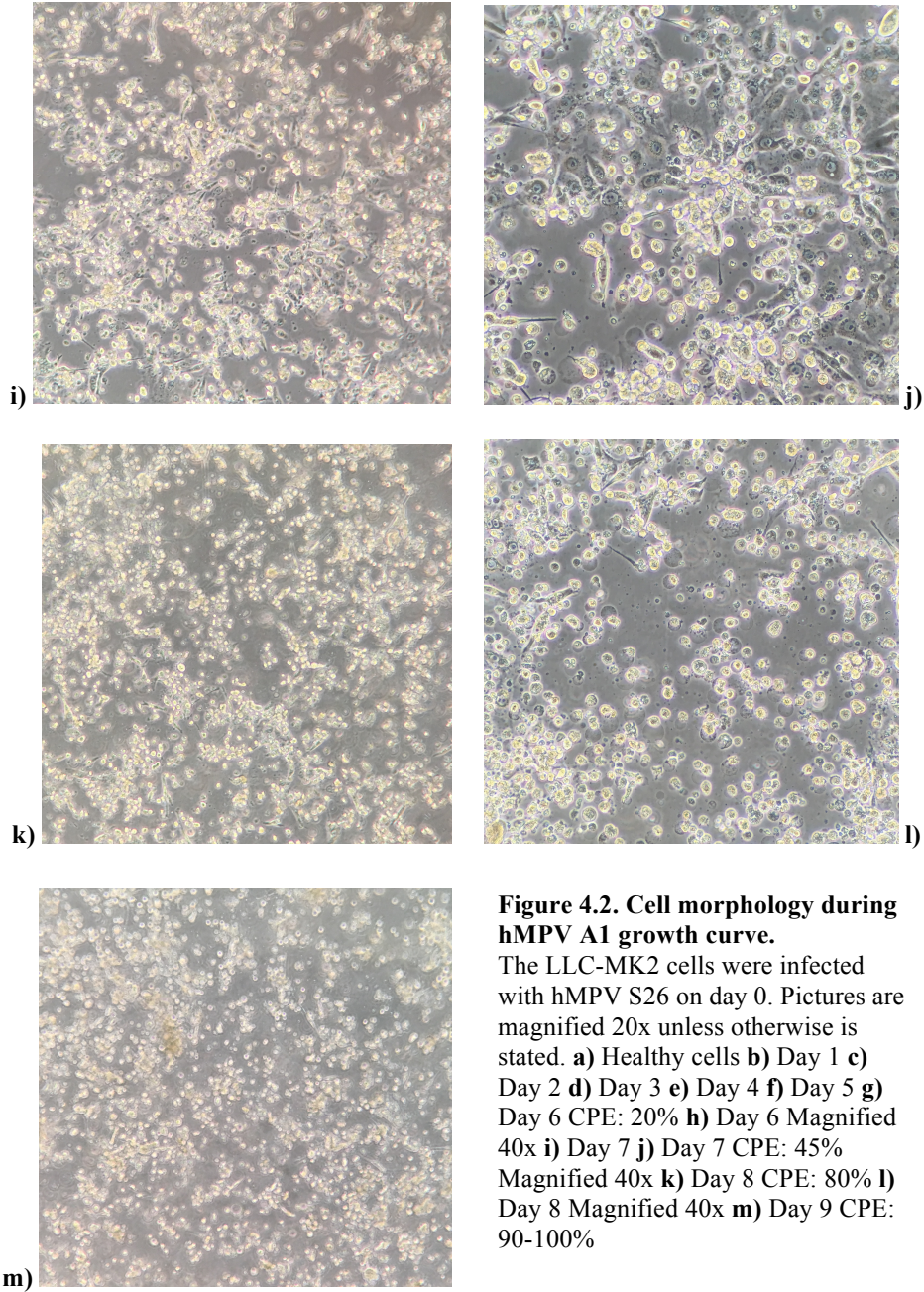


**Figure 4.2. Cell morphology during hMPV A1 growth curve.**

The LLC-MK2 cells were infected with hMPV S26 on day 0. Pictures are magnified 20x unless otherwise is stated. **a)** Healthy cells **b)** Day 1 **c)** Day 2 **d)** Day 3 **e)** Day 4 **f)** Day 5 **g)** Day 6 CPE: 20% **h)** Day 6 Magnified 40x **i)** Day 7 **j)** Day 7 CPE: 45% Magnified 40x **k)** Day 8 CPE: 80% **l)** Day 8 Magnified 40x **m)** Day 9 CPE: 90-100%

## 4.2 Determination of IFN- $\beta$ induction in virus stocks, DI+ and DI- stocks

DIs are truncated viral genomes that are produced during replication. The Van den Hoogen *et al* hypothesis is that DIs are present in hMPV stocks and could be responsible for the activation of the IFN pathway is assumed. DIs are likely recognized by the host as danger signals and lead to antiviral responses, and in this way probably play a significant role in hMPV pathogenesis (18, 19).

Virus stocks that showed greater than a 2-fold induction of IFN- $\beta$  in HEK-293 cells were considered DI+, while virus stocks that showed a fold induction of less than a 2-fold were considered DI-. This was tested because in A549 cells DI- stocks were not able to induce sufficient IFN- $\beta$ . Induction of IFN- $\beta$  in response to selected A1 stocks in HEK are shown in Figure 4.3. For WI-38 cells all stocks were able to induce sufficient amounts of IFN- $\beta$ , and thus whether the stock was considered DI+ or DI- was not of significance. In this thesis all the stocks that were used in experiments were DI-. The reason for this was that it proved to be difficult to propagate DI+ stocks. The DI- stocks showed great variation between them, both in regard to the IFN- $\beta$  induction and the TSLP fold induction. The variation might be caused by the degree of DI genomes that accumulate in the stocks. A theory is that DI particles are produced during the infection of hMPV, so that stocks that are initially DI negative might produce DI particles gradually and in this way be able to induce higher amounts of IFN- $\beta$  and could in this way be considered DI+. The theory is based upon the finding that DI- stocks in WI-38 were seen to induce IFN- $\beta$  in the same amount as stocks that were considered DI+. Whether the virus stocks were DI+ or DI- was considered to be insignificant for the experiments conducted in this thesis, because some of the DI- stocks were still able to induce sufficient amounts of TSLP in the airway epithelial (A549), while all stocks induced sufficient amounts of TSLP in lung fibroblast (WI-38) cell lines. The magnitude of the lftTSLP fold induction varied between the different A1 stocks. The variation was especially considerable in the A549 cell line, seen in Figure 4.4 while in WI-38 all stocks gave sufficient induction of lftTSLP, seen in Figure 4.5. Therefore the stocks that showed the highest induction of lftTSLP in A549 and WI-38 were chosen when conducting the experiments. The results may still vary a lot as a result of stock variation. An overview of hMPV A1 stocks used in this thesis is found in Table 4.1.

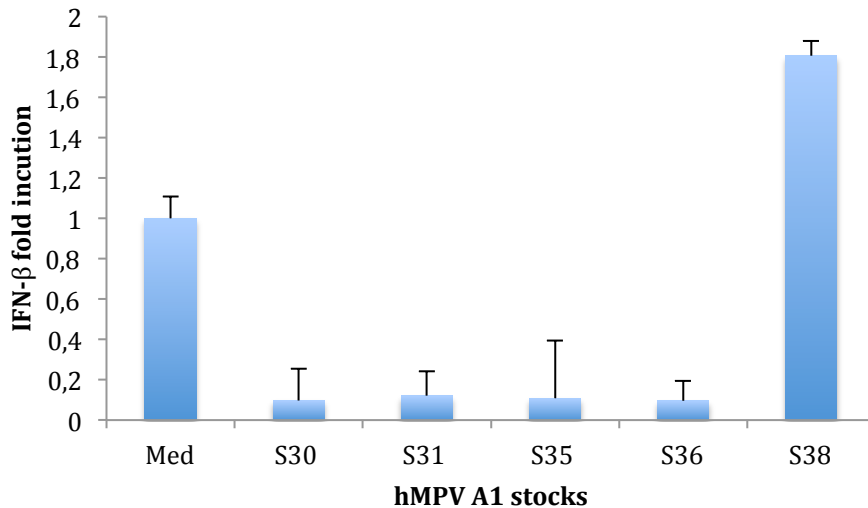


**Figure 4.3. IFN- $\beta$  induction in HEK cells infected with hMPV A1 stocks.** IFN- $\beta$  fold induction in HEK cells upon infection with hMPV stocks 30, 31, 35, 36 and 38. The cells were infected for 24 hours. The induction is measured mRNA fold compared to medium, applying qRT-PCR. SeV was used as a positive control and gave 18-fold induction (not shown). Standard deviation is represented with error bars.

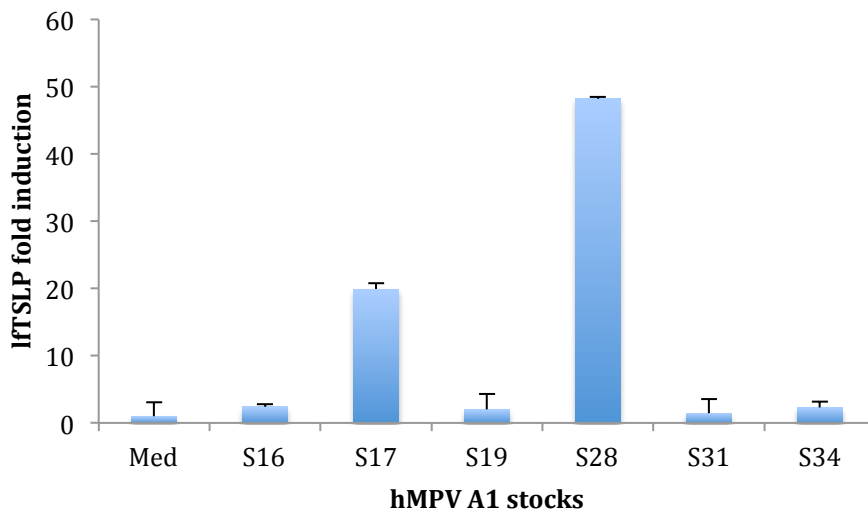


**Figure 4.4. TSLP induction in airway epithelial cells infected with hMPV A1 stocks.** The graph show IFTSLP fold change in response to hMPV stocks 16, 17, 19, 28, 31 and 34, and illustrates the stock variation in IFTSLP induction in A549 cells. The cells were infected for 24 hours. IFTSLP mRNA fold induction in A549 was measured by applying qRT-PCR. Standard deviation is represented with error bars.

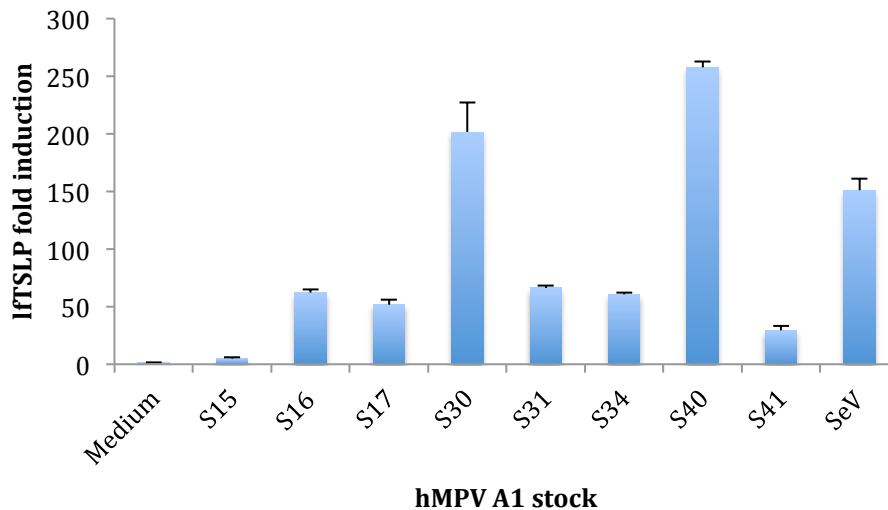


**Figure 4.5. TSLP induction in lung fibroblasts infected with hMPV A1 stocks.** IFTSLP fold induction in WI-38 cells upon infection with different hMPV A1 stock. Cells were infected for 24 hours. SeV was used as a positive control. Standard deviation is represented with error bars.

**Table 4.1. Virus stocks used in experiments.** An overview of FFU/mL, TCID50, TCID50/mL and TSLP and IFN- $\beta$  fold change of A1 stocks that are used in experiments in this thesis. N.d. = not determined.

Virus stock	FFU/mL	TCID50/mL
S15	875 000	$7.34 \times 10^5$
S17	275 000	$5.00 \times 10^5$
S21	232 500	$2.32 \times 10^5$
S26	750 000	$2.81 \times 10^6$
S28	237 500	$1.08 \times 10^5$
S30	387 500	$2.81 \times 10^5$
S31	500 000	$8.89 \times 10^5$
S35	375 000	$5.00 \times 10^5$
S38	250 000	$5.02 \times 10^5$
S40	750 000	$1.08 \times 10^6$
S41	750 000	$8.89 \times 10^6$

### **4.3 Characterization of IFN- $\beta$ response and activation of related transcription factors upon hMPV A1 infection in airway epithelial cells**

First, kinetics of IFN- $\beta$  in response to hMPV A1 infection was established, as this is the classical antiviral response (67). Next, the phosphorylation status of transcription factors known to be involved in IFN- $\beta$  induction in response to RSV and SeV was examined. This may give indications on what pathways that are triggered by hMPV and thus what pathways are likely to mediate the TSLP response.

As illustrated in Figure 7 in section 1.6, the IFN- $\beta$  promoter has binding sites for NF- $\kappa$ B, IRF3 and ATF2. NF- $\kappa$ B is involved in the induction of IFN- $\beta$  in response to SeV (68), NF- $\kappa$ B and IRF3 is involved in IFN- $\beta$  induction in response to RSV infection (13). RSV-infection in A549 cells is known to result in increased binding of ATF2 to the IL-8 promoter (69).

#### **4.3.1 Kinetics for hMPV A1-triggered IFN- $\beta$ induction in airway epithelial cells**

It is well known that IFN- $\beta$  is induced as a response to infection by RNA viruses (70, 71). To establish whether hMPV infection induce IFN- $\beta$  in airway epithelial cells, and when the IFN- $\beta$  induction reaches its high point, kinetics experiments were performed in A549 cells. The time points chosen to assess was 6h, 18h, 24h and 48h p.i. These time points were chosen on the basis of IFN- $\beta$  induction in response to SeV infection that was well established through previous observations done by the research group. These results, presented in Figure 4.6, show that hMPV indeed induce IFN- $\beta$  in airway epithelial cells. The results indicate that IFN- $\beta$  is mainly induced 48h p.i in response to hMPV A1 infection. The result is based upon one experiment. Results from other members of the research group indicate that IFN- $\beta$  is induced at 24h p.i. and even as early as 18h p.i., and this result is thus not completely representative. It may also be that hMPV is able to inhibit signaling leading to IFN- $\beta$  expression, and that this ability is stock dependent, explaining the diverging results in regard to IFN- $\beta$  induction time points.

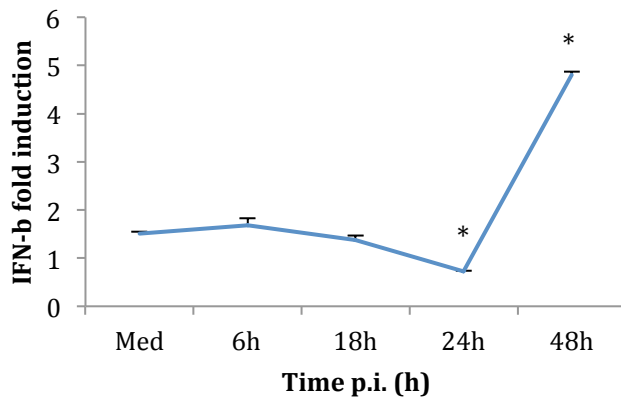


**Figure 4.6. Induction of IFN- $\beta$  in airway epithelial cells upon hMPV infection.** Induction of IFN- $\beta$  mRNA during infection with hMPV A1S21 in A549 cells. The induction starts at around 34h p.i. and peaks at 48h p.i. All fold inductions are relative to medium. Standard deviation is represented by error bars. 24h and 48h significant relative to medium, as indicated by \*. P value <0,05 relative to medium. 48h significant relative to 24h.

### 4.3.2 Activation of transcription factors upon infection with hMPV A1 in airway epithelial cells

#### *Phosphorylation status of transcription factors during hMPV A1 infection in A549*

When transcription factors are phosphorylated, they become activated and are able to translocate into the nucleus where they promote transcription of specific genes. NF- $\kappa$ B, ATF2 and IRF3 are transcription factors that are activated in response to viral infection, inducing the transcription of pro-inflammatory and antiviral genes.

Experiments by Goutagny *et al* show that these transcription factors are activated by both SeV and hMPV A1 infection. IRF3 is especially involved in to induction of IFN- $\beta$  in response to viral infections (72). NF- $\kappa$ B is known to be activated through phosphorylation on p65 in response to RSV infection in A549 cells (73), and it was therefore of interest to investigate whether p65 is phosphorylated in response to hMPV infection in these cells.

To examine whether these transcription factors are activated upon hMPV A1 infection in airway epithelial cells, time course experiments were performed in A549 cells at MOI 1. To determine activation of transcription factors upon infection, the phosphorylation status was observed. SDS-PAGE was used to separate the proteins before they were blotted onto a membrane by applying the Western Blot method. The proteins were bound by against their respective antibody, targeting a specific



phosphorylation of that protein. The results are seen in Figure 4.7. The intensity of the band is correlated to the phosphorylation status, which again suggest the amount of that specific activated transcription factor. A quantification analysis of the blots were performed to assess band intensities. To ensure equal amounts of sample in each lane, the quantification was adjusted against  $\beta$ -actin.

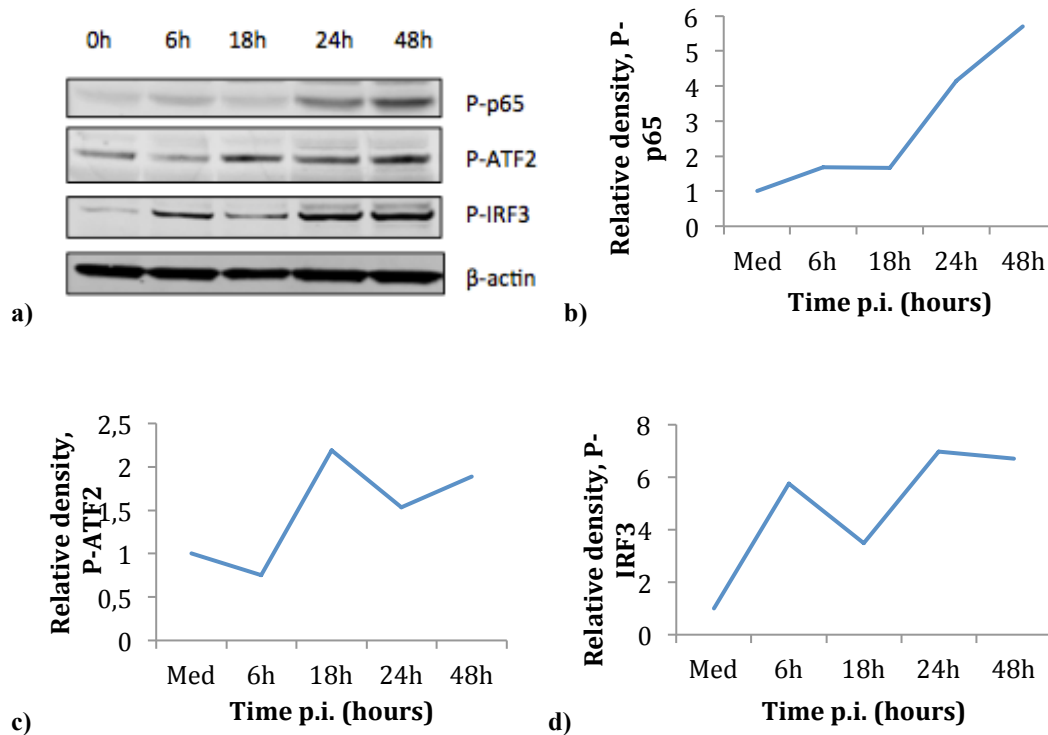


**Figure 4.7. The phosphorylation status of transcription factors upon hMPV A1 infection in A549.** **a)** Phosphorylation of p65 (65kDa), ATF2 (70kDa) and IRF3 (45-55kDa) at time points 0h, 6h, 18h, 24h and 48h p.i. **b)** Quantification of P-p65 blot. **c)** Quantification of P-ATF2 blot. **d)** Quantification of P-IRF3 blot. The quantification is measured in relative density. The relative density is adjusted against  $\beta$ -actin. Statistical analysis for the quantification graphs was not performed.

Transcription factors of the IRF family are essential players in virus-triggered type I IFN-gene expression (38). These results show that phosphorylation of IRF3 seem to peak at 24h p.i. There is also a peak at 6h p.i., however this is probably not a credible result as the results show that the phosphorylation status is decreased by 18h and this is more in line with what is expected based on the research group experience with phosphorylation of transcription factors in response to SeV infection (38).

It is also known that a number of inflammatory and immune-regulatory genes that are induced by paramyxovirus require NF- $\kappa$ B to be transcribed (36, 37). Activation of NF- $\kappa$ B requires phosphorylation of p65, and antibody against P-p65 was therefore used. The results indicate that the phosphorylation of p65 is later than expected, not until 24h p.i. and the phosphorylation of p65 even peaks at 48h p.i. The expectations are based on previous observations for SeV by the research group. It would be interesting to observe the phosphorylation of p65 at later time points, as IFN- $\beta$  in response to hMPV seems to be induced at much later time point p.i. compared to what is experienced with SeV. It has been reported that the SH-gene of hMPV inhibits phosphorylation of NF- $\kappa$ B (74), which might explain the phosphorylation status of p65 presented in this thesis, as the SH-gene might be able to inhibit the phosphorylation until 18h p.i. Experiments conducted by Wang *et al* indicate that NF- $\kappa$ B is important in regulating IFN- $\beta$  expression in response to viral infections, but that the regulation is limited to an early phase of the infection (70). In addition, their results indicate that the requirement for NF- $\kappa$ B in IFN- $\beta$  gene expression is inversely correlated with IRF3 activation, suggesting that NF- $\kappa$ B is involved in promoting the IFN- $\beta$  expression prior to the IRF3-driven IFN- $\beta$  induction. The trend indicated by the results in this thesis do not clearly support the results by Wang, however it is necessary to investigate the activation further.

The phosphorylation status of ATF2 seems to be low. The phosphorylation peaks at 18h p.i., which may indicate that ATF2 in response to hMPV is activated in the early phase of infection. It is necessary to investigate the involvement of ATF2 in hMPV-triggered IFN- $\beta$  expression further.

To confirm the results of phosphorylated transcription factors, comparing the quantification against the relative amount of that particular protein would be an advantage. This would confirm whether it the protein itself that is upregulated in response to the infection, or if the upregulation seen on the blot is representing the phosphorylated thus activated protein.

#### ***STAT1 is phosphorylated upon hMPV infection in airway epithelial cells***

The transcription factor STAT1 is an important signaling component in the Jak-STAT pathway, which is induced secondary when IFN- $\beta$  binds to the IFNAR receptor. The

binding of IFN- $\beta$  to the IFNAR is a secondary signaling pathway in response to viral infection. STAT1 phosphorylation leads to its translocation into nucleus, where it induces transcription of genes involved in the antiviral state. If STAT1 is phosphorylated upon hMPV infection, it is likely that this STAT1 activation is caused by secondary signaling by IFN- $\beta$ , initially induced in response to the viral infection. The results, seen in Figure 4.8, show that STAT1 is phosphorylated upon hMPV infection in airway epithelial cells. The phosphorylation peaks at 24h p.i. Because STAT1 seem to be phosphorylated mainly at around 24h p.i., and IFN- $\beta$  does not seem to be induced in these cells until 48h p.i., these results do not indicate a clear connection between the IFN- $\beta$  induction and the STAT1 phosphorylation seen in A549 upon hMPV infection.

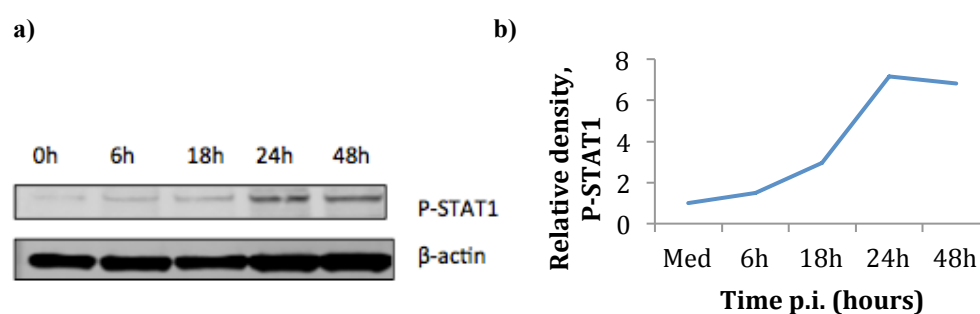


**Figure 4.8. Phosphorylation status of STAT1 upon hMPV A1 infection in A549. a)**

Phosphorylation of STAT1 (84,94kDa) at time points 0h, 6h, 18h, 24h and 48h p.i.  $\beta$ -actin was used as control to determine equal loading of the samples. **b)** Quantification of P-STAT1 blot in A549. The relative density is adjusted against  $\beta$ -actin. Statistical analysis for the quantification graph was not performed.

Contradictory it has previously been reported by Dinwiddie *et al* that hMPV infection inhibits type I IFN-induced STAT1 phosphorylation and thus nuclear translocation of P-STAT1 in A549 cells, and it has been suggested to be a way to block IFN signaling (75). Supporting the findings on STAT1 phosphorylation in airway epithelial cells in this thesis, STAT1 phosphorylation upon hMPV infection was reported by Bao *et al*. Their results show that STAT1 activation starts at around 6h p.i. (76). The results presented by Dinwiddie *et al* is based on hMPV strain CAN/97/83, which is subgroup A2. The diverging results could therefore be due to differences between the subgroups, however different experimental conditions may also be the cause. The findings must therefore be investigated further, optimally comparing the two hMPV

subgroups to confirm whether there is a difference in STAT1 involvement in IFN- $\beta$  induction in response to infection by the two subgroups or not. It would be an advantage to compare the quantification against the relative amount of the total STAT protein.

#### **4.4 Characterization of PRR signaling components involved in hMPV A1- triggered TSLP induction in airway epithelial cells**

It is not yet fully understood how TSLP is induced. To be able to fully understand the link between TSLP, respiratory virus infections like hMPV and inflammation it is necessary to characterize which PRR signaling components that are involved in regulating expression of TSLP upon hMPV infection. PRR components regulating TSLP expression in response to RSV infection has previously been assessed (77), but such characterization has not previously been done in response to hMPV. Based upon the results found for induction of IFN- $\beta$  in response to hMPV A1 infection in these cells, the kinetics of TSLP was further studied. To determine which PRR signaling components that might be involved in TSLP induction upon hMPV infection, signaling components involved in the pathways of the different transcription factors were knocked down, using siRNA-mediated knockdown method to see the impact on TSLP expression.

##### **4.4.1 Kinetics for hMPV-triggered TSLP induction in airway epithelial cells**

It has been shown that TSLP is induced in airway epithelial cells in response to RSV infection (54), and in response to hMPV infection (47). How the expression of TSLP is regulated in response to viral infection is as of today largely unknown. To be able to find strategies for treatment it is necessary to understand which components that are involved in the regulation, and how they interact. To establish the kinetics for TSLP induction in airway epithelial cells upon hMPV infection, kinetics experiments were performed. The aim of the time course experiments was to establish at what time point the TSLP induction was at its highest. The time points were initially chosen on the basis of IFN- $\beta$  induction. Both sfTSLP and lfTSLP mRNA levels were measured. As seen in Figure 4.9, the induction of lfTSLP peaks at 18h p.i. while the sfTSLP is induced later, around 48h p.i. and is thus induced at the same time as IFN- $\beta$ . The difference in induction time point could be a result of the different biological function of the two isoforms.

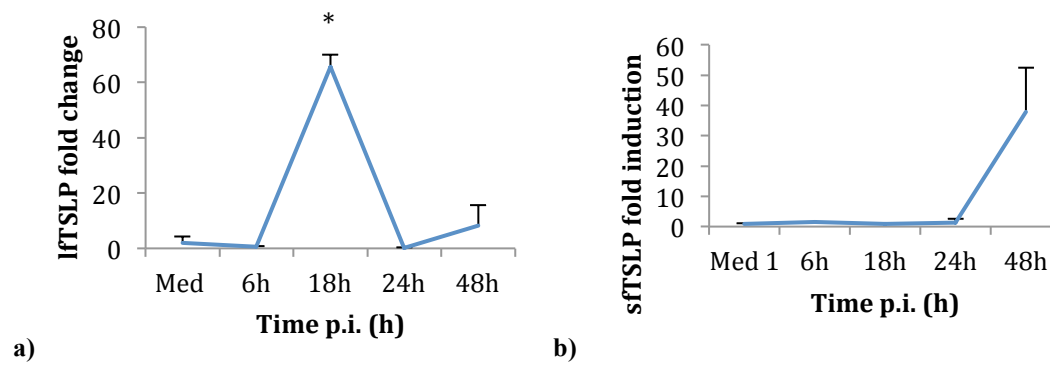


**Figure 4.9. Induction of TSLP in airway epithelial cells upon hMPV infection.** A549 cells were infected with hMPV A1S21 at MOI 1 and lysed at 6h, 18h, 24h and 48h p.i. N.i. cells used as control. Induction of TSLP mRNA was measured using qRT-PCR. All fold inductions are relative to medium. **a)** lftTSLP fold induction. **b)** sftTSLP fold induction. Standard deviation is represented by error bars. Data are representative for three experiments. Statistical significance is indicated by \*, P value <0,05 relative to medium.

#### 4.4.2 Efficiency of siRNA-mediated knockdown of PRR signaling components

Prior to conducting the siRNA-mediated knockdown experiments of PRR signaling components, a siRNA efficiency test was performed to test the efficiency of the knockdown transfection method. If the transfection was successful the cell would not be able to produce protein in as high amounts as they normally do, and thus there would be a decreased intensity of the bands for the protein in question. Transfection is not 100% effective, which leaves a mixed population of transfected and un-transfected cells. The transfection efficiency will vary from experiment to experiment, depending on the specific siRNA and how easily the cell line is transfected. Figure 4.10 shows a knockdown efficiency test of siTRAF6 in A549 cells where concentrations of 5, 10 and 20nM have been used. The knockdown of TRAF6 is clearly successful compared to the siAllstar control. The efficiency of the other siRNA sequences used in this thesis have previously been tested by the research group by Western Blot or qRT-PCR.

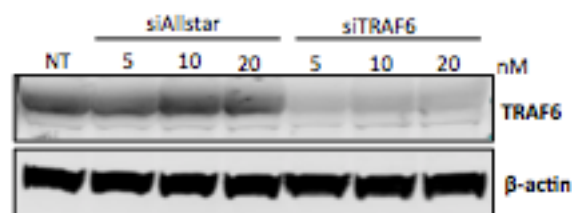


**Figure 4.10. Efficiency test of siTRAF6 in A549 cells.** A549 cells were transfected with 5, 10 or 20nM siRNA against TRAF6, or Allstar as a control. Cell lysates were separated by SDS-PAGE and immunoblotted against TRAF6 and β-actin. No transfection (NT).

#### **4.4.3 Characterization of PRR signaling components involved in hMPV A1-triggered lftTSLP expression in airway epithelial cells**

To further investigate the regulation of TSLP induction in response to hMPV infection, involvement of some PRR signaling components were analyzed. For conducting these experiments the lftTSLP isoform was chosen for further analysis. Choosing the lftTSLP isoform is based on the kinetics experiments that showed that hMPV infection in airway epithelial cells induce greater amounts of lftTSLP than the sfTSLP. LftTSLP is also induced earlier than the sfTSLP isoform. To characterize which PRR signaling components that are involved in lftTSLP induction upon hMPV infection in airway epithelial cells, knockdown experiments using siRNA transfection method was performed in A549 cell line. The cells were infected with hMPV for 18h at MOI 1 as the kinetics experiment showed peak induction for lftTSLP at this time point.

**The cytoplasmic PRR RIG-I is required for induction of lftSLP upon infection with hMPV A1 in airway epithelial cells**

RIG-I is a cytoplasmic PRR that recognizes viral genomes, and is required for the antiviral responses against viruses, including *Paramyxoviridae* (72). A study carried out by Casola *et al* confirmed that RIG-I plays an essential role in initiating cell signaling in the immune response to hMPV infection (78). Liao *et al* shows that RIG-I is important in hMPV triggered IFN- $\beta$  responses in airway epithelial cells. Their results show that inhibition of RIG-I leads to a significant decrease of IRF and NF- $\kappa$ B transcription factors as well as type I IFN and pro-inflammatory cytokines and chemokines (28). TSLP expression in epithelial cells have also been observed in response to RSV (79). RIG-I is known to be involved in the TSLP induction pathway in response to RSV and SV infection in A549 cells (54). It is therefore of interest to characterize whether RIG-I is involved in the TSLP induction pathway in response to hMPV infection as well. To investigate whether RIG-I is required for hMPV mediated induction of lftSLP mRNA in airway epithelial cells, the A549 cells were transfected with RIG-I siRNA, or Allstar siRNA as a control, and the lftSLP mRNA fold induction was measured by qRT-PCR. As a result, knockdown of RIG-I significantly suppressed hMPV-triggered lftSLP induction in compared to the siAllstar control, as seen in Figure 4.11. This suggests that RIG-I plays a significant role in the regulation of TSLP induction in airway epithelial cells upon hMPV A1 infection.

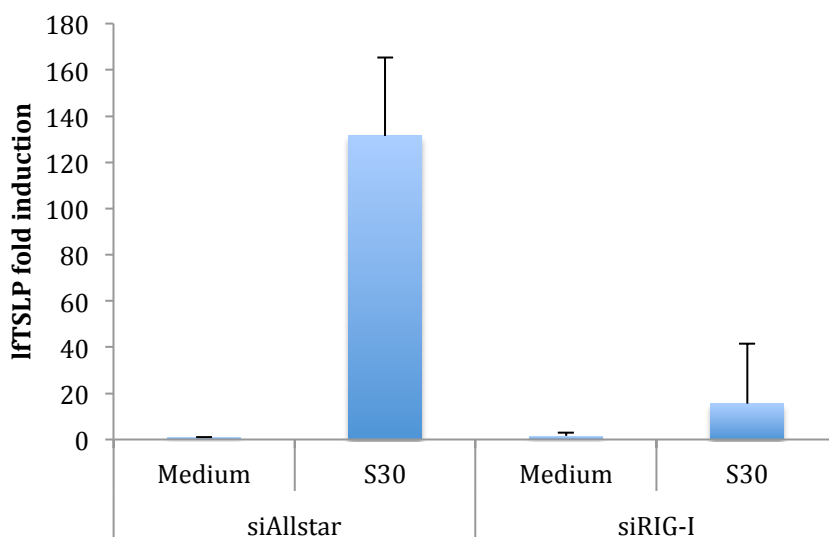


**Figure 4.11. TSLP fold induction in RIG-I depleted cells.** A549 cells were transfected with siRIG-I or siAllstar as a control, and subsequently infected with hMPV A1S30 for 18h. Induction of lftSLP mRNA was measured with qRT-PCR. Standard deviation is represented by error bars. Data are representative for three experiments.

**The adaptor protein MAVS is required for induction of lftSLP upon infection with hMPV A1 airway epithelial cells**

The mitochondrial antiviral-signaling protein MAVS is an adaptor protein that transfer signals from RIG-I to downstream kinases that activates transcription factors NF- $\kappa$ B and IRF that again leads to transcription of genes that are involved in antiviral and pro-inflammatroy responses. Liao *et al* has shown that the RIG-I-MAVS pathway is important in hMPV triggered cellular responses (28). RIG-I-MAVS signaling leading to TSLP expression has been observed in epithelial cells in response to RSV (79). It was therefore of great interest to investigate whether MAVS is involved in the regulation of TSLP induction in response to hMPV A1 infection. The cells were transfected with MAVS siRNA, or siAllstar as a control, and the lftSLP fold induction was measured. The results are seen in Figure 4.12 and show that knockdown of MAVS completely suppressed the ability of the cells to induce lftSLP compared to the siAllstar control. This suggests that MAVS plays a crucial role in the lftSLP induction in airway epithelial cells upon hMPV infection.

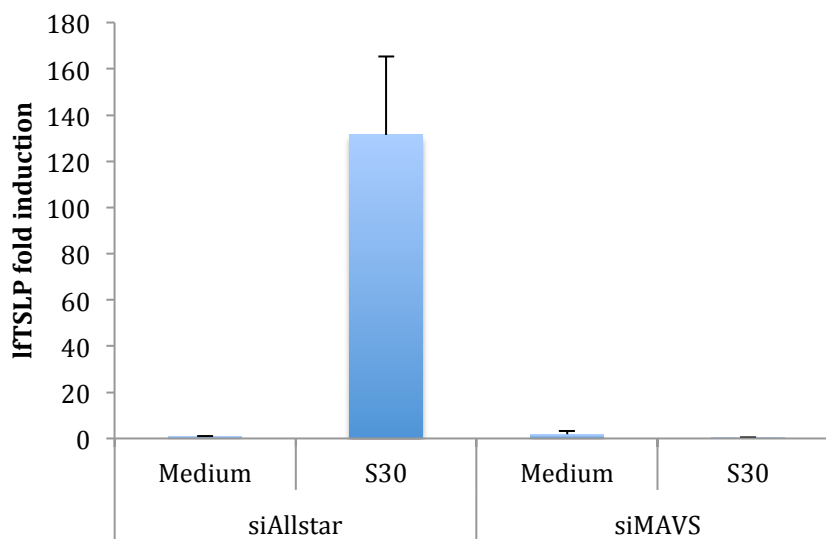


**Figure 4.12. TSLP induction in MAVS depleted cells.** Induction of lftSLP mRNA during infection with hMPV A1S30 in MAVS-depleted A549 cells. Standard deviation is represented by error bars. Data are representative for three experiments.



### *TRAF6 is involved in hMPV A1-triggered induction of lftSLP in airway epithelial cells*

TRAF6 is an intracellular protein that bind to the cytoplasmic regions of receptors (34). TRAF6 has shown to be required in RIG-I-MAVS signaling in response to RSV infection in A549 cells (73). The A549 cells were transfected with TRAF6 siRNA, or siAllstar as a control, infected with hMPV for 18h, and the lftSLP mRNA fold induction was measured. The result, seen in Figure 4.13, show that knockdown of TRAF6 significantly suppressed TSLP induction compared to the siAllstar control, suggesting that TRAF6 plays a significant role in the TSLP induction in airway epithelial cells upon hMPV infection. Yoboua et al have shown that TRAF6 is necessary in the RIG-I downstream signaling pathway leading to phosphorylation of p65 in response to RSV infection in A549 cells (73). Whether TRAF6 is involved in the signaling pathway leading to phosphorylation of p65 in response to hMPV needs to be further investigated.

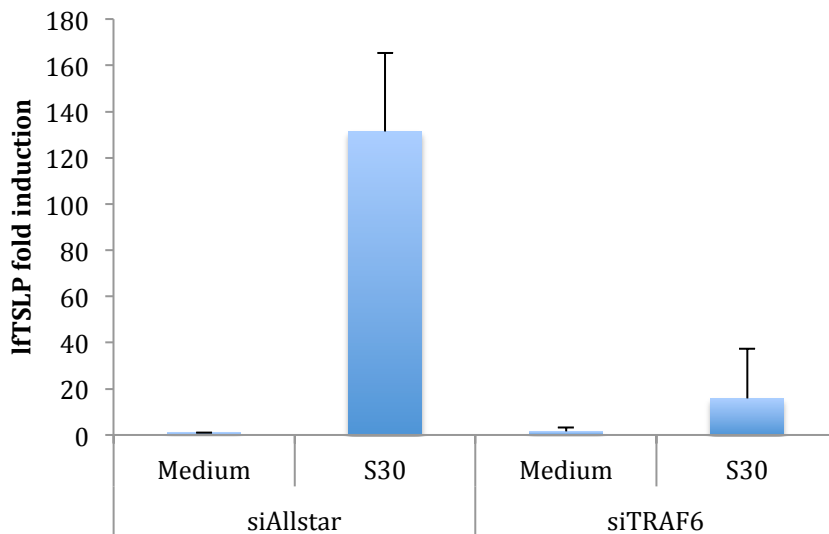


**Figure 4.13. TSLP induction in TRAF6 depleted cells.** Induction of lftSLP mRNA during infection with hMPV A1S30 in TRAF6-depleted A549 cells. Standard deviation is represented by error bars. Data are representative for three experiments.

## 4.5 Characterization of IFN- $\beta$ response and activation of related transcription factors upon hMPV A1 infection in lung fibroblasts

Because of low basal expression and high variation of TSLP induction in airway epithelial cells due to hMPV stock variation, it was decided to repeat experiments in a lung fibroblast cell line, WI-38. These cells showed higher basal expression of TSLP in addition to induce efficient amounts of TSLP for all hMPV A1 stocks.

### 4.5.1 Kinetics for hMPV-triggered IFN- $\beta$ induction in lung fibroblasts

It is well known that IFN- $\beta$  is induced in response to viral infection. Primary fibroblasts from asthmatic patients have shown poor capability to induce IFN- $\beta$  in response to human rhinovirus (HRV) (80). To establish whether hMPV A1 infection induce IFN- $\beta$  in lung fibroblasts, and to establish at what time point the IFN- $\beta$  induction is maximal in these cells, kinetics experiments were performed in the WI-38 cell line. The results, seen in Figure 4.14, show that IFN- $\beta$  is induced in WI-38 cells and that the induction reaches its high point 18h p.i. The establishment of this information on IFN- $\beta$  induction in lung fibroblasts as a response to hMPV infection was used when investigating induction of hMPV-triggered TSLP in the WI38 cell line. The time point where the IFN- $\beta$  fold induction reaches its maximum, at 18h, was further used in experiments to characterize which PRR signaling components that are involved in the TSLP induction in these cells.

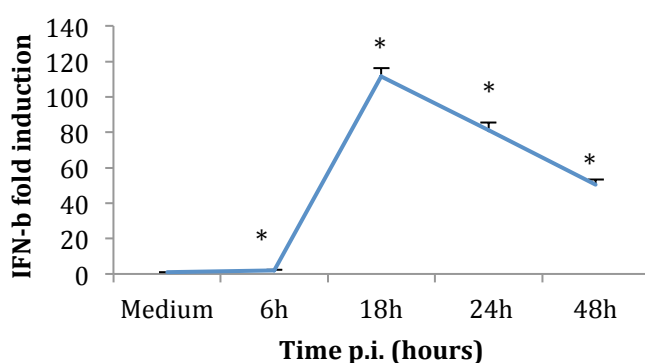


**Figure 4.14. Induction of IFN- $\beta$  in lung fibroblasts upon hMPV infection.** Induction of IFN- $\beta$  mRNA during infection with hMPV A1S38 in WI-38 cells. The induction starts at around 6h p.i. and peaks at 18h p.i. All fold inductions are relative to medium. Standard deviation is represented by error bars. Data are representative for three experiments. Statistical significance is indicated by \*, P value <0,05 relative to medium.

#### 4.5.2 Activation of transcription factors upon infection with hMPV A1 in lung fibroblasts

##### *Phosphorylation status of transcription factors during hMPV A1 infection in lung fibroblasts*

The IFN- $\beta$  promoter has binding sites for transcription factors NF- $\kappa$ B, IRF3 and ATF2, and these are activated in response to viral infection. It is as of today not completely understood how TSLP is induced in response to hMPV infection. To assess which transcription factors that are activated in response to hMPV infection, might give an indication of which transcription factors are involved in promoting TSLP induction. The results, shown in Figure 4.15, show that IRF3 is phosphorylated upon hMPV infection in WI-38 cells. However, it seems that the transcription factors NF- $\kappa$ B and ATF2 are less active in response to hMPV infection in fibroblasts. It is observed by Dey *et al* that NF- $\kappa$ B is activated in a RIG-I-dependent manner in SeV-infected fibroblasts (81). Whether hMPV infection in fibroblasts mainly induces IRF3 activation, needs to be further investigated.

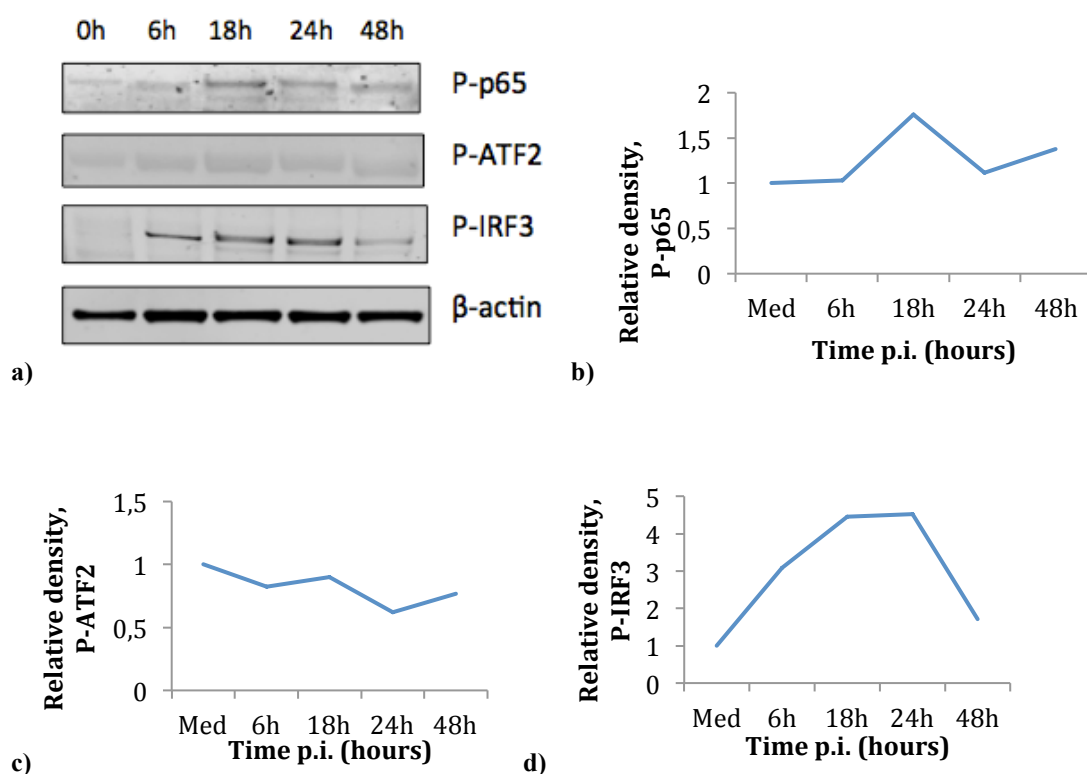


**Figure 4.15. The phosphorylation status of transcription factors upon hMPV A1 infection in WI-38. a)** Phosphorylation of p65 (65kDa), ATF2 (70kDa) and IRF3 (45-55kDa) at time points 0h, 6h, 18h, 24h and 48h p.i. **b)** Quantification of P-p65 blot. **c)** Quantification of P-ATF2 blot. **d)** Quantification of P-IRF3 blot. The quantification is measured in relative density. The relative density is adjusted against  $\beta$ -actin. Statistical analysis for the quantification graphs was not performed.

### *STAT1 is phosphorylated upon hMPV infection in lung fibroblasts*

STAT1 is found expressed constitutively in the cytoplasm of un-stimulated cells and is phosphorylated on specific tyrosine residues and post-translationally modified which leads to dimerization and translocation to the nucleus. In the nucleus, it binds to DNA and induce transcription (76). As seen in Figure 4.16, the results show that STAT1 is phosphorylated upon hMPV infection. STAT1 is mainly phosphorylated 18h to 24h p.i. This might indicate that STAT1 and the Jak-STAT pathway is activated by IFN- $\beta$  in response to hMPV infection. By quantification of blot our results show that the STAT1 phosphorylation peaks at 24h p.i. As seen in the kinetics experiment, IFN- $\beta$  mRNA is mainly induced at 18h p.i. Together, the kinetics result for IFN- $\beta$  and the results for the phosphorylation of STAT1 indicate that IFN- $\beta$  might be induced as a response to hMPV A1 infection in lung fibroblast, and that secretion of IFN- $\beta$  and the subsequent binding to the IFN- $\beta$  receptor, might lead to secondary activation of the Jak-STAT pathway and thus might result in phosphorylation of STAT1. Whether this pathway is involved in the secondary signaling pathway of TSLP upon hMPV infection would be exciting to investigate further. It is known that both STAT3 and STAT5 are activated in by TSLP binding to the TSLPR (82).

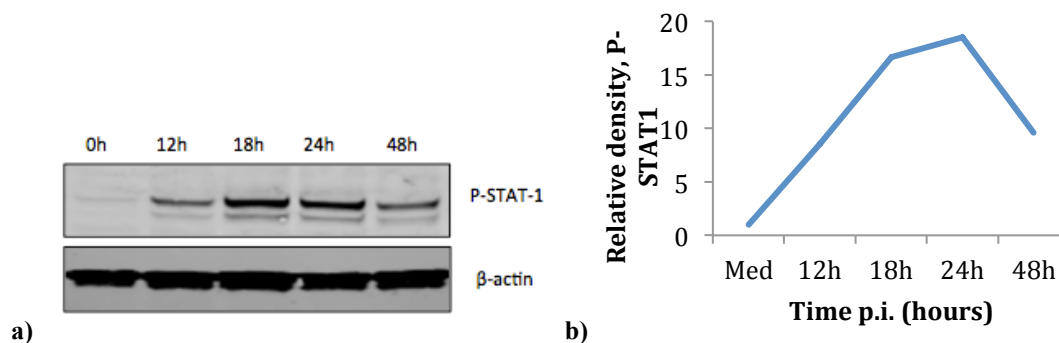


**Figure 4.16. Phosphorylation status of STAT1 upon hMPV A1 infection in WI38.**

**a)** Phosphorylation of STAT1 (84,94) at time points 0h, 6h, 18h, 24h and 48h p.i.  $\beta$ -actin was used as control to determine equal loading of the samples. **b)** Quantification of P-STAT1 blot in WI-38. The relative density is adjusted against  $\beta$ -actin. Statistical analysis for the quantification graph was not performed.

## 4.6 Characterization of PRR signaling components involved in hMPV A1-triggered TSLP induction in lung fibroblasts

It is of great interest to assess which PRR signaling components that are involved in the regulation of TSLP in response to hMPV infection. It has been reported that TSLP is able to activate fibroblasts (83).

### 4.6.1 Kinetics for hMPV-triggered TSLP induction in lung fibroblasts

To establish the kinetics for TSLP induction in lung fibroblasts upon hMPV infection, kinetics experiments were performed in WI-38 cells. The lftTSLP mRNA induction was detected by applying qRT-PCR. The aim of the kinetics experiments was to establish the time point where TSLP induction peak in response to hMPV infection. The time points were initially chosen on the basis of the IFN- $\beta$  induction results. The results, shown in Figure 4.17, show that lftTSLP show high induction 18h p.i., which also was the case for lftTSLP induction in airway epithelial cells.

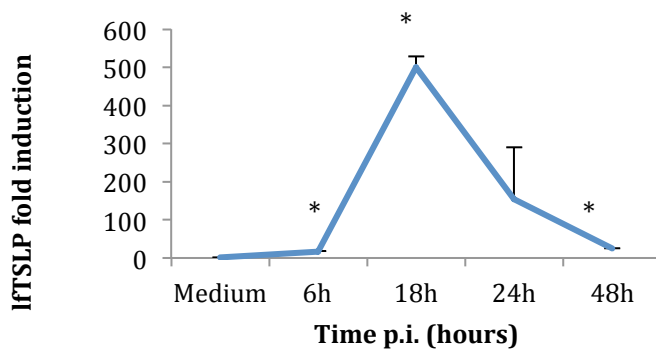


**Figure 4.17. Induction of TSLP in lung fibroblasts upon hMPV infection.** Induction of TSLP mRNA during infection with hMPV A1S38 in WI38. lftTSLP fold induction. All fold inductions are relative to medium. Standard deviation is represented by error bars. Data are representative for three experiments. Statistical significance is indicated by \*, P value <0,05 relative to medium.

#### 4.6.2 Characterization of PRR signaling components involved in hMPV A1-triggered TSLP expression in lung fibroblasts

To characterize which PRR signaling components that are involved in TSLP induction upon hMPV infection in lung fibroblasts, knockdown experiments using siRNA were performed in WI-38 cell line. Comparing the kinetics experiments of the two cell lines A549 and WI-38, the lung fibroblast cell line gave higher induction of TSLP and more stable results than A549. Because the basal expression of TSLP is low in the A549 cell line, they are very sensitive to the high differences in induction when fold induction is calculated. In addition, all hMPV A1 stocks gave sufficient induction of TSLP in the WI-38 cells. TSLP induction in response to selected hMPV A1 stocks in WI-38 cells are previously shown in Figure 4.5. Additional PRR signaling components were selected for knockdown experiments to expand the picture of the signaling pathway leading to TSLP induction upon hMPV infection. The time point for lftTSLP maximum induction was 18h p.i., and so this time point was chosen for the following knockdown experiments.

##### *The cytoplasmic PRR RIG-I is involved in the induction of lftTSLP upon hMPV A1 infection in lung fibroblasts*

RIG-I is a cytoplasmic PRR that is required for the antiviral response against *Paramyxoviridae*, by sensing the nascent 5' end triphosphate moiety of viral genomes or virus derived transcripts of -ssRNA viruses (28). RIG-I induces type I IFN responses by recruiting the CARD domain containing downstream adaptor protein MAVS and trigger IRF3 activation which activate the IFN- $\beta$  gene transcription (72). It has been shown that hMPV strain A2 induce IFN- $\beta$  in a RIG-I dependent manner (28). Goutagny *et al* have shown that RIG-I and MAVS are involved in the regulation of IFN- $\beta$  induction upon hMPV strain A1 (72). They interestingly also found that hMPV strain B1 is not able to induce IFN- $\beta$ . Mouse fibroblasts that are RIG-I deficient are unable to induce type I IFN in response to SeV infection (31).

As mentioned, it has been reported that RIG-I is involved in the TSLP regulation in response to hMPV infection in airway epithelial cells (54). Because this has been reported in airway epithelial cells, it was interesting to investigate whether this was the case in lung fibroblasts as well.

Whether TSLP was expressed in RIG-I depleted lung fibroblasts was investigated by siRNA-mediated knockdown. The cells were transfected with RIG-I siRNA, or Allstar siRNA as a control, and the lftTSLP mRNA fold induction was measured applying qRT-PCR. The result, presented in Figure 4.18, show that TSLP induction is significantly suppressed in the RIG-I depleted cells. This suggests that RIG-I plays a significant role in the TSLP induction in lung fibroblasts upon hMPV infection.

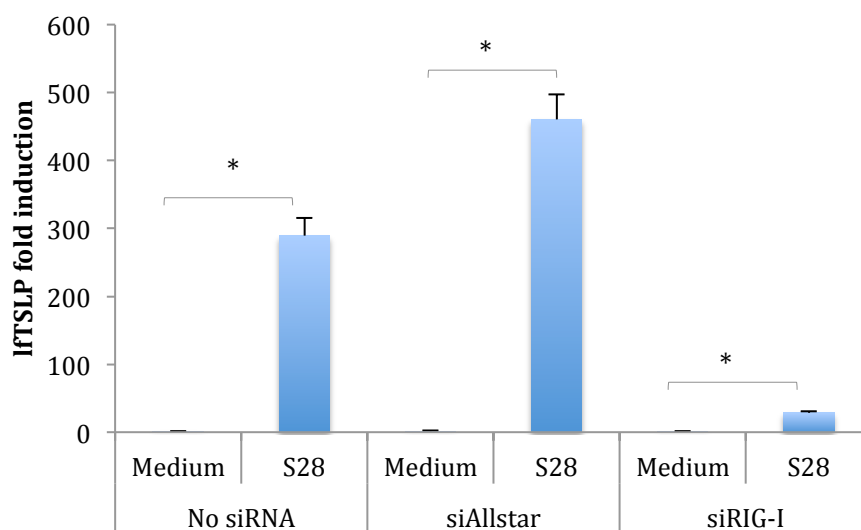


**Figure 4.18. TSLP induction in RIG-I depleted cells.** Induction of TSLP mRNA during infection with hMPV A1S28 in RIG-I-depleted WI-38 cells. Standard deviation is represented by error bars. Data are representative for three experiments. Statistical significance is indicated by \*, P value <0,05 relative to medium.

As seen in the results in Figure 4.18, the lftTSLP mRNA induction is increased for the siAllstar control. The fact that the Allstar siRNA sequence induce TSLP expression must be considered a method flaw. Ideally there should not be any difference between the no siRNA and the siAllstar control. It is necessary to compare the siRIG-I result with the siAllstar control to make sure that the transfection method itself is taken into account and not responsible for the induction. It has been shown that siRNA can induce the innate immune response (84).

#### ***The cytoplasmic PRR MDA5 is not involved in hMPV A1-triggered induction of lftTSLP in lung fibroblasts***

MDA5 is a cytoplasmic PRR that recognize viral molecules; more specifically long dsRNAs that are typical intermediates of the replication of plus-sense ssRNA viruses. MDA5 induces IFN- $\beta$  by recruitment of MAVS and activation of transcription factor IRF3. MDA5 is required for antiviral response against picornaviruses (85).

Goutagny *et al* has previously reported that MDA5 is not involved in hMPV A1 recognition in HEK293 cells, and that the IFN- $\beta$  expression is induced through the RIG-I/MAVS-dependent pathway (72). To investigate whether TSLP induction upon hMPV infection is associated with MDA5 expression in lung fibroblasts, WI-38 cells were transfected with siMDA5, or siAllstar as a control. The cells were infected for with hMPV at MOI 1 for 18h and the lftTSLP fold induction was measured by qRT-PCR. The results are presented in Figure 4.19 and show that knockdown of MDA5 gave unaltered induction of TSLP compared to the control. This suggests that MDA5 is not involved in the regulation of TSLP induction upon hMPV infection in lung fibroblasts. Based upon these results, it might seem that the MDA5 pathway is not involved in lftTSLP regulation, where RIG-I seem to work as the main sensor of hMPV and RIG-I-dependent downstream signaling is the main regulator of lftTSLP induction upon hMPV infection in lung fibroblasts. It is possible that signaling through MDA5 can lead to induction of lftTSLP, however the lung fibroblasts are able to induce lftTSLP in the same amount even in the absence of MDA5. Supporting these findings, Liao *et al* showed that MDA5 does not play a role in regulating cellular responses in upon hMPV infection in A549 (28). The role of MDA5 in response to hMPV needs to be further investigated both in airway epithelial cells and in lung fibroblasts.

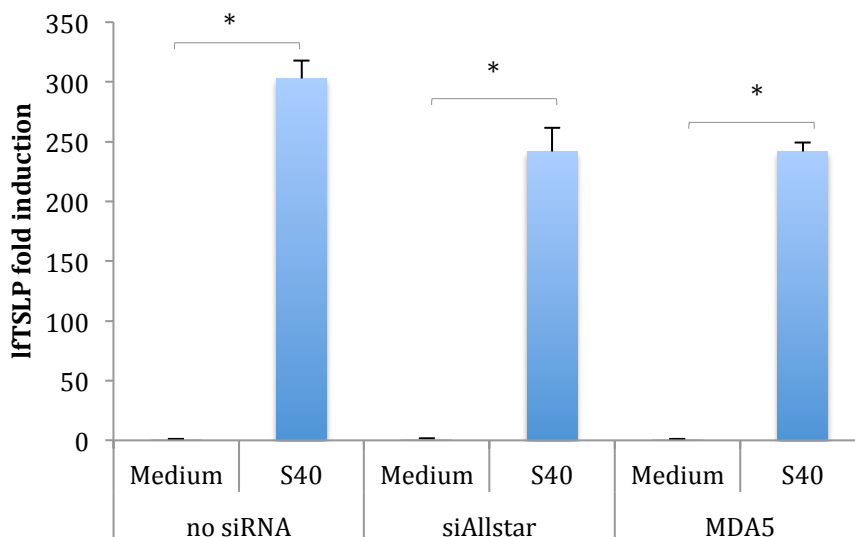


**Figure 4.19. TSLP induction in MDA5 depleted cells.** Induction of TSLP mRNA during infection with hMPV S40 in MDA5-depleted WI-38 cells. Standard deviation is represented by error bars. Data are representative for three experiments. Statistical significance is indicated by \*, P value <0,05 relative to medium.



*The cytoplasmic PRR LGP2 is not involved in hMPV A1-triggered induction of IfTSLP in lung fibroblasts*

LGP2 is a RLR that differ from RIG-I and MDA5 in that LGP2 does not contain CARD domains and is therefore thought to have a distinct role in antiviral signaling (13). To investigate whether TSLP induction upon hMPV infection is associated with LGP2 expression in fibroblasts, the cells were transfected with siLGP2 or siAllstar as a control, infected with hMPV at MOI 1 for 18h, and the IfTSLP fold induction was subsequently measured. The results are presented in Figure 4.20, and show that knockdown of LGP2 show no or little suppression of TSLP induction, suggesting that LGP2 plays a little or insignificant role in the TSLP induction in fibroblasts upon hMPV infection.

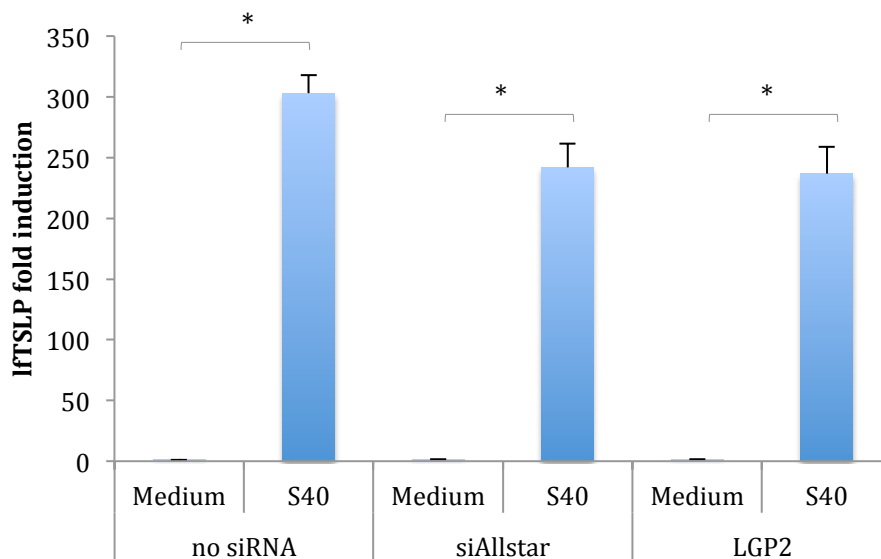


**Figure 4.20. TSLP induction in LGP2 depleted cells.** Induction of TSLP mRNA during infection with hMPV S40 in LGP2-depleted WI-38 cells. Standard deviation is represented by error bars. Data are representative for three experiments. Statistical significance is indicated by \*, P value <0,05 relative to medium.

### *The adaptor protein MAVS is involved in hMPV A1-triggered induction of IFTSLP in lung fibroblasts*

When RNA molecules bind to RIG-I and MDA5, their CARD domains interact with the CARD domain of MAVS that further recruit and activate protein kinases that phosphorylate the transcription factors (24). Whether MAVS is involved in TSLP regulation upon hMPV infection was investigated by transfecting cells with siMAVS, or siAllstar, infecting the cells at MOI 1 for 18h and the mRNA fold induction was then measured applying qRT-PCR. As a result, shown in Figure 4.21, knockdown of MAVS significantly suppressed TSLP induction, suggesting that MAVS plays a significant role in the TSLP induction in fibroblasts upon hMPV infection. Experiments carried out by Liao *et al* shows that the RIG-I-MAVS pathway is important in hMPV triggered cellular responses (28).

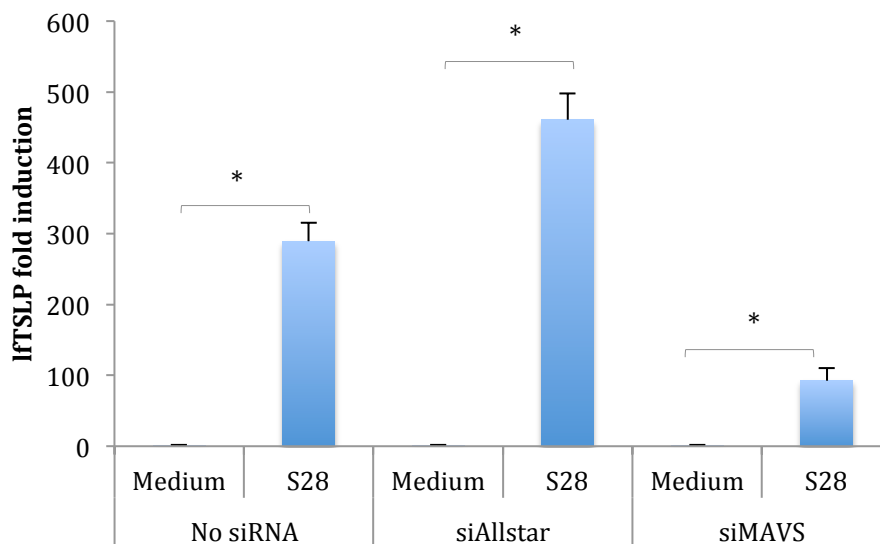


**Figure 4.21. TSLP induction in MAVS depleted cells.** Induction of TSLP mRNA during infection with hMPV A1S28 in MAVS-depleted WI-38 cells. Standard deviation is represented by error bars. Data are representative for three experiments. Statistical significance is indicated by \*, P value <0,05 relative to medium.

### *TRAF6 is not involved in hMPV A1-triggered induction of lftTSLP in lung fibroblasts*

In RLR-signaling, dimerization of MAVS leads to recruitment of TRAF6 which is involved in the downstream signaling pathway in inducing transcription factors (34). To investigate whether lftTSLP induction upon hMPV infection is associated with TRAF6 expression in fibroblasts, the cells were transfected with TRAF6 siRNA, or Allstar siRNA as a control, and the lftTSLP mRNA fold induction was measured. As a result, shown in Figure 4.22, knockdown of TRAF6 does not seem to have any impact on the lftTSLP induction compared to the control, suggesting that fibroblasts are able to induce lftTSLP production in the absence of TRAF6. This indicates that TRAF6 might not be involved in the regulation of TSLP induction in fibroblasts upon hMPV infection. As seen in figure 37, the lftTSLP mRNA induction in response to hMPV was not considered statistically significant. It has been shown by other members of the research group that TRAF6 knockdown inhibit the lftTSLP induction, contradictory indicating that TRAF6 is involved in the regulation of TSLP induction pathway in response to hMPV. Therefore, the involvement of TRAF6 in the TSLP signaling pathway must be investigated further. The result is however, in line with the result presented in Figure 4.15, suggesting that NF- $\kappa$ B is not activated in response to hMPV infection in lung fibroblasts. TRAF6 is an important signaling component in the NF- $\kappa$ B-activating pathway (25).

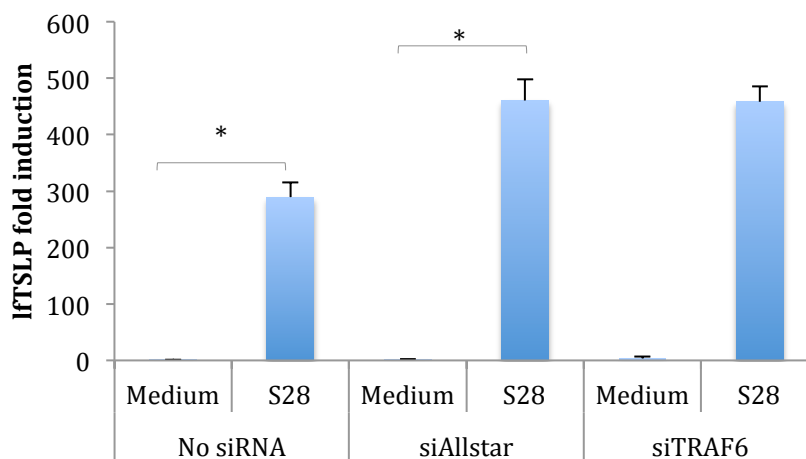


**Figure 4.22. TSLP induction in TRAF6 depleted cells.** Induction of TSLP mRNA during infection with hMPV A1S28 in TRAF6-depleted WI-38 cells. Standard deviation is represented by error bars. Data are representative for three experiments. Statistical significance is indicated by \*, P value <0,05 relative to medium.

### *TBK1 is involved in hMPV A1-triggered induction of lftSLP in lung fibroblasts*

TRAF6 may activate TBK1 that is involved in the phosphorylation of IRF3 (86). The lung fibroblasts was found to increase the activation of IRF3 in response to hMPV infection, as seen in Figure 4.15. It was therefore of interest to investigate whether TBK1 is involved in the regulation of TSLP induction in these cells. The cells were transfected with TBK1 siRNA and the lftTSLP fold induction was measured. The results are seen in Figure 4.23 and show that knockdown of TBK1 significantly suppressed TSLP induction, suggesting that TBK1 plays a significant role in the TSLP induction in fibroblasts upon hMPV infection.

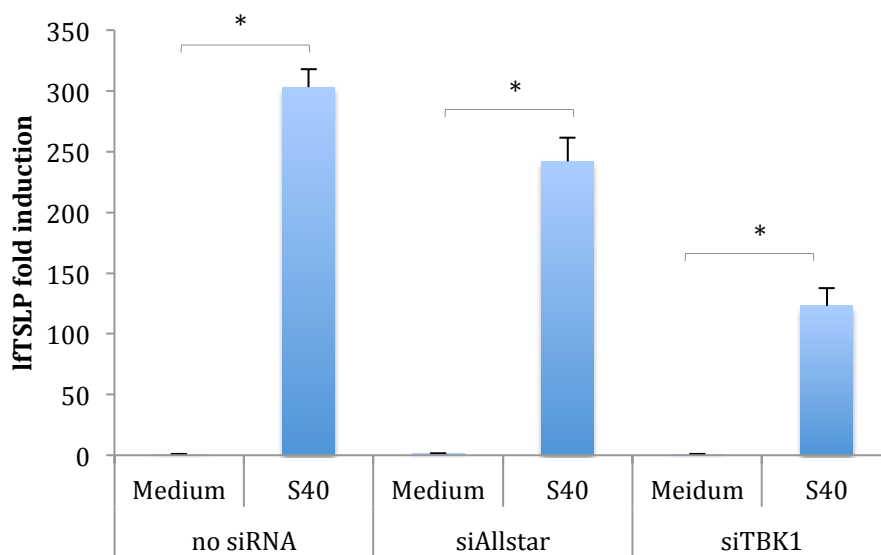
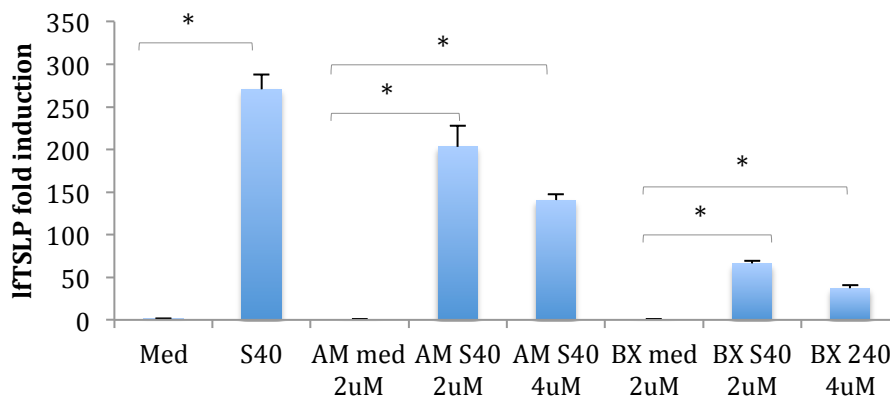


**Figure 4.23. TSLP induction in TBK1 depleted cells.** Induction of TSLP mRNA during infection with hMPV S40 in TBK-1-depleted WI-38 cells. Standard deviation is represented by error bars. Data are representative for three experiments. Statistical significance is indicated by \*, P value <0,05 relative to medium.

**The kinase activity of TBK1 is important for hMPV-triggered lftTSLP induction in lung fibroblasts**

To further investigate whether TBK1 is involved in TSLP induction upon hMPV infection in lung fibroblasts, TBK1 kinase activity was blocked by applying pharmacological inhibitors. The results are presented in Figure 4.24. lftTSLP induction was significantly suppressed in the presence of TBK1 inhibitors, suggesting that the TBK1 kinase activity is an important factor of the lftTSLP induction pathway. Increasing the concentration of kinase inhibitor led to further decrease in the lftTSLP induction, suggesting that the suppression of lftTSLP induction is a result of the inhibitor as well as indicating that the inhibition is concentration dependent. This also confirms that TBK1 is absolutely necessary in the lftTSLP induction pathway. These results are in line with the results of the phosphorylation status of IRF3 upon hMPV infection in lung fibroblasts. TBK1 has been shown to phosphorylate IRF3 which leads to IRF3 activation, translocation into the nucleus and induces the transcription of antiviral genes, like IFN- $\beta$  (32, 35). Altogether these results indicate that lftTSLP is induced in a TBK1-IRF3-dependent manner.



**Figur 4.24. Fold induction of lftTSLP upon hMPV infection in WI-38 cells transfected with TBK1 kinase inhibitors.** Fold induction of lftTSLP in WI-38 cells transfected with kinase inhibitors Amlexanox (AM) and BX-795 (BX) upon infection of hMPV S40. Standard deviation is represented by error bars. Data are representative for three experiments. Statistical significance is indicated by \*, P value <0,05 relative to medium.

#### 4.6.3 The NLRP3-inflammasome involvement in hMPV-triggered TSLP induction in lung fibroblasts

The NLRP3 inflammasome is a large protein complex that is built up by NLRs, the adaptor protein apoptosis associated speck-like protein containing a CARD (ASC) and Caspase1. The inflammasome is activated when the NLRP3s recognize DAMPs and PAMPs, like virus molecules, in the cytosol, which leads to recruitment and activation of the pro-inflammatory protease Caspase1. It has been shown that infection by both influenza virus and RSV can activate the inflammasome (87). For RSV the NLRP3/ASC inflammasome was crucial for the IL-1 $\beta$  production upon the infection. Caspase1 cleaves pro-interleukins like IL-1 and IL-18 into their active cytokine forms. Cytokine IL-1 is recognized as a potent inducer of inflammation. (30). Interestingly, IL-1 has been shown to be an inducer of TSLP in DCs (88), however it is not known if the inflammasome is involved in hMPV A1-triggered TSLP induction in lung fibroblasts. To investigate whether the inflammasome is involved in the lTSLP regulation in response to hMPV infection, siRNA-mediated knockdown of Caspase1 and NLRP3 was performed prior to infection and lTSLP mRNA induction was measured.

### *NLRP3 might be a negative regulator of lftTSLP induction in lung fibroblasts upon hMPV A1 infection*

It has recently been reported that IL-1 $\beta$  and NLRP3 is up-regulated in patients with severe respiratory tract infection associated with hMPV subgroups A2 and B2 (89). NLRP3 cells were transfected with siNLRP3, or siAllstar, infected with hMPV at MOI 1 and lysed 18h p.i. The lftTSLP mRNA induction was then measured applying qRT-PCR. The results, seen in Figure 4.25, interestingly show that knockdown of NLRP3 resulted in increased lftTSLP induction. This suggests that the NLRP3 inflammasome might work as a negative regulator in the lftTSLP induction pathway in fibroblasts. This experiment was conducted twice and it is therefore not possible to conclude based on these results. This requires further investigation before conclusions could be drawn.

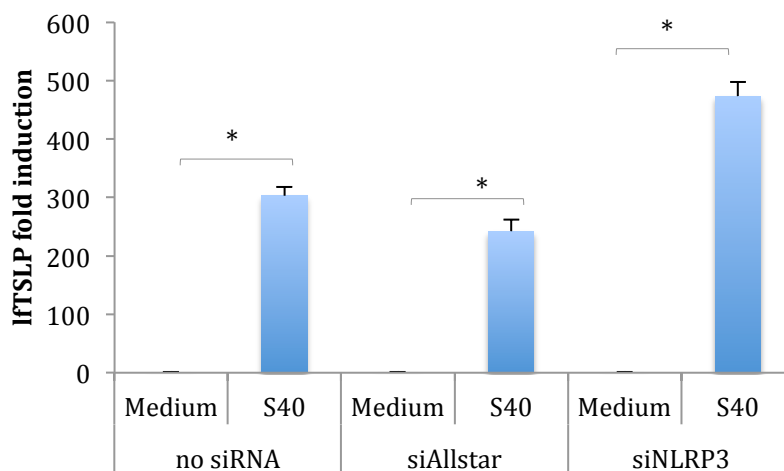


**Figure 4.25. TSLP induction in NLRP3 depleted cells.** Induction of TSLP mRNA during infection with hMPV A1S40 in NLRP3-depleted WI-38 cells. Standard deviation is represented by error bars. Data are representative for three experiments. Statistical significance is indicated by \*, P value <0,05 relative to medium.

### *Caspase1 might be involved in lftSLP in lung fibroblasts upon hMPV A1 infection*

Inflammasomes are able to recruit and activate pro-caspase1. Caspase1 is important in a variety of inflammatory responses, including converting IL-1 $\beta$  into their active cytokine form (30). The cells were transfected with siCaspase1 or siAllstar, infected with hMPV at MOI 1, lysed 18h p.i. and subsequently the lftSLP fold induction was measured. The results are presented in Figure 4.26 and show that knockdown of Caspase1 slightly decreases lftSLP induction, suggesting that lung fibroblasts are able to induce lftSLP in the absence of Caspase1, which indicates that Caspase1 is not a crucial component in the lftSLP induction pathway in lung fibroblasts upon hMPV infection. The results could also indicate that Caspase1 might possibly be involved in an inflammasome-independent manner.

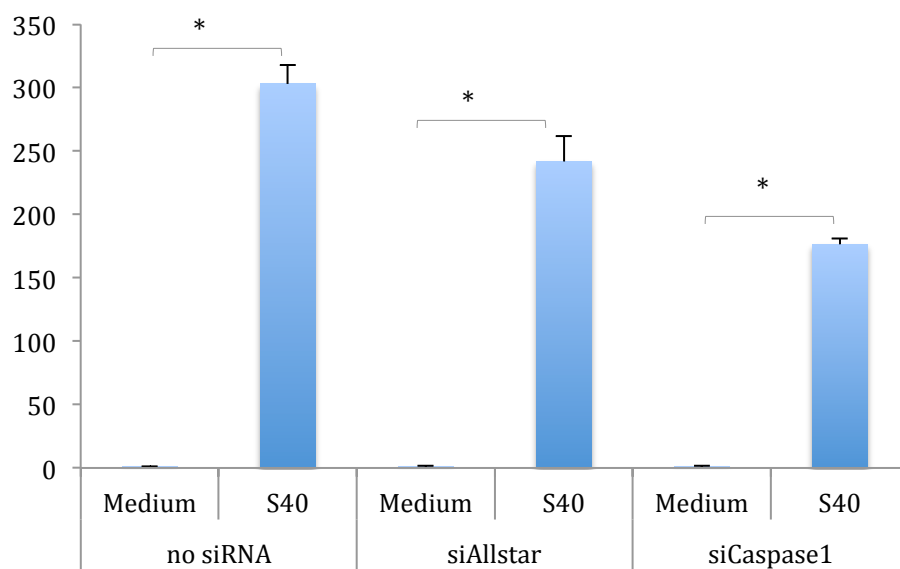


**Figure 4.26. TSLP induction in Caspase1 depleted cells.** Induction of lftSLP mRNA during infection with hMPV A1S40 in Caspase1-depleted WI-38 cells. Standard deviation is represented by error bars. Data are representative for three experiments. Statistical significance is indicated by \*, P value <0,05 relative to medium.



## 5 Conclusions

The aims of this study have been to characterize the PRR signaling components of hMPV-triggered TSLP expression, and to determine the phosphorylation status of transcription factors. The experiments that have been performed have resulted in some conclusions regarding hMPV-triggered TSLP expression and the effect on signaling components triggered by hMPV. These conclusions are listed as follows:

- hMPV A1 replication peaks at day 8-9 in LLC-MK<sub>2</sub> cells.
- sfTSLP and lftTSLP is induced upon hMPV infection in airway epithelial cells and in lung fibroblasts.
- sfTSLP induction peaks at 48h p.i. in airway epithelial cells while lftTSLP induction peaks at 18h p.i. upon hMPV A1 infection in airway epithelial cells.
- hMPV A1-triggered lftTSLP induction in airway epithelial cells and lung fibroblasts happens in a RIG-I- and MAVS-dependent pathway.
- TBK1 mediated signaling downstream of RIG-I is important in regulation of hMPV triggered lftTSLP.
- The cytoplasmic PRRs MDA5 and LGP2 play less significant roles in the hMPV A1-triggered lftTSLP-induction pathway in lung fibroblasts.

For some experiments performed in this thesis it is not possible to draw conclusions based on the results, however these results give indications that need to be further investigated. These indications are listed as follows:

- hMPV A1 stocks that are considered DI negative can still be able to induce lftTSLP in high amounts in airway epithelial cells and lung fibroblasts.
- Results in this thesis suggest that NF- $\kappa$ B is phosphorylated upon hMPV A1 infection in airway epithelial cells, while seem to be less phosphorylated upon hMPV A1 infection in lung fibroblasts. This is supported by the indication that TRAF6 seems to be involved in the lftTSLP-induction pathway in airway epithelial cells, however possibly not involved in the lftTSLP-induction pathway in lung fibroblasts. TRAF6 is known to be a signaling component resulting in NF- $\kappa$ B phosphorylation. These findings need to be further investigated.

- hMPV A1 infection in airway epithelial cells and lung fibroblasts seem to lead to IRF3 phosphorylation and thus activation. This is supported by the results indicating that TBK1 seems to be involved in the lftSLP-induction pathway in lung fibroblasts. TBK1 is shown to be necessary for the phosphorylation of IRF3. The results therefore suggest that lftSLP is induced in a TBK1-IRF3-dependent manner upon hMPV A1 infection, though this needs to be investigated further.
- STAT1 seems to be phosphorylated in response to IFN- $\beta$  signaling upon activation of hMPV A1 in fibroblasts. In airway epithelial cells, IFN- $\beta$  seems to be induced after STAT1 is phosphorylated suggesting that the phosphorylation of STAT1 is not induced by IFN- $\beta$  in these cells. These results need to be further investigated.
- The NLRP3 inflammasome does not seem to be a crucial component in the lftSLP induction upon hMPV A1 infection in fibroblasts. Further investigation is needed.

## 6 Future Studies

Further analysis is needed to provide more insight into the TSLP induction pathway in human airway cells upon hMPV infection. Understanding the role of the PRR signaling components leading to induction of TSLP upon hMPV infection this can further explain which function TSLP has in asthma development. The following experiments would be of interest to further investigate the findings of this thesis:

- It would be interesting to do additional knockdown experiments, including knockdown of transcription factors NF- $\kappa$ B, IRF3 and ATF2, and observe the effect on TSLP induction.
- Knockdown of several PRR signaling targets simultaneously would be of interest, both at mRNA level and protein level.
- Luciferase assay to investigate the promoter activity of NF- $\kappa$ B, ATF2 and IRF3 upon hMPV infection would also be of interest to supplement evidence provided by the phosphorylation analyses performed for Western Blot in this thesis.
- It would also be interesting to conduct knockdown of PRR components and apply Western Blot to analyze the phosphorylation status of transcription factors. That will provide information on how these PRR signaling components are involved in the activation of transcription factors in response to hMPV infection.
- Experiments in mice models using knockout mice would be interesting to observe the hypothesis *in vivo*.

It would also be of interest to study the differences in the induction pathways leading to sfTSLP and lfTSLP, to increase the knowledge in what the functional difference between them is. Comparing the regulation of TSLP induction in response to the different hMPV subgroups would also be highly interesting. Increased understanding of these processes would increase the understanding of the link between TSLP, hMPV and asthma, would be an important piece in the puzzle of respiratory pathogens and disease.



## References

1. WHO. WHO. Available from: <http://www.who.int/mediacentre/factsheets/fs307/en/>.
2. Encyclopædia Britannica. Available from: <http://global.britannica.com/science/respiratory-disease>.
3. Lemanske RF, Jr., Busse WW. 6. Asthma: Factors underlying inception, exacerbation, and disease progression. *The Journal of allergy and clinical immunology*. 2006;117(2 Suppl Mini-Primer):S456-61.
4. Busse WW, Lemanske RF, Jr., Gern JE. Role of viral respiratory infections in asthma and asthma exacerbations. *Lancet*. 2010;376(9743):826-34.
5. Holtzman MJ, Tyner JW, Kim EY, Lo MS, Patel AC, Shornick LP, et al. Acute and chronic airway responses to viral infection: implications for asthma and chronic obstructive pulmonary disease. *Proceedings of the American Thoracic Society*. 2005;2(2):132-40.
6. Soumelis V, Reche PA, Kanzler H, Yuan W, Edward G, Homey B, et al. Human epithelial cells trigger dendritic cell mediated allergic inflammation by producing TSLP. *Nature immunology*. 2002;3(7):673-80.
7. van den Hoogen BG, de Jong JC, Groen J, Kuiken T, de Groot R, Fouchier RA, et al. A newly discovered human pneumovirus isolated from young children with respiratory tract disease. *Nature medicine*. 2001;7(6):719-24.
8. Kahn JS. Epidemiology of human metapneumovirus. *Clinical microbiology reviews*. 2006;19(3):546-57.
9. Principi N, Bosis S, Esposito S. Human metapneumovirus in paediatric patients. *Clinical microbiology and infection : the official publication of the European Society of Clinical Microbiology and Infectious Diseases*. 2006;12(4):301-8.
10. Jartti T, Lehtinen P, Vuorinen T, Osterback R, van den Hoogen B, Osterhaus AD, et al. Respiratory picornaviruses and respiratory syncytial virus as causative agents of acute expiratory wheezing in children. *Emerging infectious diseases*. 2004;10(6):1095-101.
11. Jartti T, van den Hoogen B, Garofalo RP, Osterhaus AD, Ruuskanen O. Metapneumovirus and acute wheezing in children. *Lancet*. 2002;360(9343):1393-4.
12. Mackay IM, Bialasiewicz S, Waliuzzaman Z, Chidlow GR, Fegredo DC, Laingam S, et al. Use of the P gene to genotype human metapneumovirus identifies 4 viral subtypes. *The Journal of infectious diseases*. 2004;190(11):1913-8.
13. Kolli D, Velayutham TS, Casola A. Host-Viral Interactions: Role of Pattern Recognition Receptors (PRRs) in Human Pneumovirus Infections. *Pathogens (Basel, Switzerland)*. 2013;2(2).
14. Dimmock N, Easton A, Leppard K. *Introduction to Modern Virology*. 6th edition ed: Blackwell Publishing; 2007.
15. Schildgen V, van den Hoogen B, Fouchier R, Tripp RA, Alvarez R, Manoha C, et al. Human Metapneumovirus: lessons learned over the first decade. *Clinical microbiology reviews*. 2011;24(4):734-54.
16. Cox RG, Williams JV. Breaking in: human metapneumovirus fusion and entry. *Viruses*. 2013;5(1):192-210.

17. Schowalter RM, Smith SE, Dutch RE. Characterization of Human Metapneumovirus F Protein-Promoted Membrane Fusion: Critical Roles for Proteolytic Processing and Low pH. *Journal of virology*. 2006;80(22):10931-41.
18. Lopez CB. Defective viral genomes: critical danger signals of viral infections. *Journal of virology*. 2014;88(16):8720-3.
19. van den Hoogen BG, van Boheemen S, de Rijck J, van Nieuwkoop S, Smith DJ, Laksono B, et al. Excessive production and extreme editing of human metapneumovirus defective interfering RNA is associated with type I IFN induction. *The Journal of general virology*. 2014;95(Pt 8):1625-33.
20. Bals R, Hiemstra PS. Innate immunity in the lung: how epithelial cells fight against respiratory pathogens. *The European respiratory journal*. 2004;23(2):327-33.
21. Payne K, A W. *From Molecule to Function to Disease, Alveolar Structure and Function* 2013.
22. Manicone AM. Role of the pulmonary epithelium and inflammatory signals in acute lung injury. *Expert review of clinical immunology*. 2009;5(1):63-75.
23. Owen JA, Punt J, Stranford SA. *Kuby Immunology. Seventh Edition* ed. Houndsmills, Basingstoke RG21 6XS, England: Macmillan Higher Education; 2013.
24. Vareille M, Kieninger E, Edwards MR, Regamey N. The airway epithelium: soldier in the fight against respiratory viruses. *Clinical microbiology reviews*. 2011;24(1):210-29.
25. Akira S, Uematsu S, Takeuchi O. Pathogen recognition and innate immunity. *Cell*. 2006;124(4):783-801.
26. Bruns AM, Horvath CM. Activation of RIG-I-like receptor signal transduction. *Critical reviews in biochemistry and molecular biology*. 2012;47(2):194-206.
27. Dixit E, Kagan JC. Intracellular pathogen detection by RIG-I-like receptors. *Advances in immunology*. 2013;117:99-125.
28. Liao S, Bao X, Liu T, Lai S, Li K, Garofalo RP, et al. Role of retinoic acid inducible gene-I in human metapneumovirus-induced cellular signalling. *The Journal of general virology*. 2008;89(Pt 8):1978-86.
29. Childs KS, Randall RE, Goodbourn S. LGP2 plays a critical role in sensitizing mda-5 to activation by double-stranded RNA. *PloS one*. 2013;8(5):e64202.
30. Skeldon A, Saleh M. The inflammasomes: molecular effectors of host resistance against bacterial, viral, parasitic, and fungal infections. *Frontiers in microbiology*. 2011;2:15.
31. Kawai T, Akira S. Innate immune recognition of viral infection. *Nature immunology*. 2006;7(2):131-7.
32. Randall RE, Goodbourn S. Interferons and viruses: an interplay between induction, signalling, antiviral responses and virus countermeasures. *The Journal of general virology*. 2008;89(Pt 1):1-47.
33. Chau TL, Gioia R, Gatot JS, Patrascu F, Carpentier I, Chapelle JP, et al. Are the IKKs and IKK-related kinases TBK1 and IKK-epsilon similarly activated? *Trends in biochemical sciences*. 2008;33(4):171-80.
34. Xie P. TRAF molecules in cell signaling and in human diseases. *Journal of molecular signaling*. 2013;8(1):7.

35. Du M, Liu J, Chen X, Xie Y, Yuan C, Xiang Y, et al. Casein kinase II controls TBK1/IRF3 activation in IFN response against viral infection. *Journal of immunology (Baltimore, Md : 1950)*. 2015;194(9):4477-88.
36. Casola A, Garofalo RP, Haeberle H, Elliott TF, Lin R, Jamaluddin M, et al. Multiple cis Regulatory Elements Control RANTES Promoter Activity in Alveolar Epithelial Cells Infected with Respiratory Syncytial Virus. *Journal of virology*. 2001;75(14):6428-39.
37. Casola A, Henderson A, Liu T, Garofalo RP, Brasier AR. Regulation of RANTES promoter activation in alveolar epithelial cells after cytokine stimulation. *American journal of physiology Lung cellular and molecular physiology*. 2002;283(6):L1280-90.
38. Barnes B, Lubyova B, Pitha PM. On the role of IRF in host defense. *Journal of interferon & cytokine research : the official journal of the International Society for Interferon and Cytokine Research*. 2002;22(1):59-71.
39. Chattopadhyay S, Marques JT, Yamashita M, Peters KL, Smith K, Desai A, et al. Viral apoptosis is induced by IRF-3-mediated activation of Bax. *The EMBO journal*. 2010;29(10):1762-73.
40. Peters K, Chattopadhyay S, Sen GC. IRF-3 activation by Sendai virus infection is required for cellular apoptosis and avoidance of persistence. *Journal of virology*. 2008;82(7):3500-8.
41. Yu T, Li YJ, Bian AH, Zuo HB, Zhu TW, Ji SX, et al. The regulatory role of activating transcription factor 2 in inflammation. 2014;2014:950472.
42. Duffey D, Dolgilevich S, Razzouk S, Li L, Green R, Gorti GK. Activating transcription factor-2 in survival mechanisms in head and neck carcinoma cells. *Head & neck*. 2011;33(11):1586-99.
43. Friend SL, Hosier S, Nelson A, Foxworthe D, Williams DE, Farr A. A thymic stromal cell line supports in vitro development of surface IgM+ B cells and produces a novel growth factor affecting B and T lineage cells. *Experimental hematology*. 1994;22(3):321-8.
44. Sims JE, Williams DE, Morrissey PJ, Garka K, Foxworthe D, Price V, et al. Molecular cloning and biological characterization of a novel murine lymphoid growth factor. *The Journal of experimental medicine*. 2000;192(5):671-80.
45. Quentmeier H, Drexler HG, Fleckenstein D, Zaborski M, Armstrong A, Sims JE, et al. Cloning of human thymic stromal lymphopoietin (TSLP) and signaling mechanisms leading to proliferation. *Leukemia*. 2001;15(8):1286-92.
46. Reche PA, Soumelis V, Gorman DM, Clifford T, Liu M, Travis M, et al. Human thymic stromal lymphopoietin preferentially stimulates myeloid cells. *Journal of immunology (Baltimore, Md : 1950)*. 2001;167(1):336-43.
47. Lay MK, Cespedes PF, Palavecino CE, Leon MA, Diaz RA, Salazar FJ, et al. Human metapneumovirus infection activates the TSLP pathway that drives excessive pulmonary inflammation and viral replication in mice. *European journal of immunology*. 2015;45(6):1680-95.
48. West EE, Kashyap M, Leonard WJ. TSLP: A Key Regulator of Asthma Pathogenesis. *Drug discovery today Disease mechanisms*. 2012;9(3-4).
49. Bjerkan L, Schreurs O, Engen SA, Jahnsen FL, Baekkevold ES, Blix IJ, et al. The short form of TSLP is constitutively translated in human keratinocytes and has characteristics of an antimicrobial peptide. *Mucosal immunology*. 2015;8(1):49-56.

50. Fornasa G, Tsilingiri K, Caprioli F, Botti F, Mapelli M, Meller S, et al. Dichotomy of short and long thymic stromal lymphopoietin isoforms in inflammatory disorders of the bowel and skin. *The Journal of allergy and clinical immunology*. 2015;136(2):413-22.
51. Ziegler SF, Liu YJ. Thymic stromal lymphopoietin in normal and pathogenic T cell development and function. *Nature immunology*. 2006;7(7):709-14.
52. He R, Geha RS. Thymic stromal lymphopoietin. *Annals of the New York Academy of Sciences*. 2010;1183:13-24.
53. Allakhverdi Z, Comeau MR, Jessup HK, Yoon BR, Brewer A, Chartier S, et al. Thymic stromal lymphopoietin is released by human epithelial cells in response to microbes, trauma, or inflammation and potently activates mast cells. *The Journal of experimental medicine*. 2007;204(2):253-8.
54. Lee HC, Headley MB, Loo YM, Berlin A, Gale M, Jr., Debley JS, et al. Thymic stromal lymphopoietin is induced by respiratory syncytial virus-infected airway epithelial cells and promotes a type 2 response to infection. *The Journal of allergy and clinical immunology*. 2012;130(5):1187-96.e5.
55. Hull RN, Cherry WR, Tritch OJ. Growth characteristics of monkey kidney cell strains LLC-MK1, LLC-MK2, and LLC-MK2(NCTC-3196) and their utility in virus research. *The Journal of experimental medicine*. 1962;115:903-18.
56. Tollefson SJ, Cox RG, Williams JV. Studies of culture conditions and environmental stability of human metapneumovirus. *Virus research*. 2010;151(1):54-9.
57. Scientific T. Available from: <http://www.nanodrop.com/Library/T009-NanoDrop 1000-&NanoDrop 8000-Nucleic-Acid-Purity-Ratios.pdf>.
58. Aldrich S. Sigma Aldrich. Available from: <http://www.sigmaaldrich.com/technical-documents/protocols/biology/resuscitation-of-frozen.html>.
59. Flint S, Enquist L, Racaniello V, Skalka A. *Principles of Virology*. Third edition ed: ASM Press; 2009.
60. Aagaard L, Rossi JJ. RNAi therapeutics: principles, prospects and challenges. *Advanced drug delivery reviews*. 2007;59(2-3):75-86.
61. Bio M. Available from: <https://http://www.mirusbio.com/applications/gene-silencing/sirna-mediated-pathway>.
62. TOCRIS. Available from: <https://http://www.tocris.com/dispprod.php?ItemId=374318-.V0Hmvma3eOk>.
63. InvivoGen. Available from: <http://www.invivogen.com/bx795>.
64. Whitney SE, Sudhir A, Nelson RM, Viljoen HJ. Principles of rapid polymerase chain reactions: mathematical modeling and experimental verification. *Computational biology and chemistry*. 2004;28(3):195-209.
65. Overbergh L, Giulietti A, Valckx D, Decallonne R, Bouillon R, Mathieu C. The use of real-time reverse transcriptase PCR for the quantification of cytokine gene expression. *Journal of biomolecular techniques : JBT*. 2003;14(1):33-43.
66. Livak KJ, Schmittgen TD. Analysis of relative gene expression data using real-time quantitative PCR and the 2(-Delta Delta C(T)) Method. *Methods (San Diego, Calif)*. 2001;25(4):402-8.



67. Haller O, Kochs G, Weber F. The interferon response circuit: induction and suppression by pathogenic viruses. *Virology*. 2006;344(1):119-30.
68. Garoufalidis E, Kwan I, Lin R, Mustafa A, Pepin N, Roulston A, et al. Viral induction of the human beta interferon promoter: modulation of transcription by NF-kappa B/rel proteins and interferon regulatory factors. *Journal of virology*. 1994;68(8):4707-15.
69. Mastrorarde JG, Monick MM, Mukaida N, Matsushima K, Hunninghake GW. Activator protein-1 is the preferred transcription factor for cooperative interaction with nuclear factor-kappaB in respiratory syncytial virus-induced interleukin-8 gene expression in airway epithelium. *The Journal of infectious diseases*. 1998;177(5):1275-81.
70. Wang J, Basagoudanavar SH, Wang X, Hopewell E, Albrecht R, Garcia-Sastre A, et al. NF-kappa B RelA subunit is crucial for early IFN-beta expression and resistance to RNA virus replication. *Journal of immunology (Baltimore, Md : 1950)*. 2010;185(3):1720-9.
71. Conzelmann KK. Transcriptional activation of alpha/beta interferon genes: interference by nonsegmented negative-strand RNA viruses. *Journal of virology*. 2005;79(9):5241-8.
72. Goutagny N, Jiang Z, Tian J, Parroche P, Schickli J, Monks BG, et al. Cell type-specific recognition of human metapneumoviruses (HMPVs) by retinoic acid-inducible gene I (RIG-I) and TLR7 and viral interference of RIG-I ligand recognition by HMPV-B1 phosphoprotein. *Journal of immunology (Baltimore, Md : 1950)*. 2010;184(3):1168-79.
73. Yoboua F, Martel A, Duval A, Mukawera E, Grandvaux N. Respiratory syncytial virus-mediated NF-kappa B p65 phosphorylation at serine 536 is dependent on RIG-I, TRAF6, and IKK beta. *Journal of virology*. 2010;84(14):7267-77.
74. Bao X, Kolli D, Liu T, Shan Y, Garofalo RP, Casola A. Human metapneumovirus small hydrophobic protein inhibits NF-kappaB transcriptional activity. *Journal of virology*. 2008;82(16):8224-9.
75. Dinwiddie DL, Harrod KS. Human metapneumovirus inhibits IFN-alpha signaling through inhibition of STAT1 phosphorylation. *American journal of respiratory cell and molecular biology*. 2008;38(6):661-70.
76. Bao X, Liu T, Spetch L, Kolli D, Garofalo RP, Casola A. Airway epithelial cell response to human metapneumovirus infection. *Virology*. 2007;368(1):91-101.
77. Lee HC, Ziegler SF. Inducible expression of the proallergic cytokine thymic stromal lymphopoietin in airway epithelial cells is controlled by NFkappaB. *Proceedings of the National Academy of Sciences of the United States of America*. 2007;104(3):914-9.
78. Casola A, Garofalo RP, Jamaluddin M, Vlahopoulos S, Brasier AR. Requirement of a novel upstream response element in respiratory syncytial virus-induced IL-8 gene expression. *Journal of immunology (Baltimore, Md : 1950)*. 2000;164(11):5944-51.
79. Lay MK, Bueno SM, Galvez N, Riedel CA, Kalergis AM. New insights on the viral and host factors contributing to the airway pathogenesis caused by the respiratory syncytial virus. *Critical reviews in microbiology*. 2015:1-13.
80. Bedke N, Haitchi HM, Xatzipsalti M, Holgate ST, Davies DE. Contribution of bronchial fibroblasts to the antiviral response in asthma. *Journal of immunology (Baltimore, Md : 1950)*. 2009;182(6):3660-7.

81. Dey N, Liu T, Garofalo RP, Casola A. TAK1 regulates NF-KappaB and AP-1 activation in airway epithelial cells following RSV infection. *Virology*. 2011;418(2):93-101.
82. Wu J, Liu F, Zhao J, Wei Y, Lv J, Dong F, et al. Thymic stromal lymphopoietin promotes asthmatic airway remodelling in human lung fibroblast cells through STAT3 signalling pathway. *Cell biochemistry and function*. 2013;31(6):496-503.
83. Christmann RB. Another Piece in the Fibrotic Puzzle: TSLP as a Novel Ligand for Fibrocyte Activation. *The Journal of investigative dermatology*. 2016;136(2):360-2.
84. Whitehead KA, Dahlman JE, Langer RS, Anderson DG. Silencing or stimulation? siRNA delivery and the immune system. *Annual review of chemical and biomolecular engineering*. 2011;2:77-96.
85. Kato H, Takeuchi O, Sato S, Yoneyama M, Yamamoto M, Matsui K, et al. Differential roles of MDA5 and RIG-I helicases in the recognition of RNA viruses. *Nature*. 2006;441(7089):101-5.
86. Johnsen IB, Bergstroem B, Stiberg KA, Thommesen L, Anthonsen MW. Inducible cAMP early repressor (ICER) is a novel regulator of RIG-I mediated IFN-beta production. *Cellular signalling*. 2013;25(9):1804-12.
87. Kim TH, Lee HK. Innate immune recognition of respiratory syncytial virus infection. *BMB reports*. 2014;47(4):184-91.
88. Elder MJ, Webster SJ, Williams DL, Gaston JS, Goodall JC. TSLP production by dendritic cells is modulated by IL-1beta and components of the endoplasmic reticulum stress response. *European journal of immunology*. 2016;46(2):455-63.
89. Malmo J, Moe N, Krokstad S, Ryan L, Loevenich S, Johnsen IB, et al. Cytokine Profiles in Human Metapneumovirus Infected Children: Identification of Genes Involved in the Antiviral Response and Pathogenesis. *PloS one*. 2016;11(5):e0155484.

## Appendix A: Instruments and Computer Software

Purpose	Instrument/machine	Producer	Software
<b>Cell culture</b>			
Microscope	AE3IE	MOTIC	
Centrifuge	5810R	Eppendorf	
Cell counter	Z2 Coulter® Particle Count and Size Analyzer	Beckman Coulter	
<b>Virus propagation</b>			
Titration Assay	C-SHG1 Inverted Microscope Diaphot-TMD	Nikon	
Ultracentrifuge, virus isolation	Sorvall Discovery 100SE	Hitachi	
<b>Western Blot</b>			
Dry Blot	iBlot™	Invitrogen	
Western blot membrane scanner	Odyssey	LI-COR	Odyssey
Membrane analysis		LI-COR	Image Studio
Quantification of blots			ImageJ
<b>qRT-PCR</b>			
qRT-PCR machine	Step One Plus Real-Time PCR System	Applied Biosystems	Step One Plus
Centrifuge cDNA synthesis	Rotina 35 TC-512	Hettich Zentrifugen TECHNE	